Applications of Gauge-Gravity Duality
Haifa, 4 June 2012

Effective Holographic Theories for finite density systems

Elias Kiritsis

University of Crete APC, Paris

Bibliography

Based ongoing work with

T. Alho (Jyvaskyla U.) K. Kajantie (Helsinki U.), K. Tuominen (Jyvaskyla U.), M. Järvinen (Crete)

C. Charmousis (Orsay) and B. Gouteraux, (APC)

and published recent work with

V. Niarchos (Crete) arXiv:1205.6205 [hep-th]

M. Jarvinnen (Crete) arXiv:1112.1261 [hep-ph]

B. Gouteraux (APC) arXiv:1012.3464 [hep-th]

B. S. Kim and C. Panagopoulos (Crete) arXiv:1012.3464 [cond-mat.str-el]

C. Charmousis, B. Gouteraux (Orsay), B. S. Kim and R. Meyer (Crete)
. arXiv:1005.4690 [hep-th]

The plan of the talk

- Introduction
- The program of Effective Holographic Theories
- The dynamics in the single scalar case
- Generalized Criticality and hyperscaling violations
- Symmetry breaking IR asymptotics and the holographic effective potential.
- Two scalar operators: a interesting example with both QC and symmetry breaking.
- Outlook

Introduction

• Holographic techniques offer a new look into strongly-coupled, semiclassical theories, at finite density.

• The goal is to (a) extend our understanding of known CM mechanisms at strong coupling (b) Look for novel phenomena.

• Like in QFT, a very useful and efficient tool is that of an effective theory: Effective Holographic Theory $\rightarrow$ EHT.

The reason is that it is useful to:

(1) Develop intuition

(2) Do efficient model building

(3) Be useful as an intermediary between theory and data.

• Unlike QFT we know much less about EHT.

• The first step is to hierarchically treat, the

(a) Field content

(b) IR classification of interactions

• The next step is to assess which EHTs are sensible and which are not.

• Eventually a calculation of observables (thermodynamics and transport data for example) should be done in EHT.

• Finally, by matching thresholds, any string derived supergravity and truncation ansatz can be matched to a EHT solution.

♠ The exploration of EHT is an important tool because in gravity/string theory, there is no simple and direct connection between (action+solutions) and physical observable properties.

Effective Holographic Theory Program

The strategy advocated in

Charmousis+Gouteraux+Kim+E.K.+Meyer

is:

1. Select the operators expected to be important for the dynamics

2. Write an effective (gravitational) holographic action that captures the (IR) dynamics by parametrizing the IR asymptotics of interactions .

3. Find the scaling solutions describing extremal saddle points. Built the $T \to 0$ bh solutions around them

4. Study the physics around each acceptable saddle point.

This strategy started bearing fruit as it dealt with

• Einstein-Maxwell-Dilaton theories with the most general AdS and Lifshitz asymptotics.

Charmousis+Gouteraux+Kim+E.K.+Meyer, Gouteraux+E.K.

• Einstein-Maxwell-Dilaton theories with also massive asymptotics and non-abelian (Bianchi) scaling symmetries.

Iizuka+Kachru+Kundu+Narayan+Sircar+Trivedi

• Einstein-Maxwell theories with CP-couplings and a magnetic field.

Donos+Gauntlett

• Einstein-Maxwell-Dilaton+axion theories with broken rotational symmetry.

Iizuka+Maeda

• Einstein-Maxwell-Scalar theories in the symmetry broken regime (to be described later in this talk).

Gouteraux+E.K.

• Einstein-two-scalar theories (special classes to be described later in this talk)

Jarvinnen+E.K.

• The bulk metric $g_{\mu\nu} \leftrightarrow T_{\mu\nu}$ is always sourced in any theory. In CFTs it captures all the dynamics of the stress tensor and the solution is AdS_{p+1}.

• In a theory with a conserved U(1) charge, a gauge field is also necessary, $A_\mu \leftrightarrow J_\mu$. If only $g_{\mu\nu}, A_\mu$ are important then we have an AdS-Einstein-Maxwell theory with saddle point solution=AdS-RN.

• The thermodynamics and CM physics of AdS-RN has been analyzed in detail in the last few years, revealing rich physical phenomena

Chamblin+Emparan+Johnson+Myers (1999), Hartnoll+Herzog (2008), Bak+Rey (2009),Cubrovic+Schalm+Zaanen (2009), Faulkner+Liu+McGreevy+Vegh (2009)

1. Emergent AdS_2 scaling symmetry in the IR at finite density

2. Interesting fermionic correlators

and also

3. Is unstable (in N=4) to both neutral and charged scalar perturbations

Gubser+Pufu (2008), Hartnoll+Herzog+Horowitz (2008)

4. Has a non-zero (large) entropy at $T = 0$.

Einstein-Scalar-U(1) theory

• To go beyond RN, we must include the most important (relevant) scalar operator in the IR.

• The most general 2d action (after field redefinitions) is

$$S = \int d^{p+1}x\sqrt{g}\left[R - \frac{1}{2}(\partial\phi)^2 + V(\phi) - Z(\phi)F^2\right]$$

• It involves two arbitrary functions of ϕ.

Consider first the zero density case:

• There are two types of critical points.

♠ Standard (AdS) critical points: $V'(\phi_*) = 0$ for finite ϕ_*. This is a standard IR or UV fixed point at zero density (depending whether $V''(\phi_*)$ is positive or negative).

♠ "decompactication" asymptotics, $\phi_* \to \pm\infty$. These correspond to geometric "singularities" (sometimes decompactification) in string theory.

These also lead to scale invariant saddle points despite the fact that the extremal solutions have a nontrivial running for ϕ. To find the leading physics at extremality it is enough to parametrize

$$V(\phi) \sim e^{-\delta\phi} \quad , \quad Z(\phi) \sim e^{\gamma\phi} \quad , \quad \phi \to \pm\infty$$

• γ,δ capture the leading physics except if $|\delta| = \sqrt{\frac{2}{p-2}}$.

Finite Density scaling

The fate of zero density Quantum Critical asymptotics, at finite density is as follows:

♠ Standard (AdS) critical points: There is a new density dependent "effective potential" for ϕ

Goldstein+Iizuka+Kachru+Prakash+Trivedi+Westphal

$$V_{eff} = V(\phi) - \frac{q^2}{Z(\phi)}$$

and generically there is a new fixed point at ϕ_{**} at a special density q_*.

$$V'(\phi_{**}) = q_*^2 \frac{Z'(\phi_{**})}{Z^2(\phi_{**})} \quad , \quad V(\phi_{**}) = \frac{2q_*^2}{Z(\phi_{**})}$$

E.K.+Meyer

• If $Z'(\phi_*) = 0$ then $\phi_* = \phi_{**}$. This is the generalization of Reissner-AdS case with the usual IR AdS_2 geometry. In the near IR region, the AdS-RN bh is a solution.

• $Z'(\phi_*) \neq 0$. There is a new QC point at a special value of the density. The metric is $AdS_2 \times R^n$.

Scaling IR asymptotics

• In the IR-AdS region, the IR-extremal metrics are AdS_{p+1} at zero density and AdS_2 at finite density.

• In the case of runaway $\phi \to \pm\infty$ QC points, with $V \sim e^{-\delta\phi}$, $Z \sim e^{\gamma\phi}$, the extremal metrics are general scaling metrics of the form

$$ds^2 = \frac{dr^2}{r^2} + \frac{-dt^2 + dx^i dx^i}{r^{2a}}$$

at zero density and

$$ds^2 = \frac{dr^2}{r^2} - \frac{dt^2}{r^{2a}} + \frac{dx^i dx^i}{r^{2b}}$$

at finite density.

• Their near-extremal asymptotics (small temperatures) are also simply constructed.

• In several cases, the extremal metrics are solutions to the full equations. (as with exponential potentials)

The hidden scale invariance

Gouteraux+E.K.

- At zero density:

$$ds^2 = \frac{dr^2}{f} + \frac{(-f dt^2 + dx\cdot dx)}{r^{-\frac{4}{(p-1)\delta^2}}} \quad , \quad f = 1 - \left(\frac{r_0}{r}\right)^{\frac{2p}{(p-1)\delta^2}-1} \quad , \quad e^{\delta\phi} \sim r^2$$

Changing variables

$$w = r^{1-\frac{2}{(p-1)\delta}}$$

$$ds^2 = e^{2\chi(r)}\left[\frac{dw^2}{w^2 f(w)} + \frac{-f(w)dt^2 + dx\cdot dx}{w^2}\right] \quad , \quad e^{2\chi} \sim r^2 \sim e^{\delta\phi} \sim \frac{1}{V(\phi)}$$

- This is conformal to the AdS-Schwarzschild black hole.

- It is a scaling solution that violates hyperscaling.

- Such solutions can be obtained by dimensional reduction from a higher dimensional theory without a scalar.

• When $\delta^2 < \frac{2}{p-1}$ this is the dimensional reduction of an AdS_{p+1+n} solution on T^n with

$$\delta^2 = \sqrt{\frac{1}{1+\frac{p-1}{n}}} \cdot \frac{2}{p-1} \quad \leq \frac{2}{p-1}$$

Gubser+Nellore, Skenderis+Taylor

• This explains the continuous spectrum and absence of mass gap for $\delta^2 < \frac{2}{p-1}$.

• Therefore, the theory is quantum critical in the IR, despite the non-trivial potential.

• The singularity is resolved by the KK-modes (oxydation). The IR scale becomes the AdS scale in the higher dimensions.

• Different δ can be obtained by extending to real $n > 0$.

• The crossover value $\delta^2 = \frac{2}{p-1}$ is obtained when $n \to \infty$.

- Dimensional Reduction of AdS_{p+1+n} solution on S^n

Gouteraux+E.K.

$$\delta^2 = \frac{2}{p-1} + \frac{2}{n} \geq \frac{2}{p-1}$$

and a naturally discrete spectrum and mass gap.

- Violation of the Gubser bound: $n \leq 1$. Marginal case: $n \to \infty$.

- The theory is again quantum critical in the IR,

Scaling and hyperscaling at finite density

- The extremal solutions for all (γ, δ) are simple powers, and therefore scaling.
- The metric can always be written as

Gouteraux+E.K.

$$ds^2 = e^{\chi}\, d\hat{s}^2 \quad , \quad e^{\chi} \sim e^{\delta\phi} \quad , \quad d\hat{s}^2 = -\frac{dt^2}{w^{2z}} + \frac{dw^2 + dx^i dx^i}{w^2}$$

with

$$z = \frac{(\gamma-\delta)(\gamma+(2p-3)\delta)+2(p-1)}{(\gamma-\delta)(\gamma+(p-2)\delta)}$$

- They are conformal to Lifshitz or AdS solutions.

$$x^i \to \lambda x^i \quad , \quad w \to \lambda w \quad , \quad t \to \lambda^z\, t \quad , \quad ds^2 \to \lambda^{\theta}\, ds^2 \quad , \quad \theta = \frac{2(p-1)\delta}{\gamma+(p-2)\delta}\,.$$

- θ, the hyperscaling exponent, is set by the scaling of the inverse scalar potential, and controls the violation of hyperscaling.

• They can be also written in a different frame as

Huisje+Sachdev+Swingle

$$ds^2 = \frac{dr^2}{r^{4\frac{\theta-1}{\theta-2}}} - \frac{dt^2}{r^{2\frac{\theta-2z}{\theta-2}}} + \frac{dx^i dx^i}{r^2}$$

with scaling transformations

$$x^i \to \lambda\ x^i \quad , \quad r \to \lambda^{1-\frac{\theta}{2}}\ r \quad , \quad t \to \lambda^z\ t \quad , \quad ds^2 \to \lambda^\theta\ ds^2$$

• Most of these can be lifted to solutions in higher dimensions with generalized scaling symmetry (Boosted AdS black-holes or black AdS q-branes).

• They represent the most general critical behavior at zero temperature, generalizing the AdS and Lifshitz geometries.

• Note that at $\gamma + (p-2)\delta = 0$ we obtain an $AdS_2 \times R^2$ geometry at extremality but with $S = 0$.

• Like the zero density case, they are dimensional reductions of regular or Lifshitz higher-dimensional solutions.

- The higher-dimensional theories are of the following types:

$$S = \int d^{p+q+1}x\sqrt{G}\,[R + 2\Lambda]\,.$$

reduced along a torus with a boost.

$$S = \frac{1}{16\pi G_D}\int \mathrm{d}^{p+q+1}x\,\sqrt{-g}\left[R - \frac{1}{2(n+2)!}G^2_{[n+2]}\right].$$

reduced on a sphere.

$$S = \frac{1}{16\pi G_D}\int \mathrm{d}^{p+q+1}x\,\sqrt{-g}\left[R - \frac{1}{2(q+2)!}G^2_{[q+2]} + 2\Lambda\right],$$

reduced on a torus.

- The spectra (continuous vs discreet) follow from the curvature of the internal space.

- The thermodynamic variables have the natural scaling of the higher-dimensional theory.

The higher-dimensional picture:

1. Explains the near T=0 scaling behavior.

2. Explains the qualitative difference between EHTs with $C_p < 0$ and $C_p > 0$. In the neutral case it explains the crossover value, δ_c.

3. Provides and alternative view of the Gubser bound.

4. Provides one possible resolution of the zero temperature naked singularity of the original solution.

5. Gives a direct and efficient way to compute the scaling transport coefficients by dimensionally reducing scale invariant hydrodynamics.

Gouteraux+(Smolic)^2+Skenderis+Taylor

(Lifshitz) Scaling in the broken-symmetry phase

• The minimal description of the broken symmetry phase contains the metric, a gauge field and a complex scalar ($D_\mu \Psi = \partial_\mu \Psi + iqA_\mu \Psi$)

$$S = M^2 \int d^4x \sqrt{-g} \left[R - \frac{G(|\Psi|)}{2} |D\Psi|^2 + \tilde{V}(|\Psi|) - \frac{\tilde{Z}(|\Psi|)}{4} F_{\mu\nu} F^{\mu\nu} \right]$$

• In the broken phase, Ψ is non-trivial, $\Psi = \chi \, e^{i\theta}$. Choose the gauge $\theta = 0$ and change variables $\chi \to \phi$ so that the kinetic term of ϕ is properly normalized

$$S = M^2 \int d^4x \sqrt{-g} \left[R - \frac{1}{2} (\partial\phi)^2 + V(\phi) - \frac{Z(\phi)}{4} F_{\mu\nu} F^{\mu\nu} - \frac{W(\phi)}{2} A_\mu A^\mu \right]$$

• Again the interesting IR behavior appears if V,W,Z have extrema, or decompactification (exponential) behavior.

• It can be shown, that both at finite ϕ, or runaway ϕ with exponential IR asymptotics for V, Z, W, we obtain generalized Lifshitz scaling in the IR geometry.

• The Lifshitz exponent z depends non-trivially on the IR asymptotics of the EHT.

Gouteraux+E.K

Constant scalar

- $\phi = \phi_*$ is constant and

$$ds^2 = B_0 \frac{dr^2}{r^2} + \frac{dx^2 + dy^2}{r^2} - \frac{dt^2}{r^{2z}} \quad , \quad A_t = Q\ r^{-z}$$

$$Q^2 = \frac{2(z-1)}{zZ(\phi_*)} \quad , \quad B_0 = 2z \frac{Z(\phi_*)}{W(\phi_*)}$$

with the Lifshitz exponent z satisfying

$$z^2 + \left(1 - \frac{2V(\phi_*)Z(\phi_*)}{W(\phi_*)}\right) z + 4 = 0$$

and

$$\frac{V_*'}{V_*} + \frac{2(z-1)}{z^2+z+4}\frac{W_*'}{W_*} + \frac{z(z-1)}{z^2+z+4}\frac{Z_*'}{Z_*} = 0$$

- This has non-trivial real solutions unless

$$-\frac{3}{2} \leq \frac{V(\phi_*)Z(\phi_*)}{W(\phi_*)} \leq \frac{5}{2}$$

- When $\frac{V(\phi_*)Z(\phi_*)}{W(\phi_*)} = 3$ we obtain $z = 1$ namely AdS.

Running scalar

- A decompactification case

$$V(\phi) = V_0 e^{-\delta\phi} \quad , \quad Z(\phi) = Z_0\, e^{\gamma\phi} \quad , \quad W(\phi) = W_0 e^{(\gamma-\delta)\phi}$$

- We also obtain a Lifshitz geometry in the IR with

$$z = \frac{\epsilon(\epsilon-2\gamma)x + 2(\epsilon^2-\epsilon\gamma-2)}{(\epsilon^2+2\gamma^2-4\epsilon\gamma-2)x + 2\epsilon(\epsilon-\gamma)}$$

with

$$(4-\epsilon^2+4\epsilon\gamma)x^2+\left(2-2\epsilon^2+2\gamma^2+(-4+\epsilon^2-4\epsilon\gamma)\frac{V_0 Z_0}{W_0}\right)x+\left(4+2\epsilon^2\frac{V_0 Z_0}{W_0}\right)=0$$

- In the rest of the cases we obtain, Lifshitz geometries or generalized Lifhitz geometries (with hyperscaling violation).

Extremal geometries

- The analysis above seems to suggest that in all systems studied so far, the $T \to 0$ asymptotics involve non-trivial scale invariant holographic theories.

- This conclusion remains the same when charge densities are present.

- The scaling geometries are generalized AdS or Lifshitz geometries with hyperscaling violations.

- Point Charges generate AdS_2, string charges AdS_3 etc.

- This is valid both in broken (superfluid) and unbroken phases.

- How general is this???

The holographic effective potential

Niarchos+E.K

• In QFT a very useful tool is the quantum effective potential: it is the Legendre transform of the source action, and is a function of the expectation values of fields.

It is a valuable tool in the investigation of dynamical symmetry breaking and the study of phase transitions.

• The analogous concept in holography is in principle computable, but has not been used so far (but for a few exceptions).

• I will outline the formalism in a model class of theories: EMD

$$S = M_P^{p-1} \int d^{p+1}x\sqrt{g}\left[R - \frac{1}{2}(\partial\phi)^2 + V(\phi) - Z(\phi)F^2\right] + \text{boundary terms}$$

$$ds^2 = e^{2A(u)}\left(-f(u)dt^2 + dx^i dx^i\right) + \frac{du^2}{f(u)}\ , \quad \mathbf{A} = A_t(u)dt\ , \quad \phi = \phi(u)$$

• We will

(a) Find the classical solution with temperature T, charge density ρ, and scalar source $\phi = \phi_0 = constant$ in (t, x^i).

(b) Evaluate the on-shell action, $S_{on-shell}(\phi_0)$.

(c) Legendre transform in ϕ_0 to obtain the effective potential $V_{eff}(\phi_c; T, \rho, M)$ as a function of the classical field $\phi_c = \frac{\partial S_{on-shell}(\phi_0)}{\partial \phi_0}$ and the RG scale $M = e^{A_0}$, at which all field variables are defined.

• The key step here is to introduce the "superpotential" $W(\phi)$ that will be related both to the effective potential and the holographic β-function.

Gursoy+E.K.+Nitti

$$\frac{d\phi}{du} = \frac{dW(\phi)}{d\phi} \quad , \quad \frac{dA}{du} = -\frac{W(\phi)}{2(p-1)} \quad \Rightarrow$$

$$\Rightarrow \quad \frac{d\phi}{dA} = \frac{d\phi}{d\log M} = -2(p-1)\ \partial_\phi \log W = \beta(\phi)$$

• Note that the ϕ equation is solvabe with a single initial condition: $\phi(A_0) \equiv \phi_0$. The vev is hidden in the determination of W.

• The equations of motion for the unknown functions: $W(\phi), A(\phi), f(\phi)$ become

$$\frac{\mathcal{R}'}{\mathcal{R}} = \frac{W}{W'}\ , \quad \mathcal{R} \equiv e^{-2(p-1)A} \tag{1a}$$

$$W'(W'f')' - \frac{pWW'}{2(p-1)}f' = \frac{\rho^2\mathcal{R}}{Z} \tag{1b}$$

$$\left(\frac{pW^2}{2(p-1)} - W'^2\right) f - WW'f' = 2V - \frac{\rho^2\mathcal{R}}{Z} \tag{1c}$$

The second order equation can be integrated to a first order one:

$$f' = \frac{e^{-dA}}{W'}\left[D + \rho^2 \int_{\phi_0}^{\phi} \frac{d\chi}{e^{(d-2)A(\chi)}Z(\chi)W'(\chi)}\right]$$

$$D = -4\pi e^{(d-1)A_0}\, T\ S - \rho^2 \int_{\phi_0}^{\phi_h} \frac{d\tilde{\phi}}{e^{(d-2)A} Z W'}$$

• The three constants of integration amount to $T, \langle\phi\rangle$ and the RG scale $M = e^{A_0}$.

• $\langle\phi\rangle$ is tuned to the value that makes the bulk solution "regular".

• We now calculate the Free Energy (on-shell action):

$$\mathcal{F} = S_{on-shell} = M_P^{p-1}\beta V_{p-1}\ e^{pA_0}\ \left(-W + \dot{f}\right)_{u=u_0}$$

and from the equations we obtain $Z(\phi_0, T, \rho, A_0)$.

$$Z = \frac{\mathcal{F}}{M_P^{p-1}\beta V_{p-1}} = -e^{pA_0}W(\phi_0) - 4\pi e^{(p-1)A_0}\ T\ S + \rho^2 \int_{\phi_h}^{\phi_0} \frac{d\tilde{\phi}}{e^{(p-2)A} Z W'}$$

• Z is the single-trace effective action for the source ϕ_0. The full effective action contains possible multitrace deformations:

$$Z_{total} = Z + Z_{\text{multi-trace}} \quad , \quad Z_{\text{multi-trace}} = \sum_{n=2}^{\infty} \frac{g_n}{N^{n-2}}\ \phi_0^n$$

• The Legendre transform of Z with respect to ϕ_0 is the effective potential, $V_{eff}(\phi_c;\ T, \rho, A_0)$.

- The effective potential, is evaluated at an RG scale $M = e^{A_0}$.

- ϕ_c depends implicitly on A_0 as determined by the bulk flow equations.

- RG invariance $(T = \rho = 0)$:

$$\boxed{\frac{d}{dA_0} Z = 0}$$

- In the scaling region around an IR or UV fixed point, V_{eff} can be obtained by a perturbative calculation. It is in general non-polynomial in ϕ_c and provides a generalization of the LG ansatz.
- From scaling:

$$\phi_r \equiv e^{-(p-\Delta)A_0}\phi_0 \quad , \quad \hat{T} \equiv e^{-A_0}T \quad , \quad \hat{\rho} \equiv e^{(2-p)A_0}\rho$$

$$Z = \phi_r^{\frac{p}{p-\Delta}}\, \zeta(\phi_r^{\frac{1}{p-\Delta}}, \hat{T}, \hat{\rho}) \quad , \quad \lim_{A_0 \to \infty} \zeta = \text{constant}$$

- Transition temperatures can be calculated directly via perturbation theory if they occur in the scaling region.

The effective action

- We can go beyond the effective potential, to the first terms in the effective action

$$S_{source} = \int d^4x\sqrt{g}\left[U(\phi)R - \frac{1}{2}Z(\phi)(\partial\phi)^2 + V(\phi) + \cdots\right]$$

- V was calculated already

- U can be calculated by turning on constant spacial curvature

$$U(\phi_0) = -\int_{\infty}^{\phi_0} \frac{d\phi}{W'} e^{-\frac{1}{4}\int_{\phi_0}^{\phi}\frac{W}{W'}d\phi}$$

at zero temperature and density.

- Calculating $Z(\phi)$ is more complicated.

- Such effective actions are very useful both in condensed matter (generalizations of the LG framework) and cosmology (inflaton as a strongly coupled bound state)

EHT with two scalar fields

• This is the next case that provides a new dimension in the possible phenomena that may happen.

$$S = \int d^{p+1}x\sqrt{g}\left[R - \frac{1}{2}G\ \partial\phi\partial\bar{\phi} + V(\phi,\bar{\phi})\right] \quad , \quad G = \partial_\phi\partial_{\bar{\phi}}K(\phi,\bar{\phi})$$

• The presence and mixing of the two scalar operators opens the possibility that the new phenomena can appear dynamically.

• With a single scalar, to obtain such phenomena we must change parameters of the bulk Lagrangian (like masses or charges).

• Now these changes can happen during RG flows.

• A new element appears here: the (Zamolodchikov) metric in field space, controlled by the (pseudo) Kahler potential K.

A startup example: V-QCD

Jarvinnen+E.K.

• The theory contains a metric and two scalars, a real one, λ and a complex one T. There is also a U(1) symmetry under which T is charged.

$$S = S_{glue} + S_{flavour} \quad , \quad S_{glue} = \int d^5x\sqrt{g}\left[R - \frac{1}{2}\frac{(\partial\lambda)^2}{\lambda^2} + V_g(\lambda)\right]$$

$$S_{flavour} = -x\int d^5x\ V_f(\lambda,T)\sqrt{-\det(g_{ab} + h(\lambda)\partial_a T\partial_b T)}$$

Fixed points of the potential:

UV: $(\lambda = 0, T = 0)$, $\Delta_\lambda = 4, \Delta_T = 3$, unbroken U(1) symmetry.

IR: $(\lambda = \lambda_*, T = 0)$ (non-trivial CFT), unbroken U(1) symmetry or

$(\lambda = \infty, T = \infty)$, broken U(1) symmetry and a different (free) CFT of the Goldstone boson.

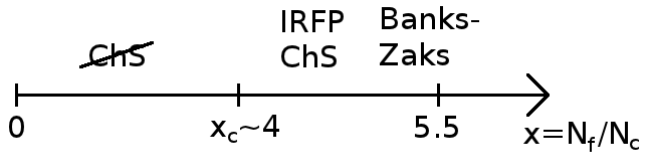

Condensate dimension at the IR fixed point

• By expanding the DBI action we obtain the IR tachyon mass at the IR fixed point $\lambda = \lambda_*$ which gives the chiral condensate dimension:

$$-m_{\rm IR}^2 \ell_{\rm IR}^2 = \Delta_{\rm IR}(4 - \Delta_{\rm IR})$$

• Must reach the Breitenlohner-Freedman (BF) bound (horizontal line) at some x_c.

• x_c marks the *conformal phase transition*

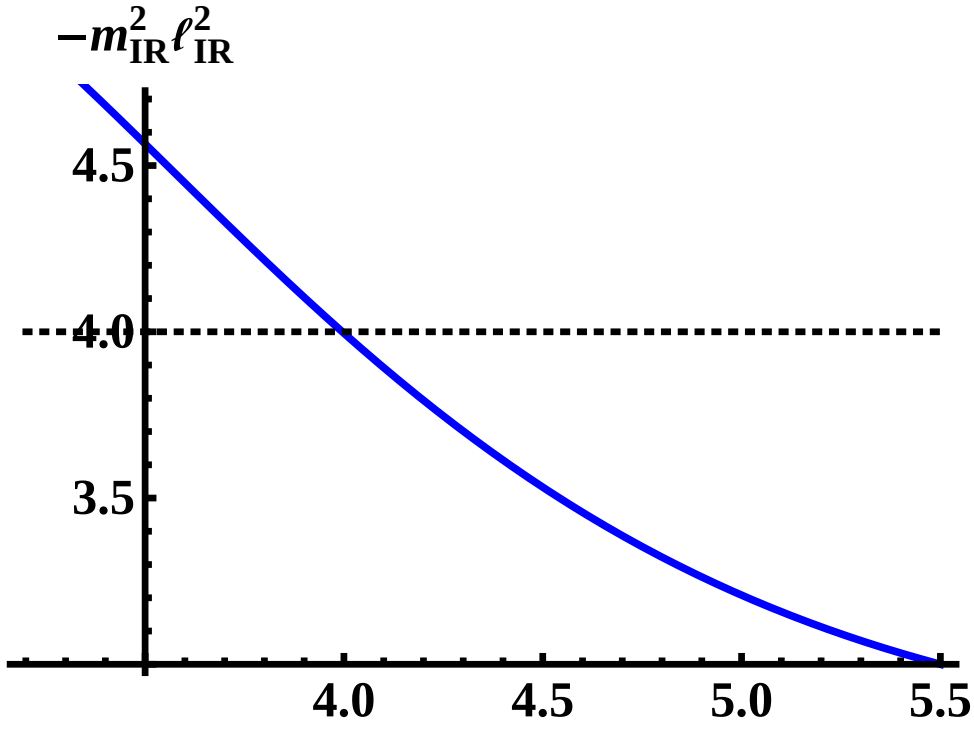

The symmetry breaking regime

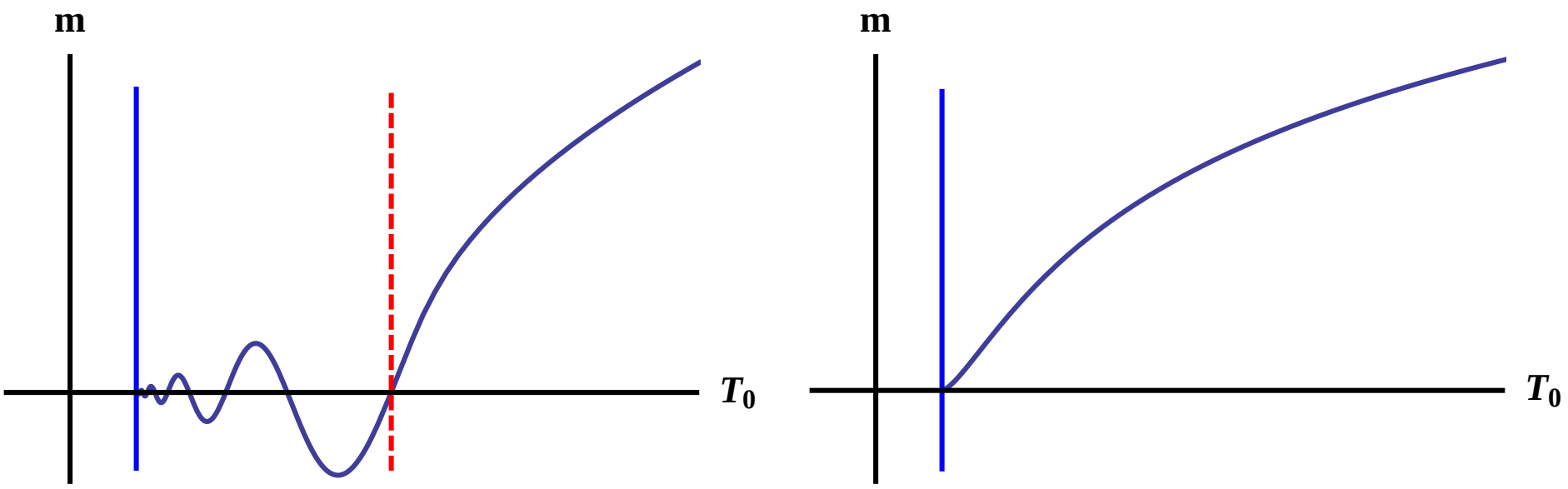

- In the symmetry breaking region there is an infinite number of saddle points.

- Their Free energies are ordered

$$F_0 < F_1 < F_2 < \cdots < \quad F \quad _{T=0}$$

BKT scaling

• In the symmetry region we have BKT scaling for all symmetry breaking scales

$$\sigma \sim \frac{1}{r_{\rm UV}^3} \exp\left(-\frac{2K}{\sqrt{x_c - x}}\right) \ .$$

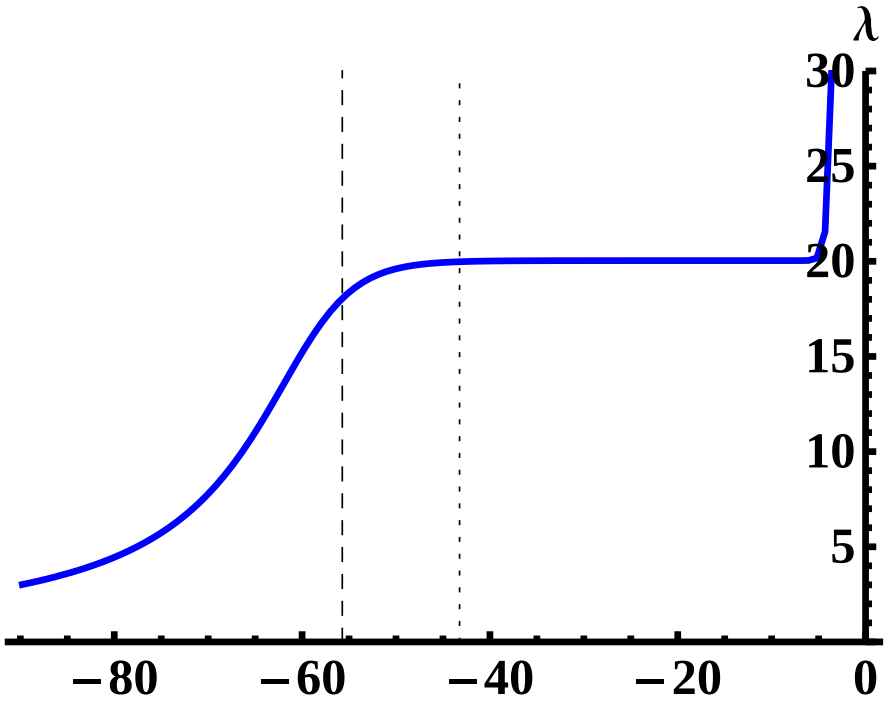

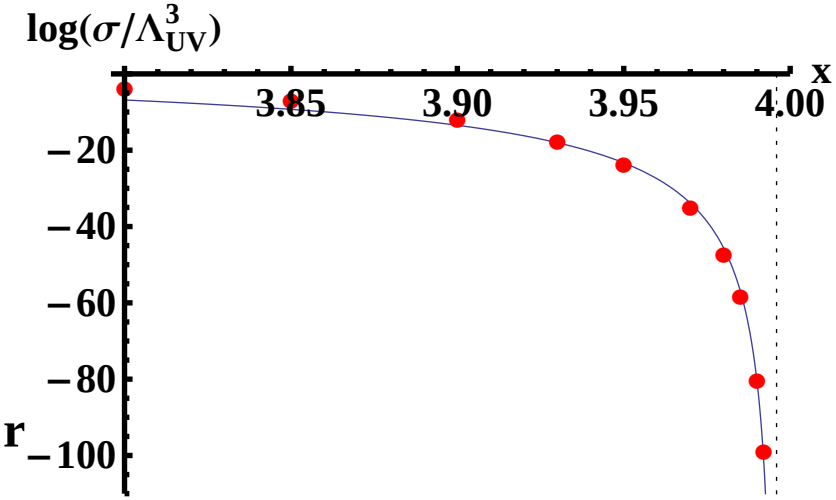

Efimov spiral

Ongoing work: $\sigma(m)$ dependence

❑ For $x < x_c$ spiral structure

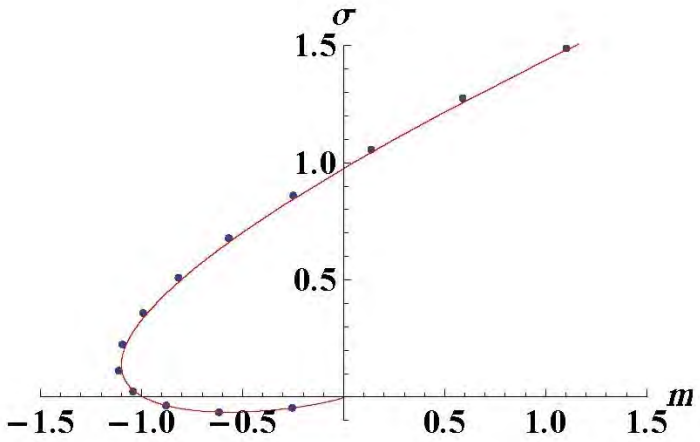

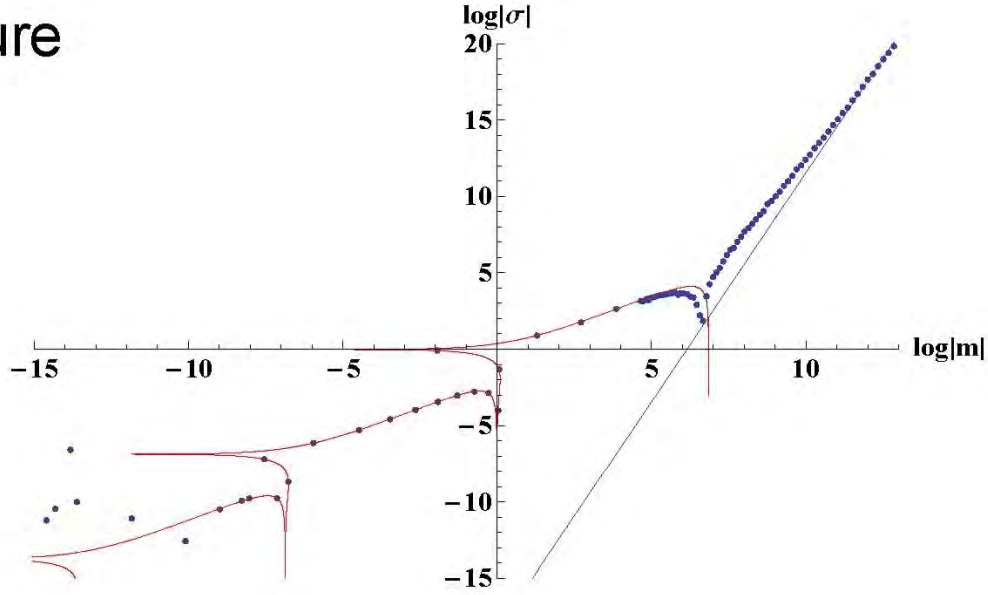

• This suggests that the presence of double trace deformations can alter the ground state of the system and make the second Effimov vacuum be the ground state.

Finite temperature

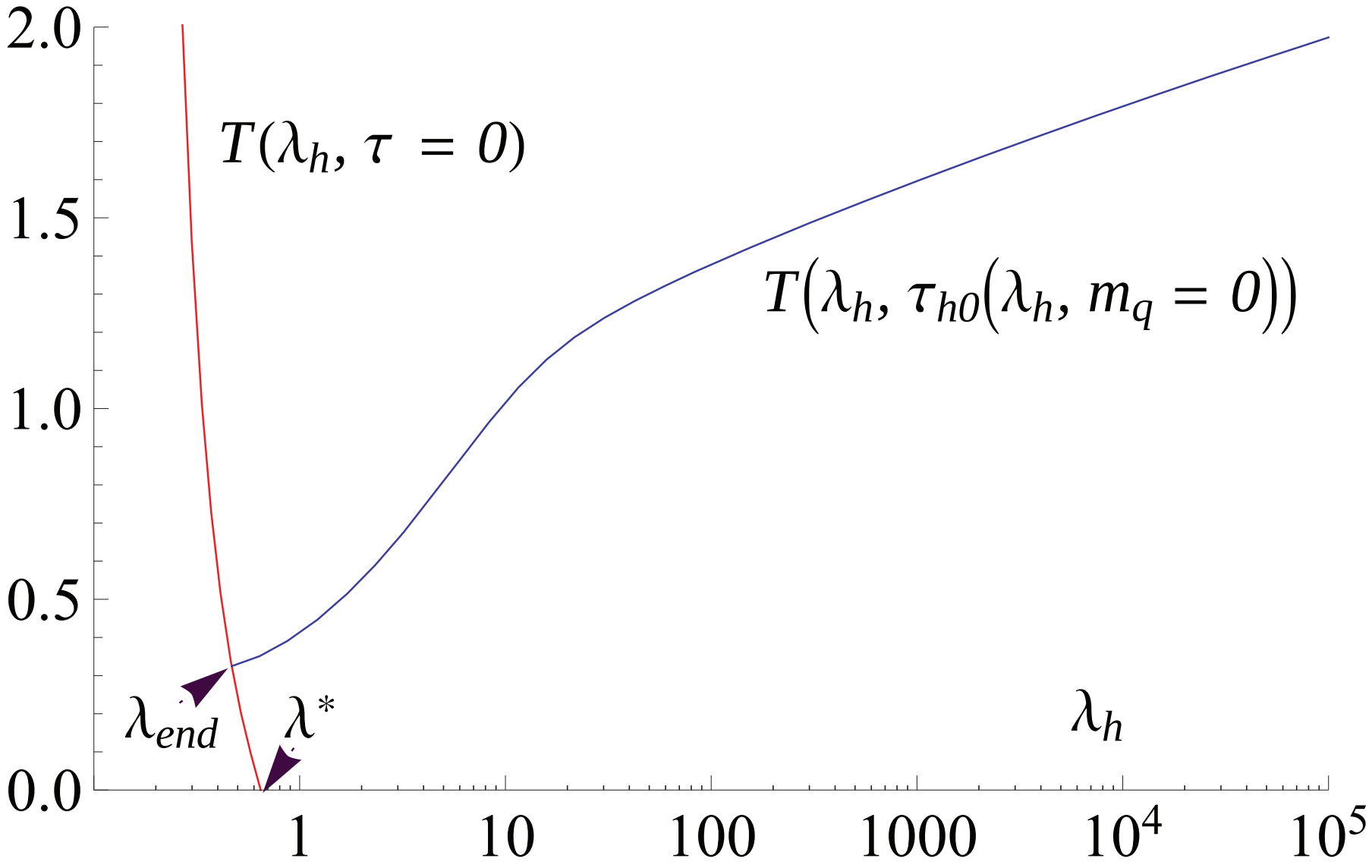

The temperature as a function of λ_h for solutions for Pot II at $x_f = 3\,W_0 = 12/11$, for zero mass

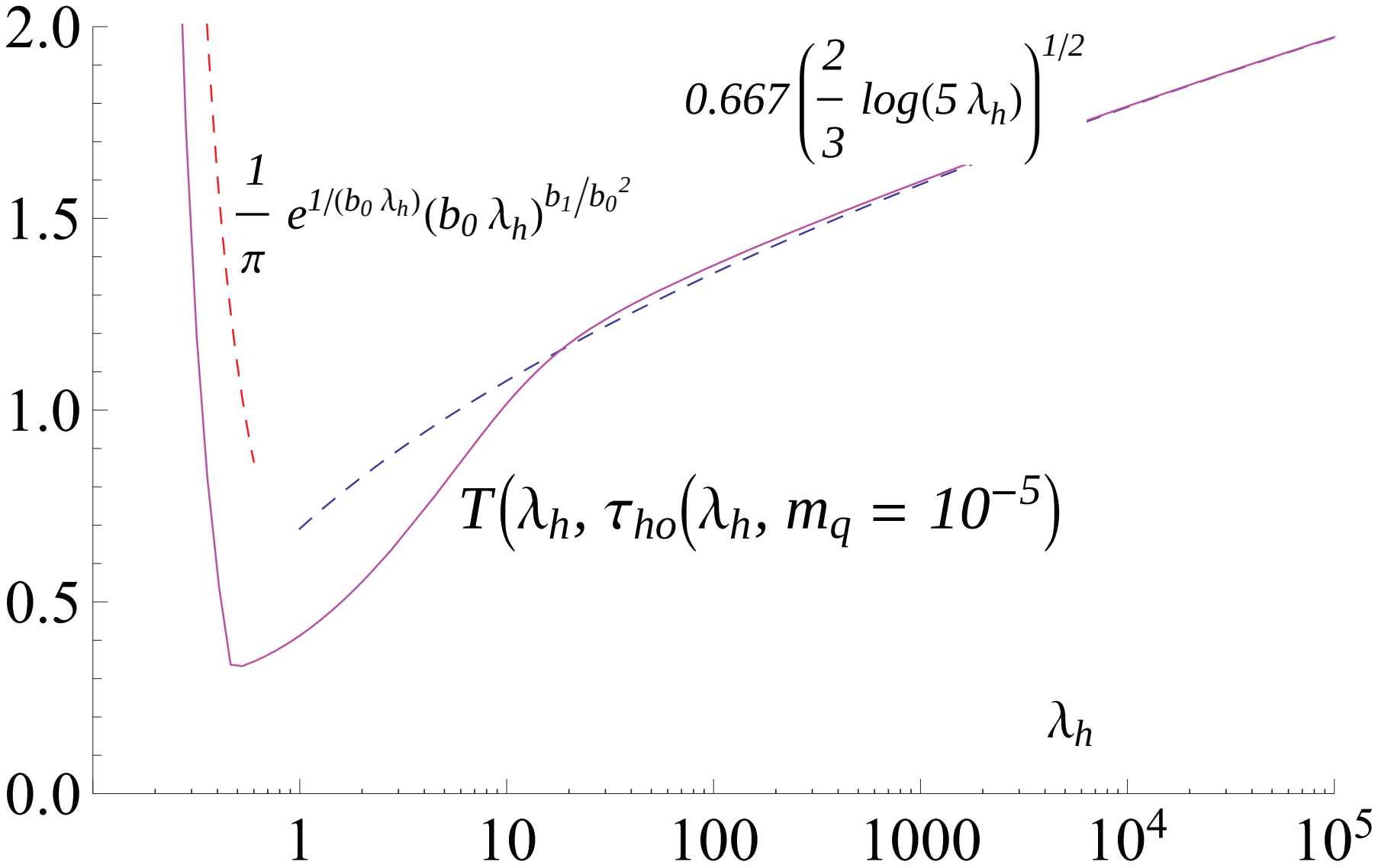

The temperature as a function of λ_h for solutions for Pot II at $x_f = 3\,W_0 = 12/11$, and very small mass . The asymptotic limits are also shown for $m_q = 10^{-5}$, in the range of the figure the UV limit is not yet accurate.

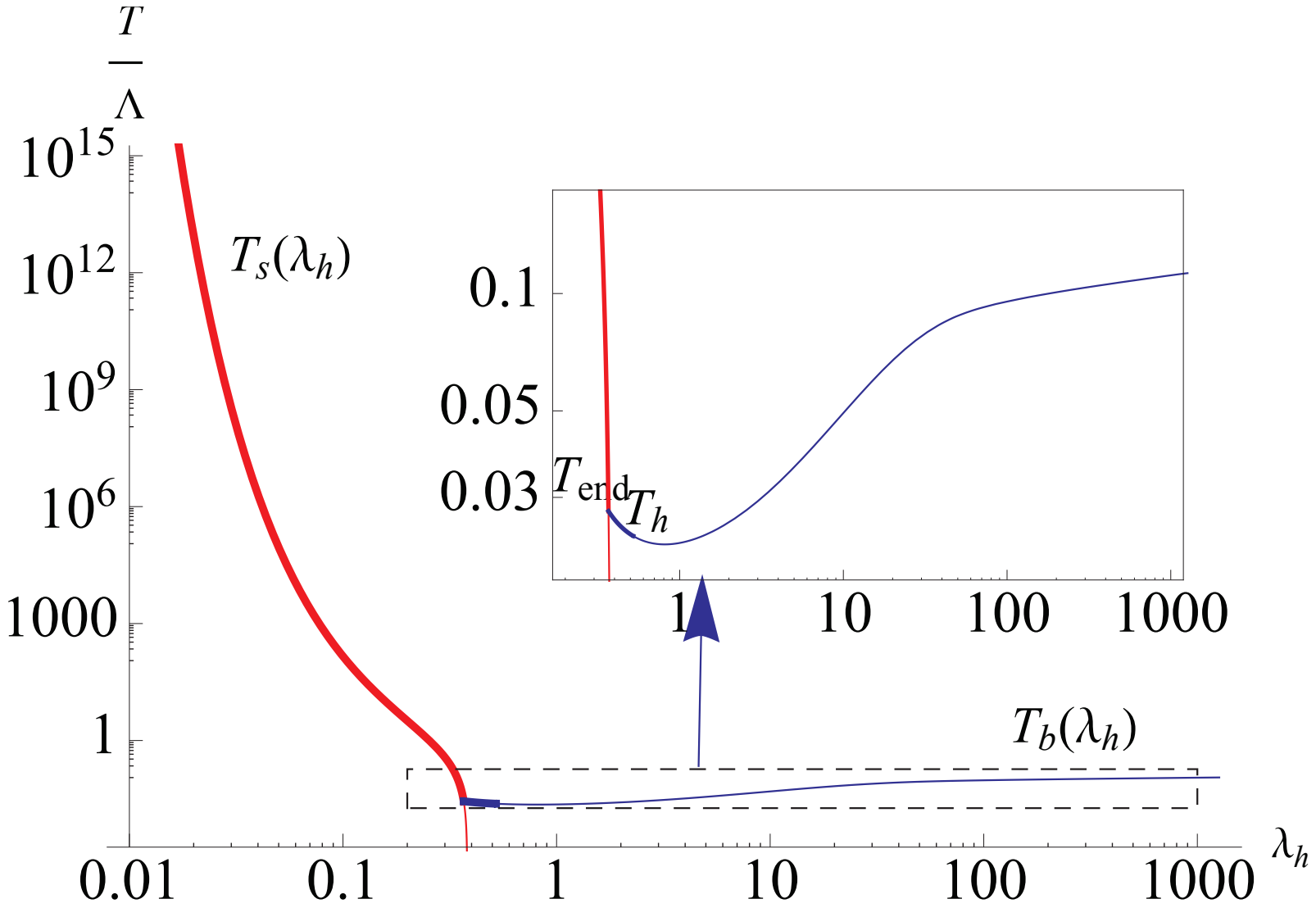

Examples of the $T_{\rm end}$, T_h and $T_{\rm crossover}$ transitions in potential II with Stefan-Boltzmann -normalization of $\mathcal{L}_{\rm UV}$ and with $x_f = 3$. Here: The temperature $T(\lambda_h)$. The curving of $T_s(\lambda_h)$ at $\lambda_h \sim 0.2$, $T \sim 2$ is related to the crossover transition. The inset shows the minimum of $T_b(\lambda_h)$, which causes p_b to be positive between T_h and $T_{\rm end}$.

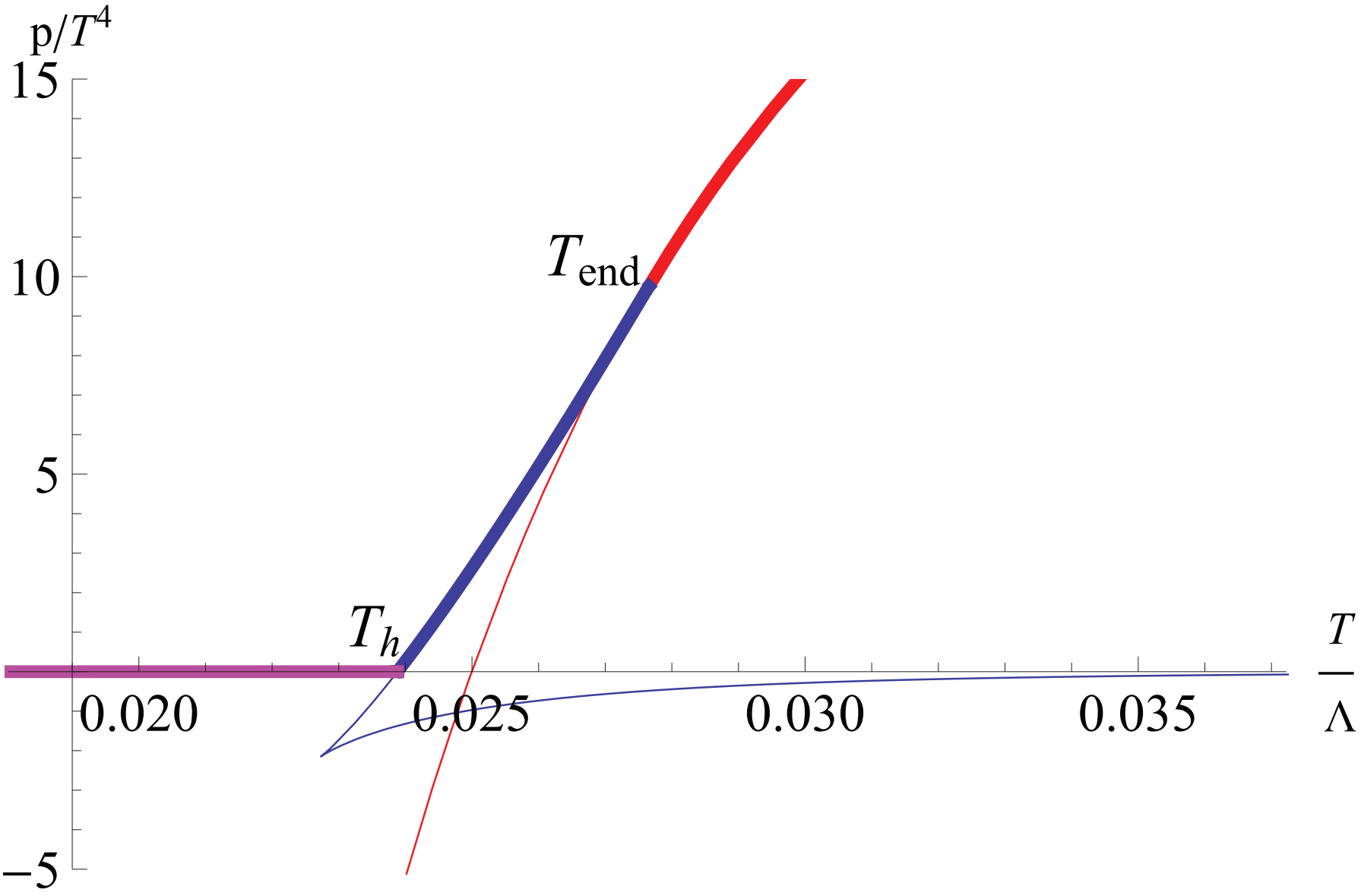

p/T^4 in a close-up around the region of the T_h and T_{end} -transitions.

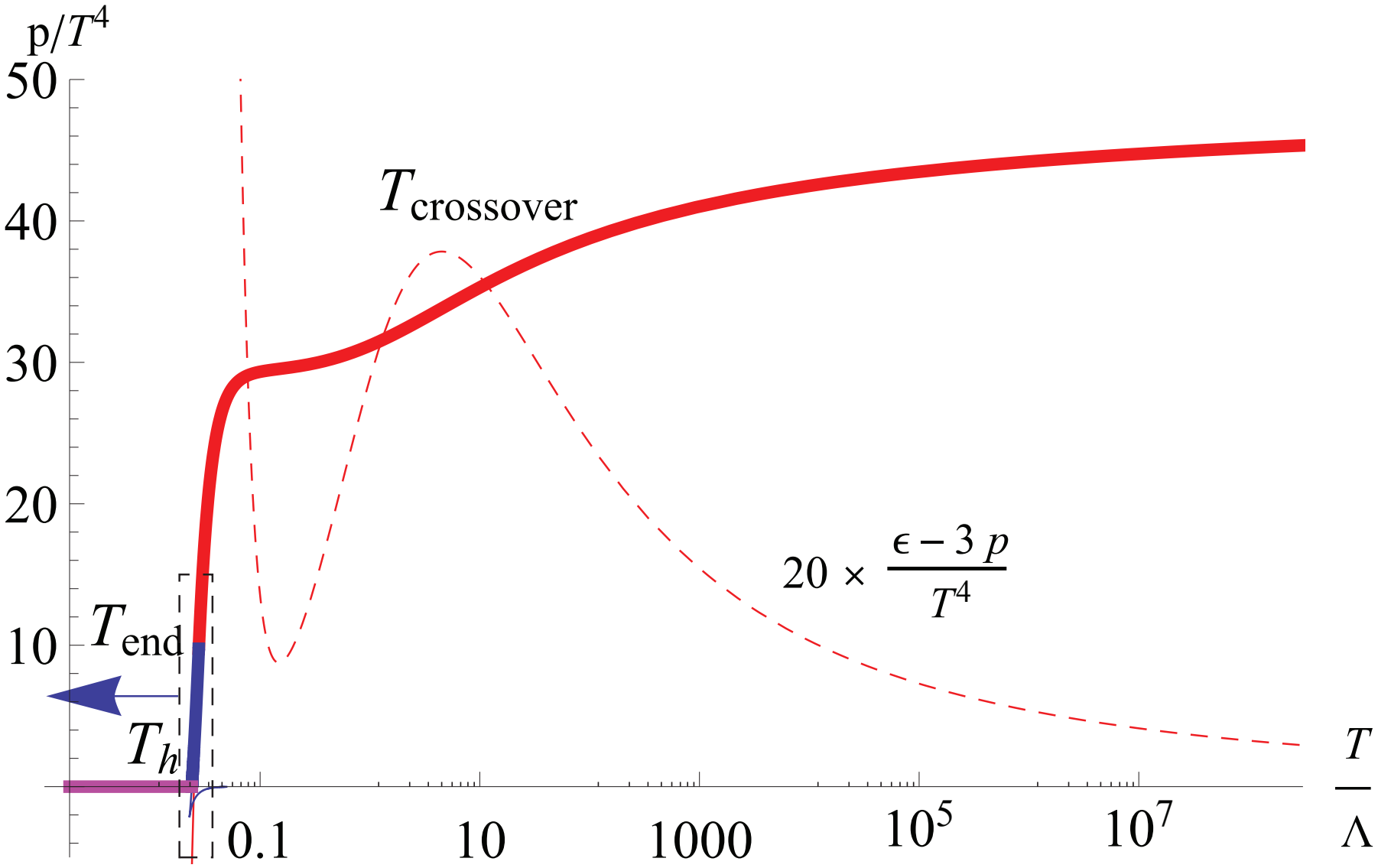

An overview of the pressure in the same case, also showing the interaction measure, which's peak determines the position of $T_{\text{crossover}}$.

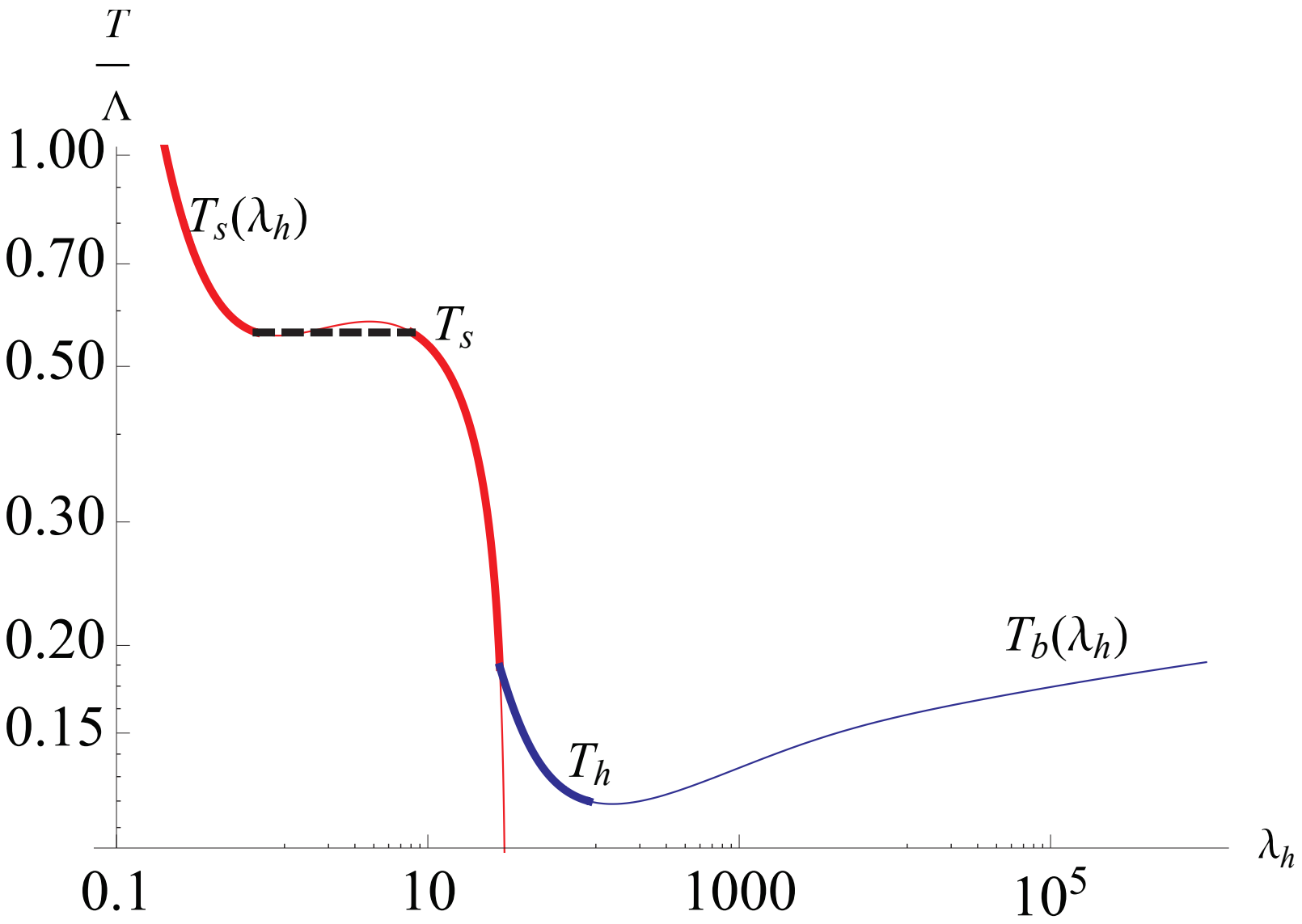

An example of the T_S transition in potential I with $W_0 = 24/11$ and with $x_f = 3$. The local maximum and minimum which generate the first order T_S -transition.

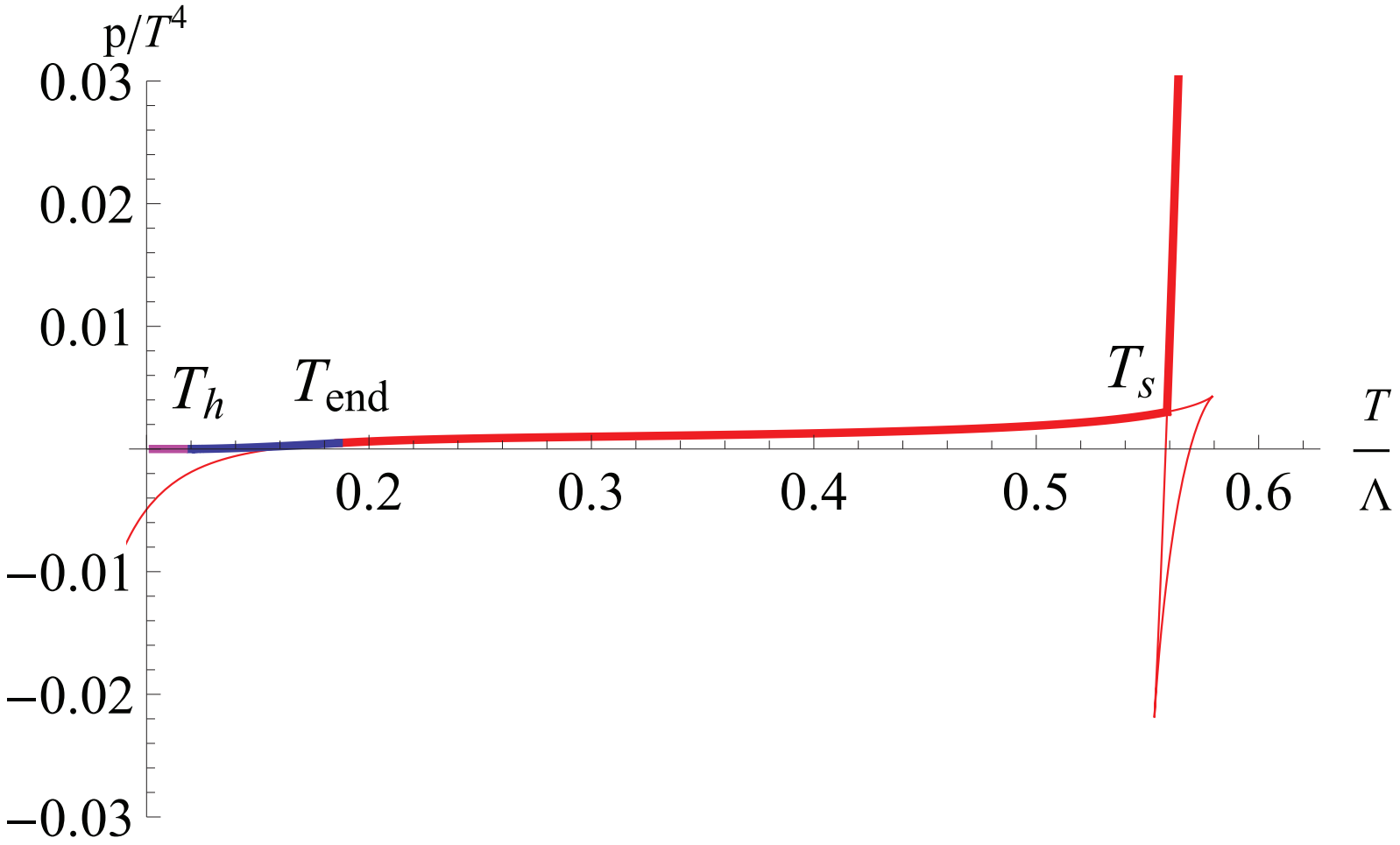

An example of the T_{S} transition in potential I with $W_0 = 24/11$ and with $x_f = 3$. $p(T)/T^4$ in the region around which the first order T_{S} transition takes place, extending to smaller T in order to show the relation to the T_h and T_{end} transitions.

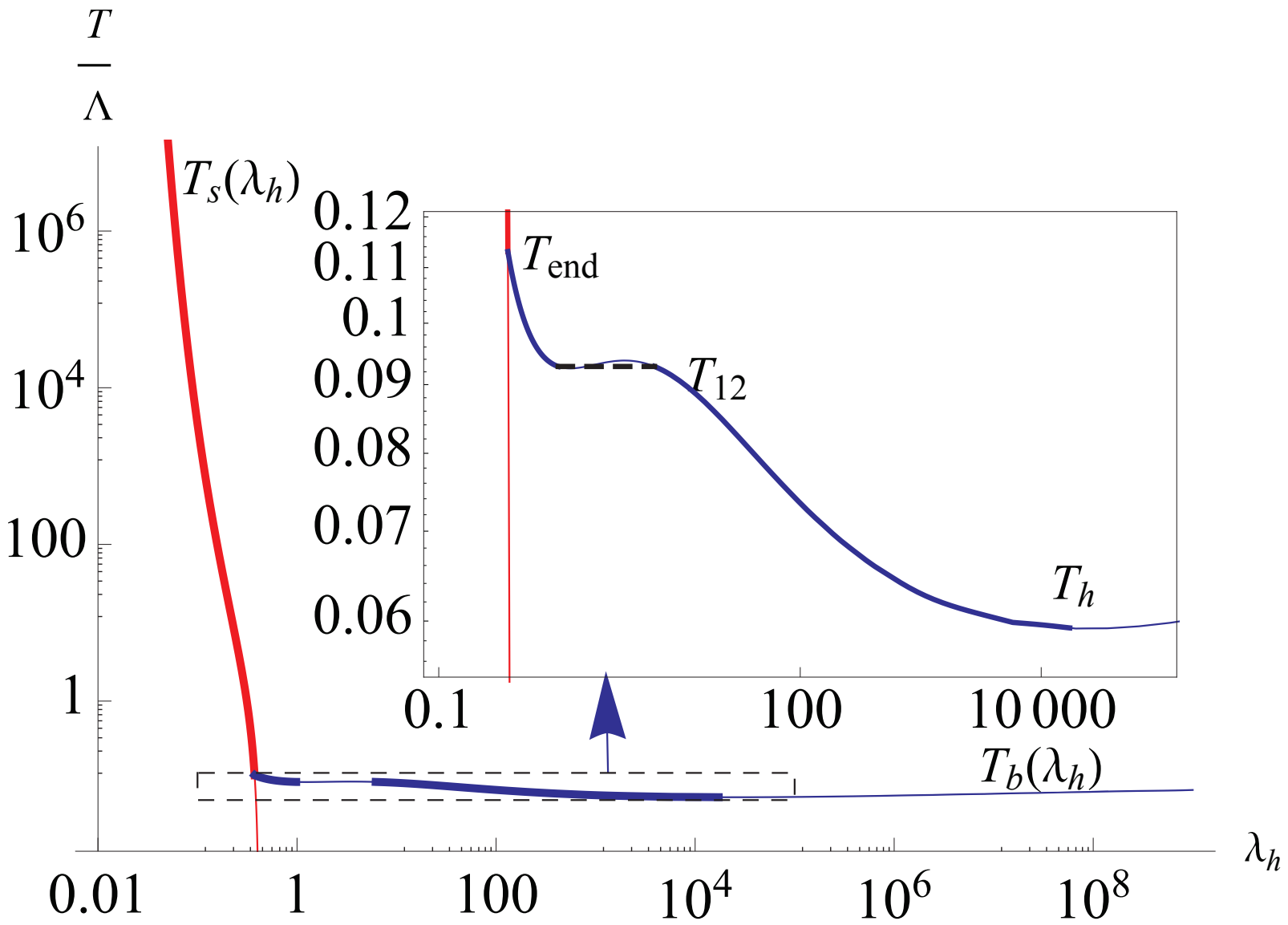

An example of the T_{12} transition in potential I with $W_0 = 12/11$ and with $x_f = 3.5$. The overall structure of $T(\lambda_h)$, with an inset showing the maximum and minimum in more detail.

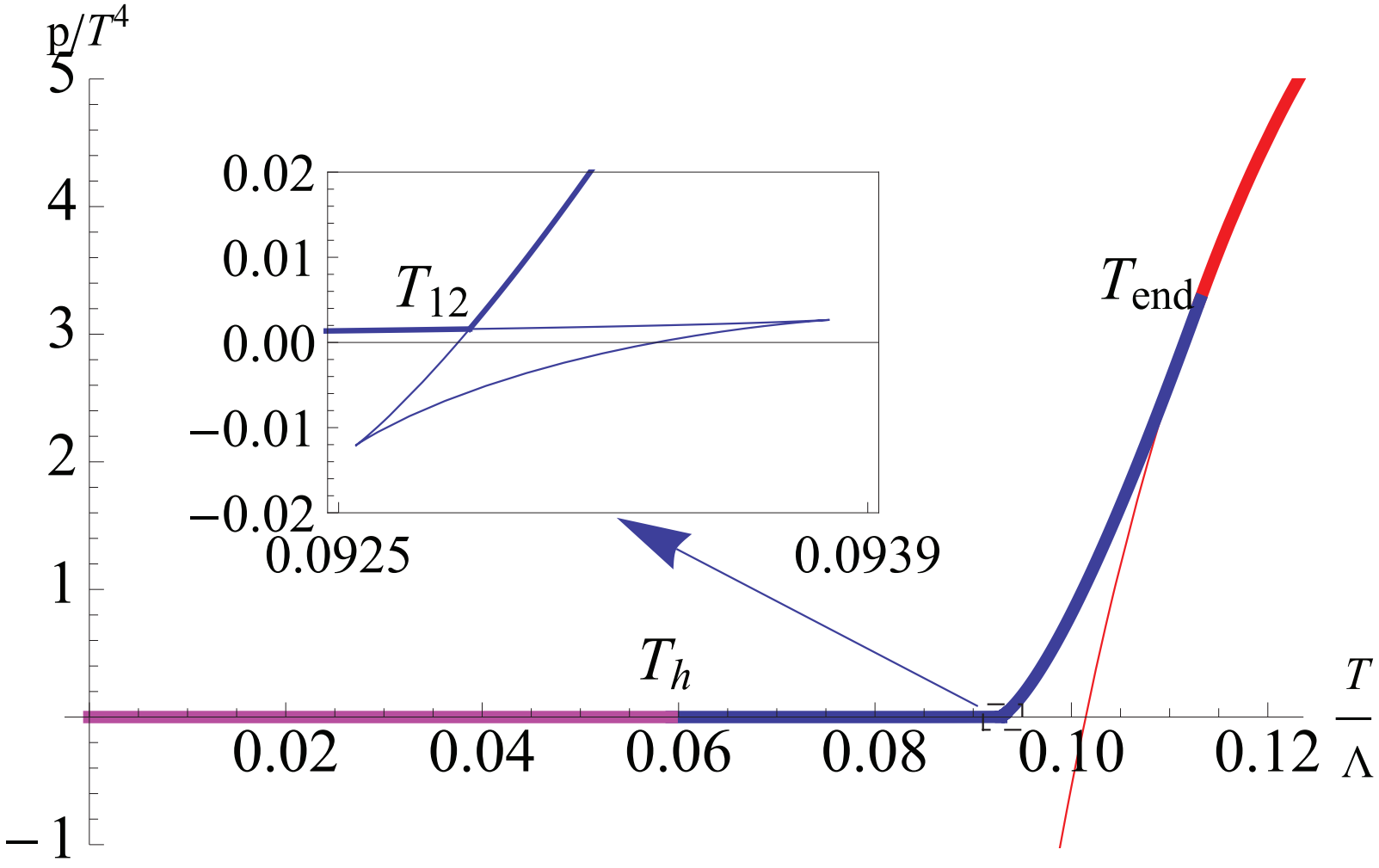

An example of the T_{12} transition in potential I with $W_0 = 12/11$ and with $x_f = 3.5$. A close-up of $p(T)/T^4$ in the region where the T_{12} -transition happens, with an inset showing further detail.

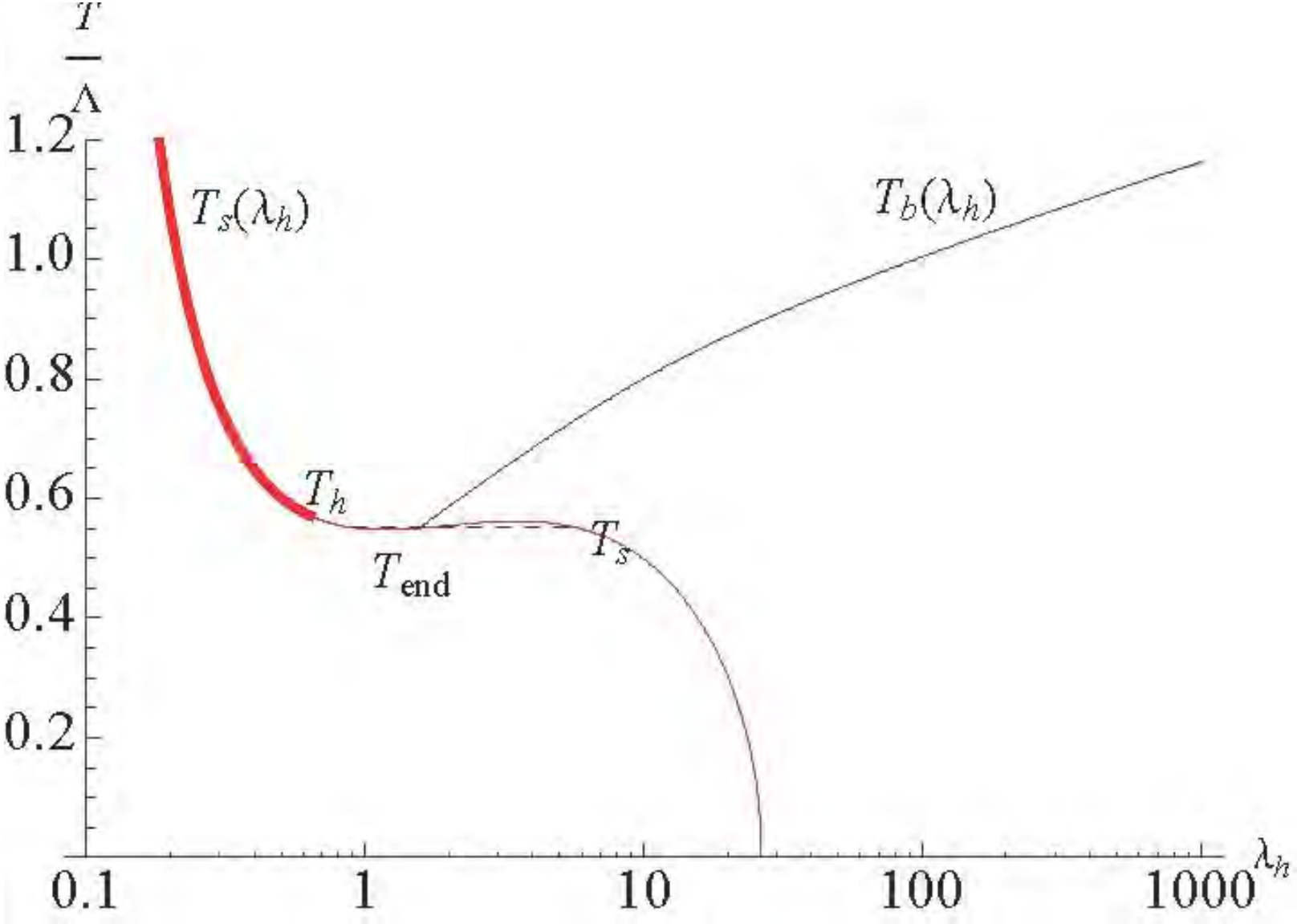

An example of a configuration where all but the crossover and hadronisation transitions $T_{\text{crossover}}$, T_h, are in the thermodynamically unstable region, in the initial stages of the approach to the IHQCD limit. The potential is II with $W_0 = 12/11$ and with $x_f = 0.4$ *Left*:The temperature $T(\lambda_h)$. Note that everything to the right of the T_h transition is in the unstable phase.

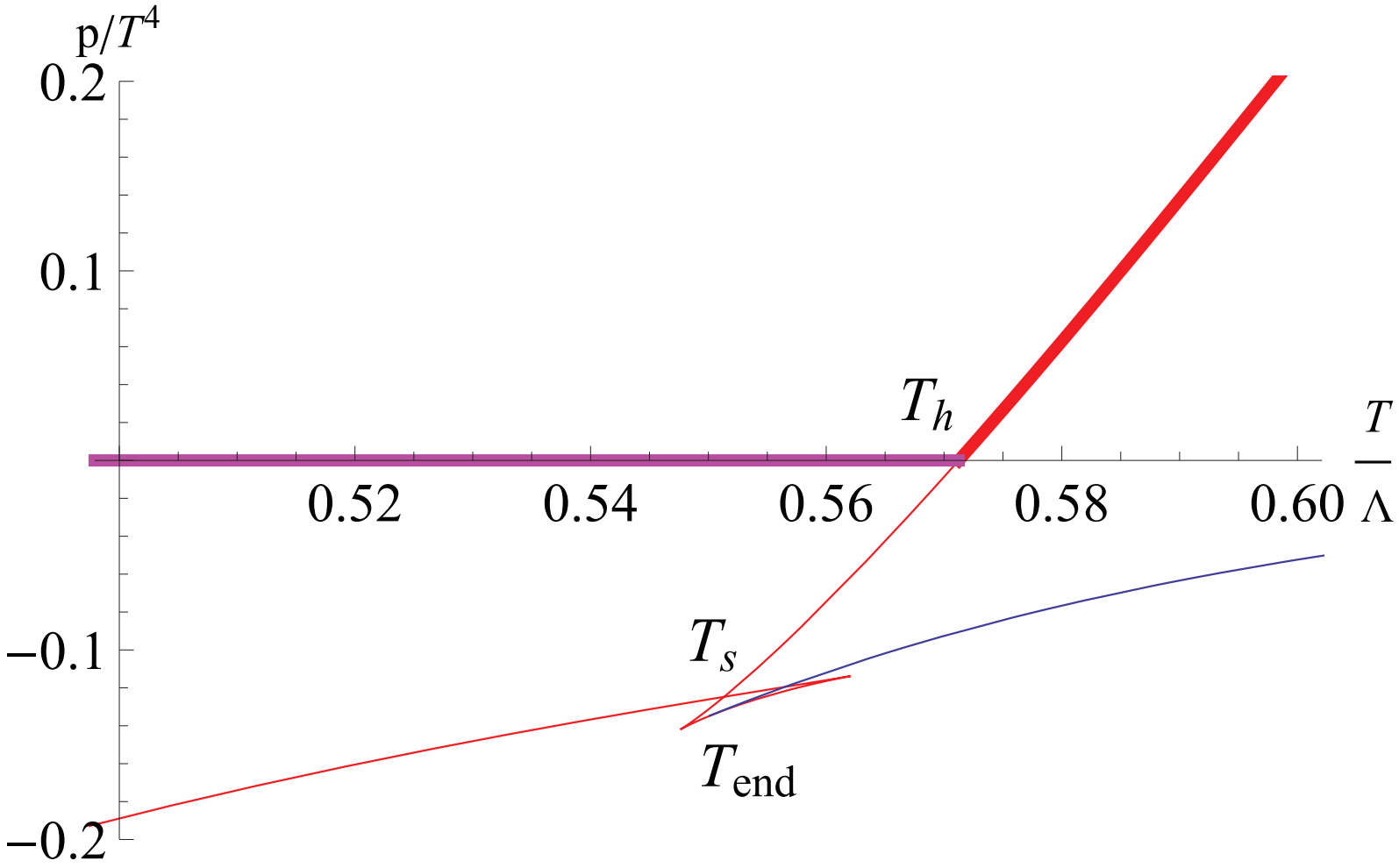

An example of a configuration where all but the crossover and hadronisation transitions $T_{\text{crossover}}$, T_h, are in the thermodynamically unstable region, in the initial stages of the approach to the IHQCD limit. $p(T)/T^4$ in the region where the T_h transition and the unstable T_{end} and T_{S} -transitions happen.

The phase diagram for potential II_2.

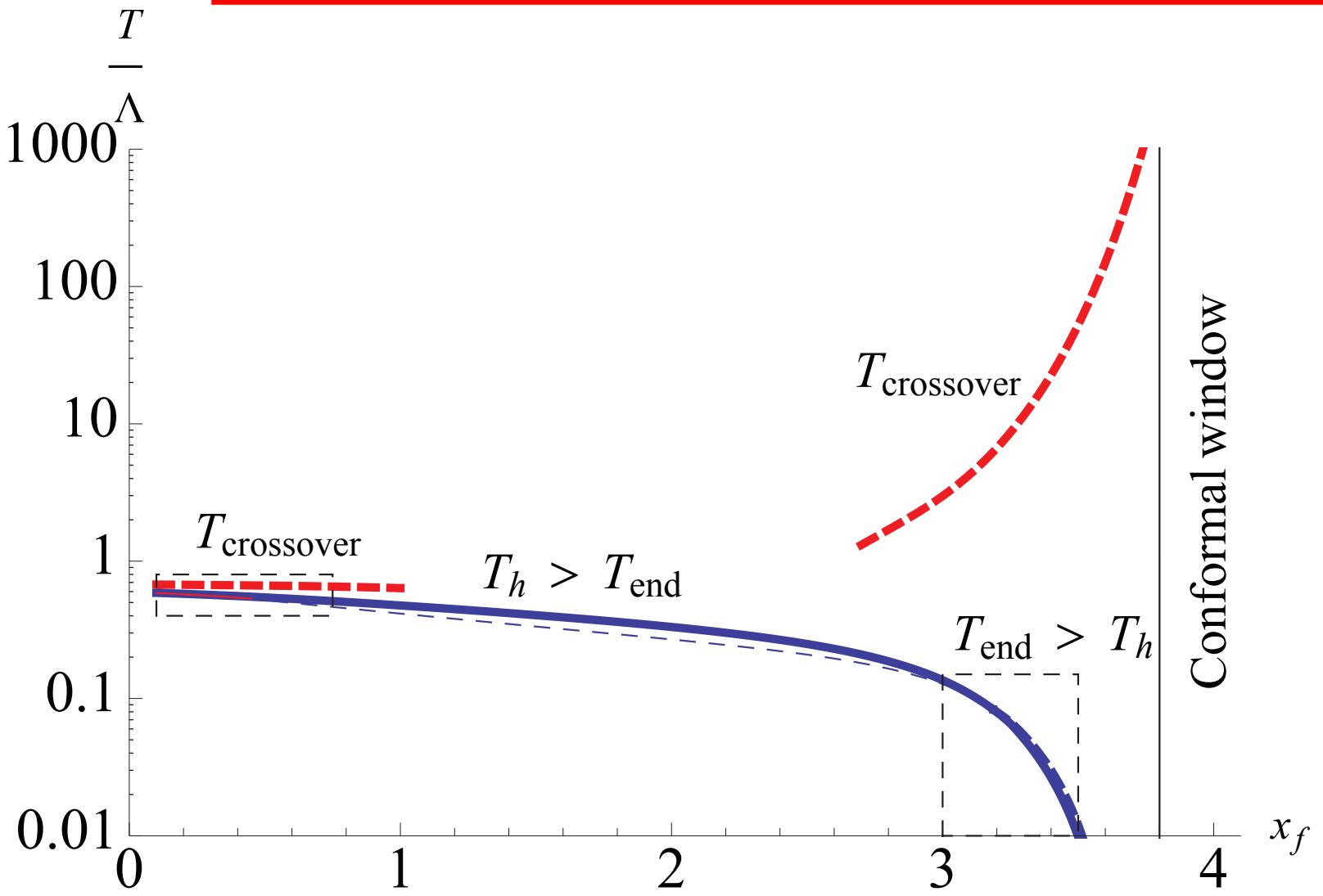

The chirally symmetric crossover transition $T_{\text{crossover}}$ is everywhere the highest temperature stable transition, except between $x_f \sim 1$ to $x_f \sim 2.7$, where the interaction measure does not have a maximum and the crossover does not therefore exist.

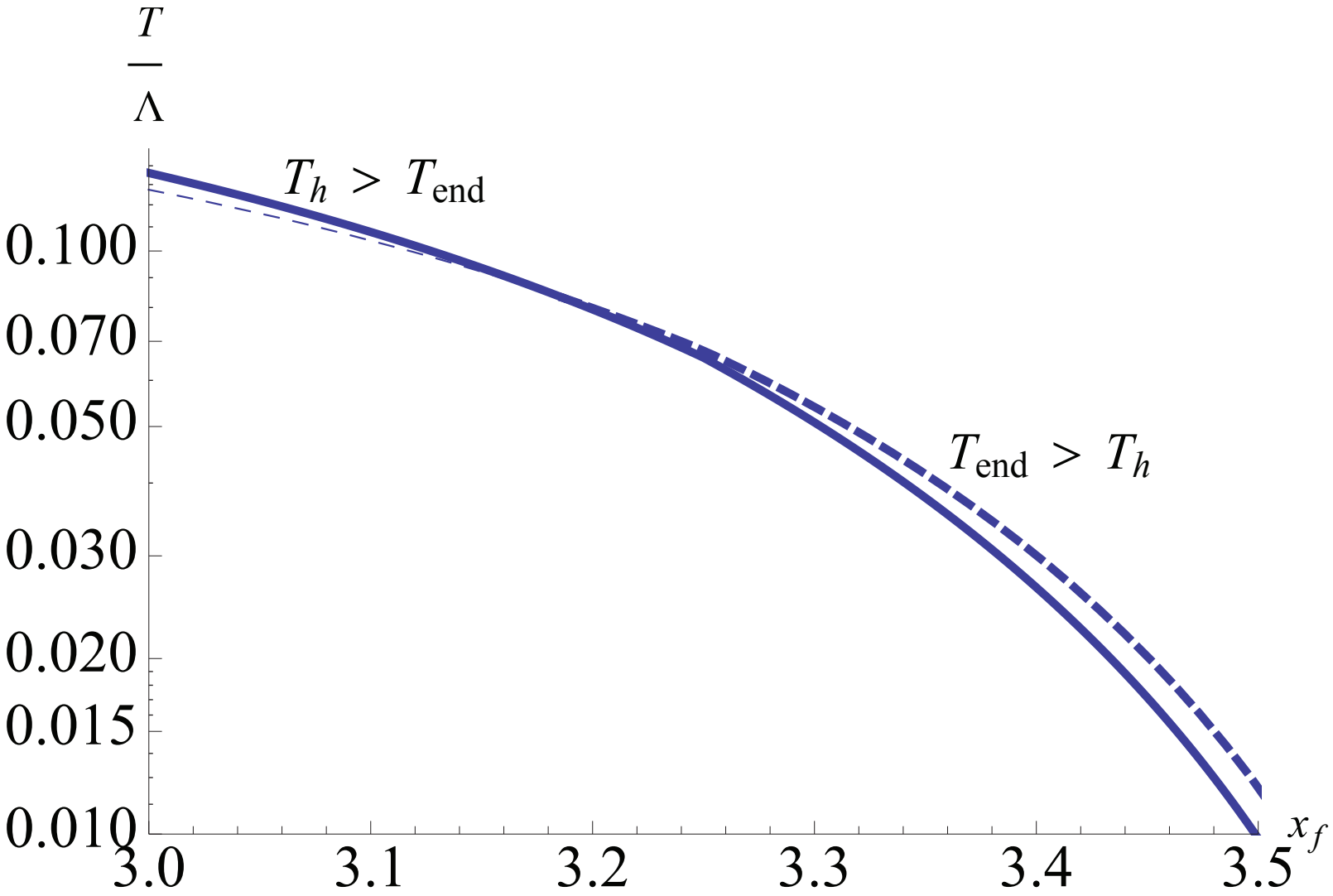

Above $x_f = 3.19$, the next transition is the second order T_{end}, which goes from the chirally symmetric high-T phase to the chirally broken low-T phase. This is very quickly followed by the T_h transition to the thermal gas solution. Below $x_f = 3.19$ the T_h transition happens first, and therefore T_{end} is in the unstable branch of the solution.

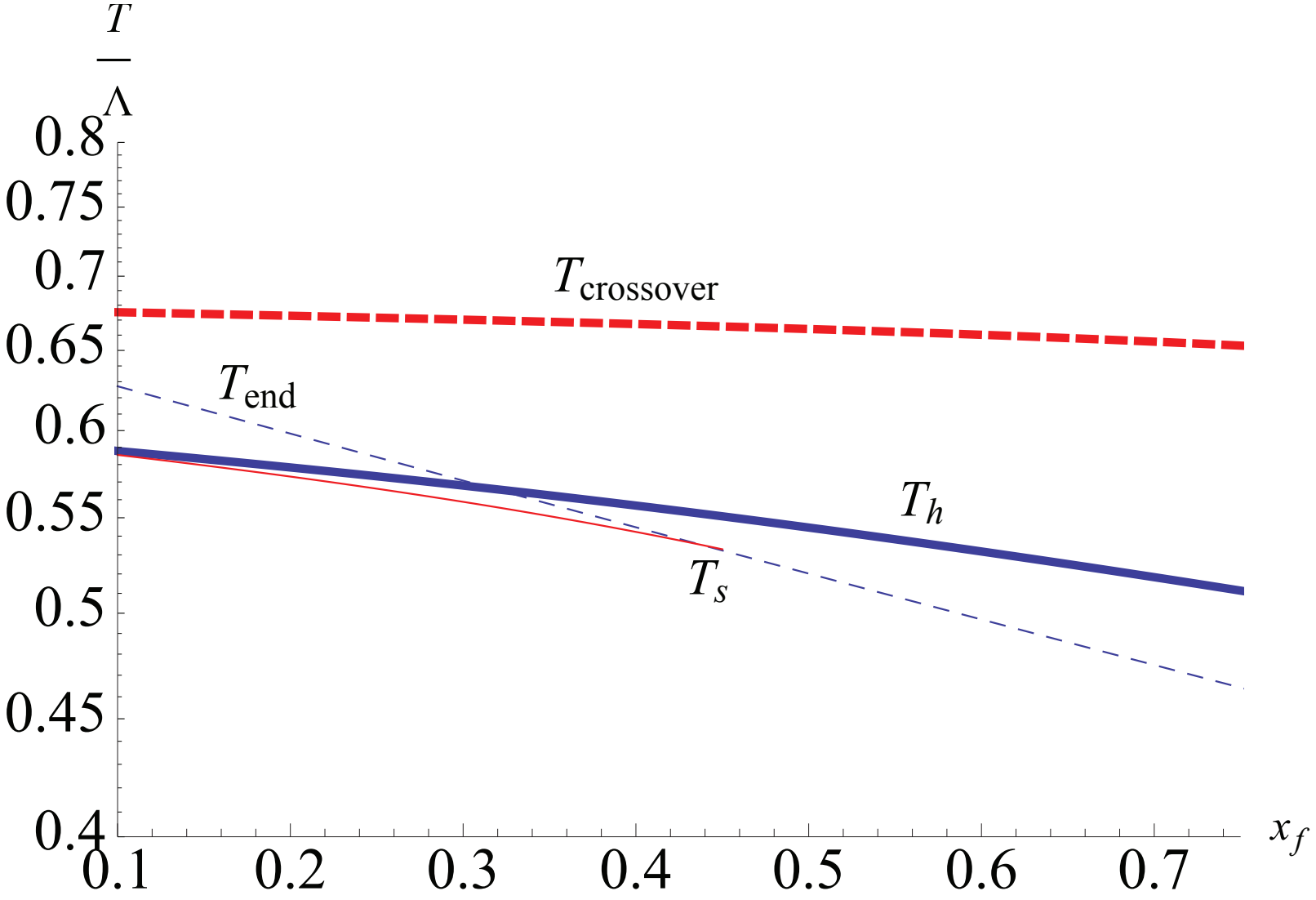

There is further structure at small x_f. a close-up of the small-x_f region. At $x_f \sim 0.4$, the first order T_S transition appears in the unstable branch just slightly below T_h. This transition nonetheless develops into the YM -transition at the $x_f \to 0$ -limit. T_{end} crosses above the T_h transition, but it is also in the unstable branch. A close-up of the $x_f \sim 3.2$ -region, where the T_{end} -transition crosses into the unstable branch.

Outlook

• We have used the concept of EHT to study IR asymptotics of a class of theories involving a scalar, a graviton and a vector.

• This is a part of an EHT program that is currently extended to more general situations: symmetry breaking, CP-odd interactions, more scalars and U(1)'s etc can be extended to more fields and more interactions.

• The behaviors we find are rich and calculable, giving a wide set of phase diagrams and transport behavior.

• Some of these systems have observables that bear a remarkable resemblance to what is seen in strange metals.

• A more detailed analysis of this physics and its link to microscopics is in need.

.

THANK YOU

On naked holographic singularities

• If no IR AdS/Lifshitz, all Poincaré invariant solutions end up in a naked IR singularity.

• In GR naked singularities are proscribed.

• In holographic gravity some may be acceptable. The reason is that they do not always signal a breakdown of predictability as is the case in GR. They could be resolved by stringy or KK physics, or they could be shielded for finite energy configurations.

• Are they resolvable? Does the near-singularity physics depends on the resolution?

• An important task in EHT is to therefore ascertain when such naked singularities are acceptable and when are reliable (alias "good")
(A priori these are different things)

♠ Gubser gave a criterion for good (acceptable) singularities: They should be limits of solutions with a regular horizon.

Gubser (2000)

• The second criterion amounts to having a well-defined spectral problem for fluctuations around the solution: The second order equations describing all fluctuations are Sturm-Liouville problems (no extra boundary conditions needed at the singularity).

Gursoy+E.K.+Nitti (2008)

• The singularity is "repulsive" (like the Liouville wall). It has an overlap with the previous criterion. It involves the calculation of "Wilson loops"

Gursoy+E.K.+Nitti (2008)

• It is not known whether the list is complete.

Solutions at zero charge density

.

Gursoy+Kiritsis+Mazzanti+Nitti (2009)

• The only parameter relevant for the solutions is $\delta \in R$ in $V \sim e^{-\delta\phi}$. Take $p+1=4$.

• $0 \leq |\delta| < 1$. T=0 singularity acceptable. Continuous spectrum/no mass gap. Continuous transition to BH phase at $T > 0$

• $1 < |\delta| < \sqrt{3}$. Discrete spectrum/mass gap. BH is thermodynamically subdominant and unstable. $1 < |\delta| < \sqrt{\frac{5}{3}}$. The spin-2 and spin-0 spectral problem is reliable without resolution.

• $|\delta| \geq \sqrt{3}$. Gubser bound violated, singularity→unacceptable.

The crossover value here is $|\delta| = 1$. For all other $\delta \neq 1$, corrections like $V = e^{-\delta\phi}\phi^k + e^{-\delta'\phi}\phi^{k'} + ...$ give subleading corrections.

• $1 < |\delta| < \sqrt{3}$. In the gapped case, the BH is unstable and thermodynamically irrelevant. The complete story at finite T depends on the subleading terms in the potential (aka the UV completion).

• There is a first order phase transition at T_c to a large BH.

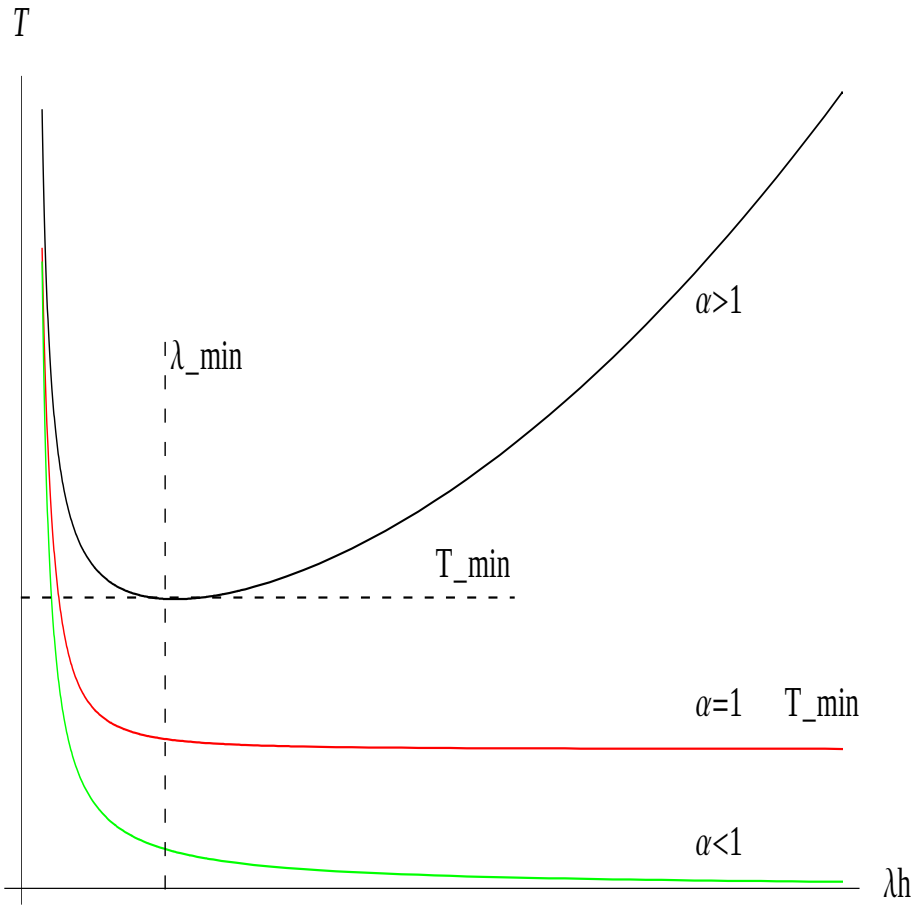

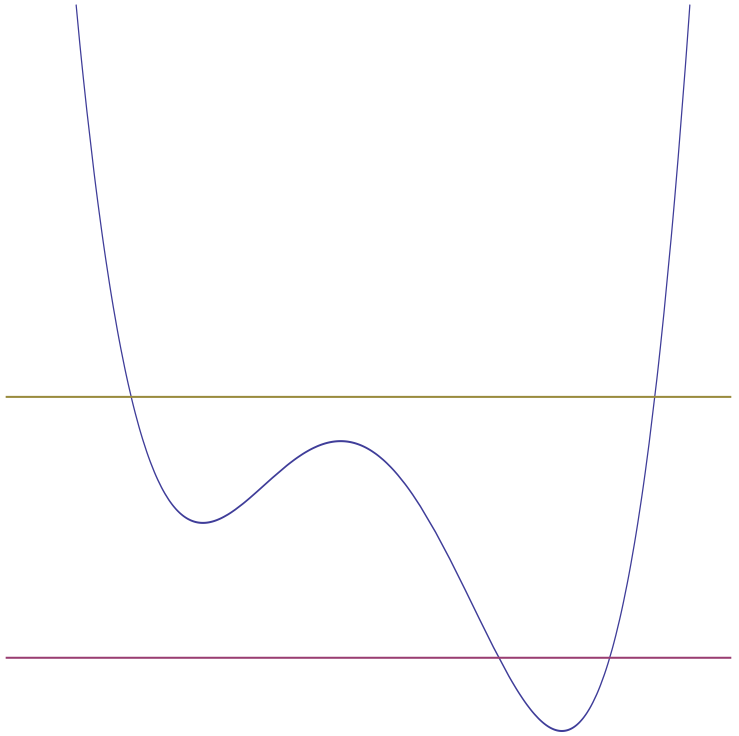

• For more complicated potentials multiple phase transitions are possible.
Gursoy+Kiritsis+Mazzanti+Nitti (2009), Alanen+Kajantie+Tuominen (2010)

• $|\delta| = 1$. This is the "marginal" case. It has a good singularity, a continuous spectrum and a gap. A lot of the physics of finite temperature transitions depends on subleading terms in the potential:

♠ If $V = e^{\phi}\left[1 + C\ e^{-\frac{2\phi}{n-1}} + \cdots\right]$, then at $T = T_{min} = T_c$ there is an n-th order continuous transition.

♠ If $V = e^{\phi}\left[1 + C/\phi^k + \cdots\right]$, then at $T = T_{min} = T_c$ there is a generalized KT phase transition

Gursoy (2010)

♠ If $V = e^{\phi}\ \phi^P$, with $P < 0$ this behaves as in $|\delta| < 1$. When $P > 0$ like $|\delta| > 1$.

The spectra depend importantly on P, when $P > 0$.

In particular, we will see that $P = \frac{1}{2}$ is very much like what we expect in 4D large-N YM.

Charged near-extremal scaling solutions

$$ds^2 = r^{\frac{(\gamma-\delta)^2}{2}}\left[dx^2 + dy^2 - f(r)dt^2\right] + \frac{dr^2}{f(r)}$$

$$f(r) = \frac{16\,(-\Lambda)}{wu^2}e^{-\delta\phi_0}\quad r^{1-\frac{3}{4}(\gamma-\delta)^2+\frac{wu}{4}}\quad\left(1-\frac{2m}{r^{\frac{wu}{4}}}\right),$$

$$e^{\phi} = e^{\phi_0}r^{-(\gamma-\delta)}\quad,\quad \mathcal{A} = \frac{8}{wu}\sqrt{\frac{v\Lambda}{u}}e^{-\frac{(\gamma+\delta)}{2}\phi_0}\quad\left[r^{\frac{wu}{4}}-2m\right]dt$$

$$wu = 3\gamma^2 - \delta^2 - 2\gamma\delta + 4 > 0\,,\quad u = \gamma^2 - \gamma\delta + 2\,,\quad v = \delta^2 - \gamma\delta - 2\,, \delta^2 \leq 3$$

- These are near extremal solutions (the charge density is fixed).
- The Entropy vanishes at extremality if $\gamma \neq \delta$.
- If $\gamma = \delta$ the extremal solution is $AdS_2 \times R^2$.
- The charge entropy dominates the $Q = 0$ entropy almost everywhere.
- When $\frac{dS}{dT} < 0$ the BH is unstable$\rightarrow$ gapped spectra.

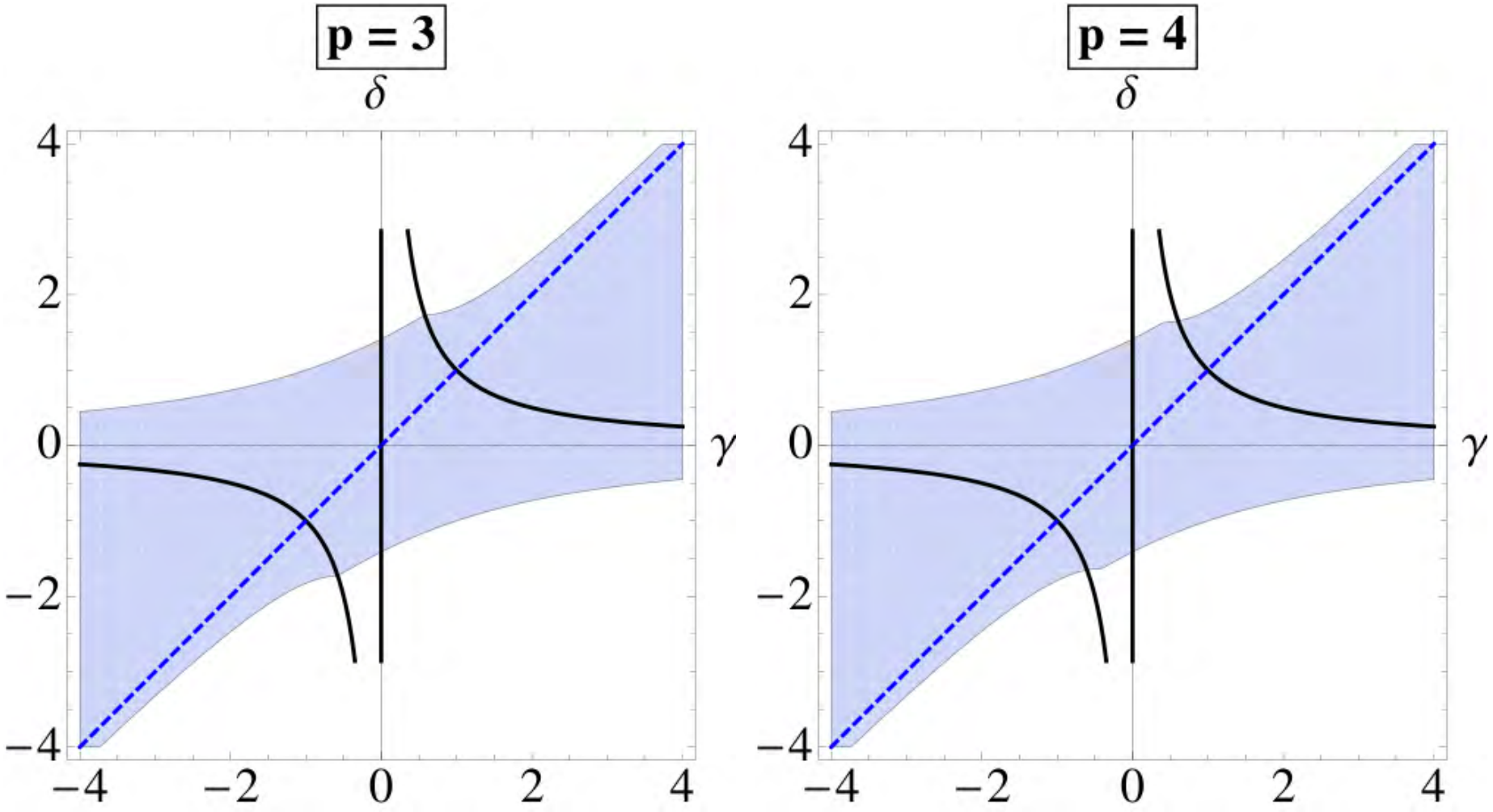

This graph shows the Gubser bounds on the near extremal solution on the whole of the (γ, δ) plane for $p = 3$ and $p = 4$. The blue regions are the allowed regions where the near extremal solutions are black-hole like. The white regions are solutions of a cosmological type and therefore fail the Gubser bound. The dashed blue line is the $\gamma = \delta$ solutions while the solid black line corresponds to the $\gamma\delta = 1$ solutions.

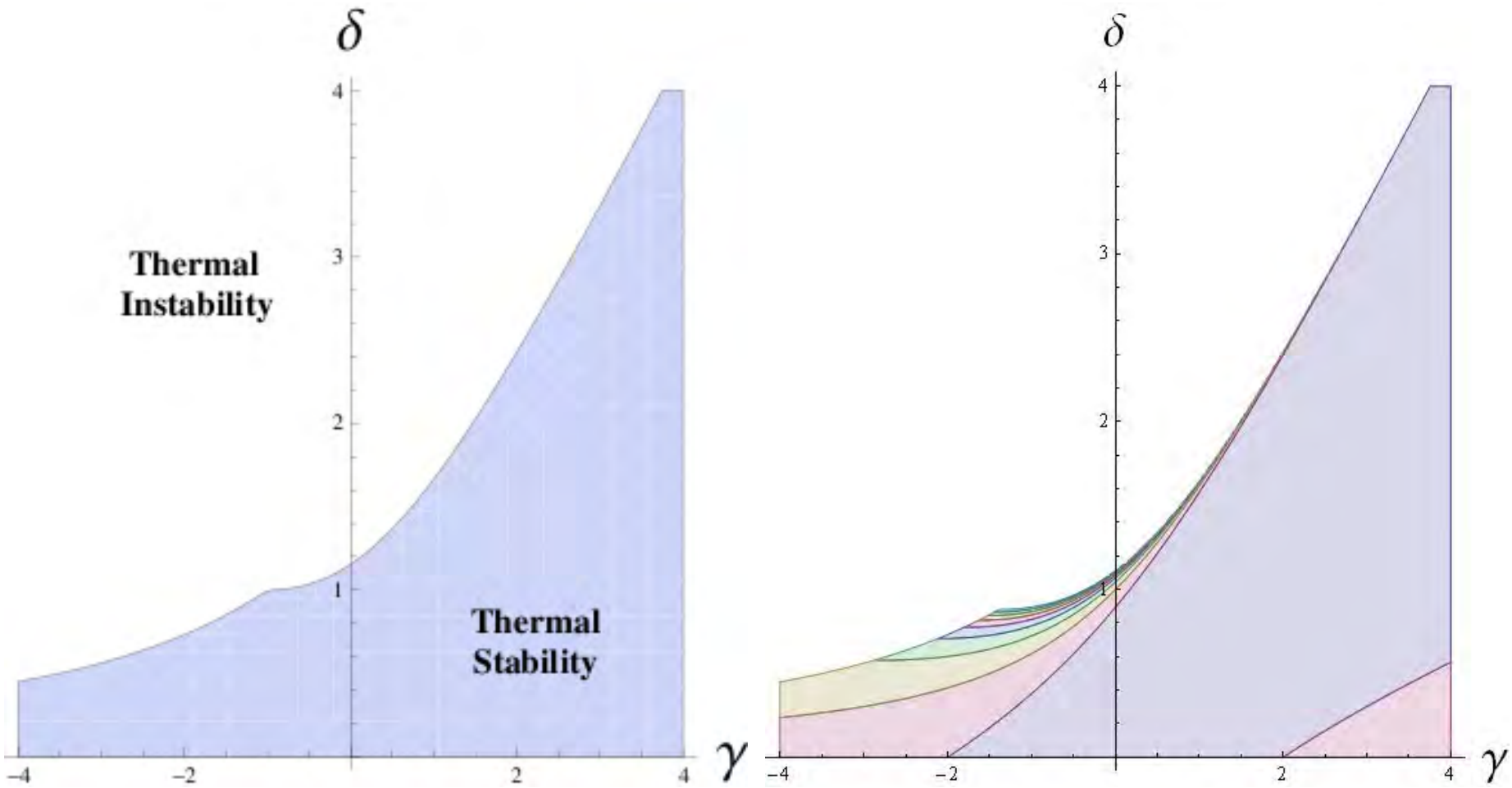

On the left: region of local stability of the near extremal black hole. Right: The variety of phase transitions of the near extremal black hole to the background at zero temperature. In the blue region continuous transitions occur, in the purple region adjacent to the blue one the transitions are of third-order. The stripes starting with yellow to the left of the blue and purple regions depicts transitions of fourth-(yellow) up to tenth-order. Above them all higher-order transitions also occur.

Mott-like spectra

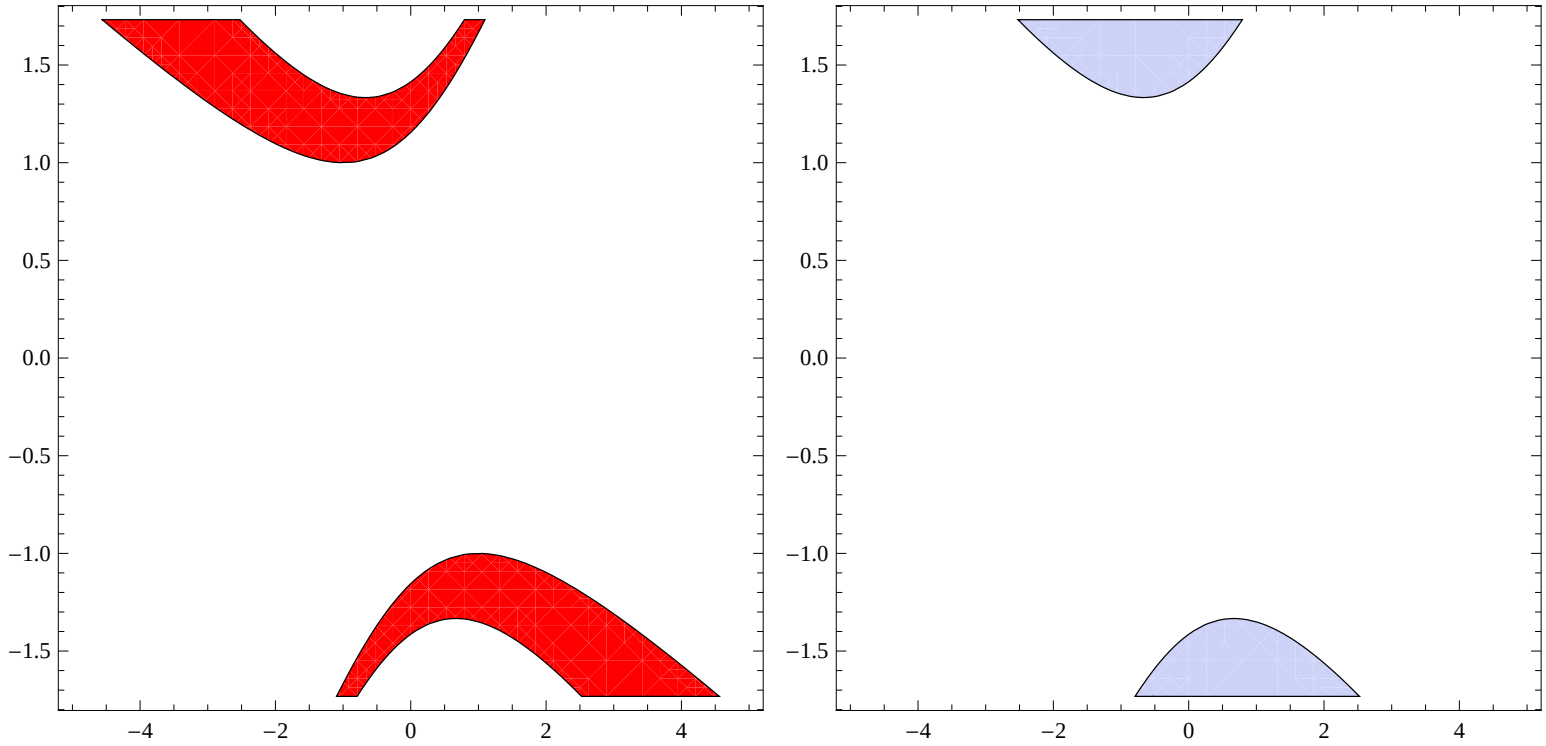

Left: The region on the $(\gamma\delta)$ plane where the IR black holes are unstable and $c > 0$. Here the extremal finite density system has a mass gap and a discrete spectrum of charged excitations, when $\Delta < 1$. This resembles a Mott insulator and the figure provides the Mott insulator "islands" in the (γ, δ) plane. Right:The region where the IR black holes are unstable, and $c < 0$. In this region the extremal finite density system has a gapless continuous spectrum at zero temperature. In both figures the horizontal axis parametrizes γ, whereas the vertical axis δ.

A similar system was analyzed independently by Mc Greevy and Balasubramanian

Exact charged solutions

- The full set of solutions for $\gamma\delta = 1$ and $\gamma = \delta$ are known.

- $\delta^2 < 3$ otherwise the solutions are De-Sitter like (cf Gubser).

- For $\gamma\delta = 1$ there are three distinct classes of dynamics:
  $\delta^2 \in [0,1] \cup [1, 1+\frac{2}{\sqrt{3}}] \cup [1+\frac{2}{\sqrt{3}}, 3)$

- At $Q = 0$ all $|\delta| > 1$ systems were insulators. Now this range is split in two in $\gamma\delta = 1$.

- $\gamma\delta = 1$ has zero entropy but $\gamma = \delta$ has finite entropy at extremality .

$\gamma\delta = 1$ solutions

- $0 \leq |\delta| < 1$

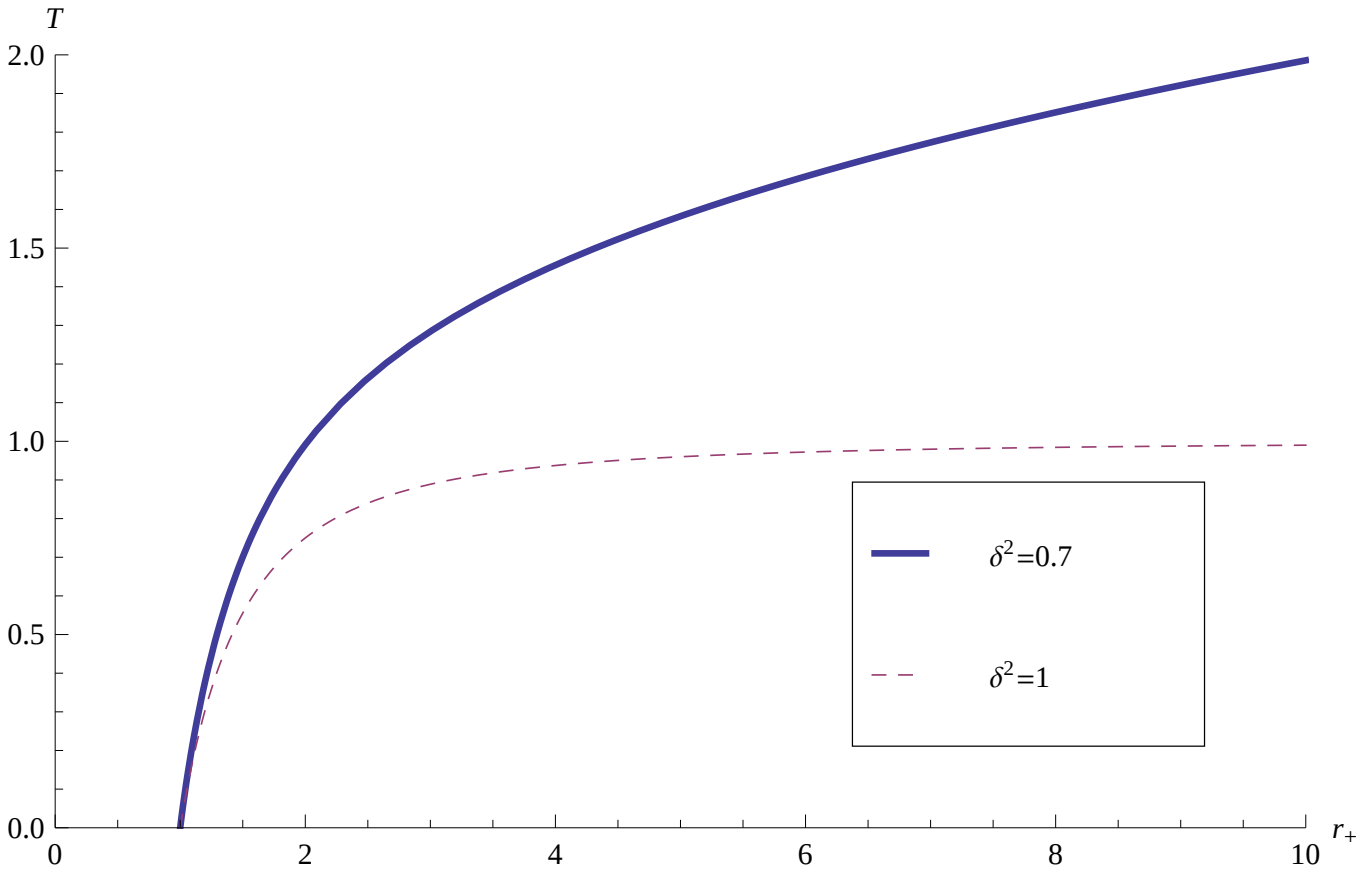

- A single branch of BH that dominate at $T > 0$. The transition at $T = 0^+$ is between 2nd and 3rd order.

- The system is a conductor.

- $\delta^2 \in [1, 1+\frac{2}{\sqrt{3}}]$

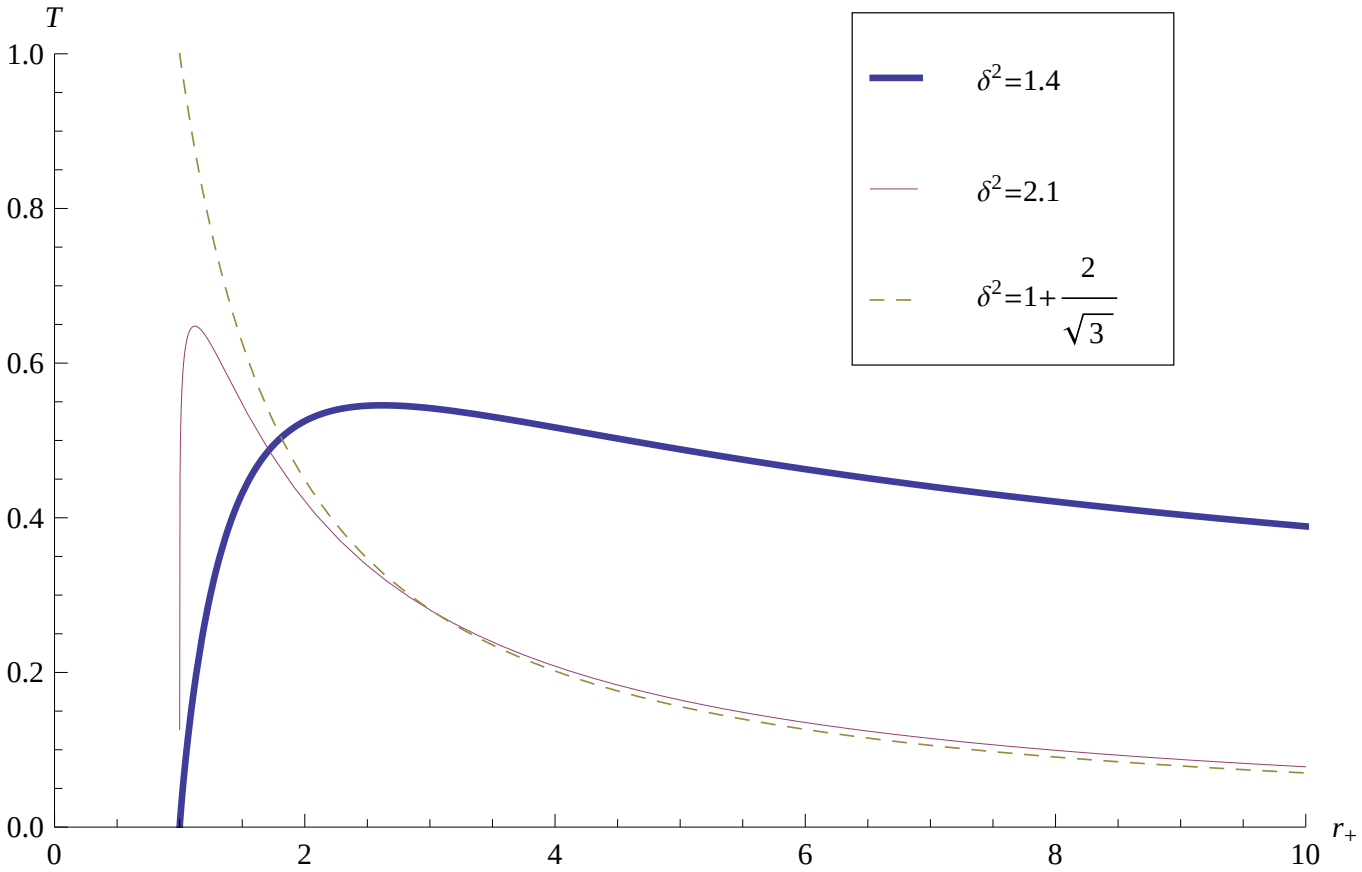

- There are two black holes at a given temperature $T < T_{max}$.

- At $T_{max} > T > 0$ it is the small black hole branch that dominates thermodynamically. The transition at $T = 0^+$ is continuous of any order. Upon UV completion, at $T_c \sim T_{max}$ a transition is expected to an RN-BH.

- $\delta^2 \in [1+\frac{2}{\sqrt{3}}, 3]$

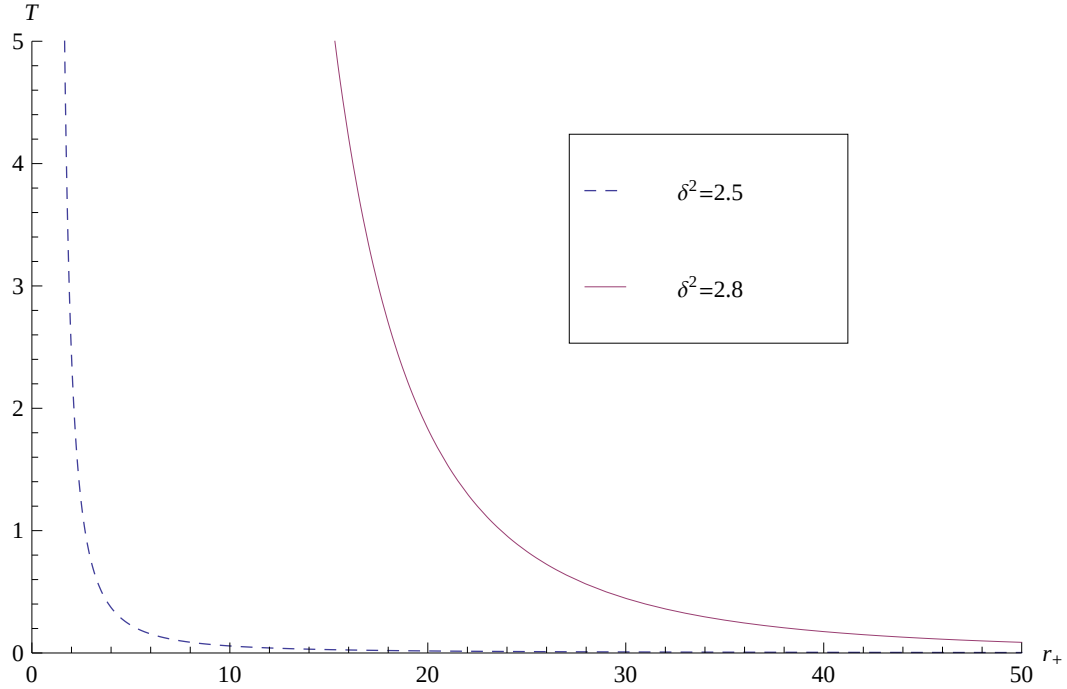

- The BH solution is unstable and never dominant. This is like the $\delta^2 > 1$ case at zero density.

- For $1+\frac{2}{\sqrt{3}} \leq \delta^2 \leq \frac{5+\sqrt{33}}{4}$ the system has a mass gap and discrete spectrum in the current correlator if $\Delta < 1$. It is a Mott-like insulator.

- Upon UV completion a RN-like new stable BH solution is expected to appear for $T > T_{min}$. There will be a first or second order phase transition to a conducting phase at $T_c > T_{min}$.

- For $\frac{5+\sqrt{33}}{4} \leq \delta^2 < 3$ The system has a continuous spectrum and is again a conductor.

A typical phase diagram

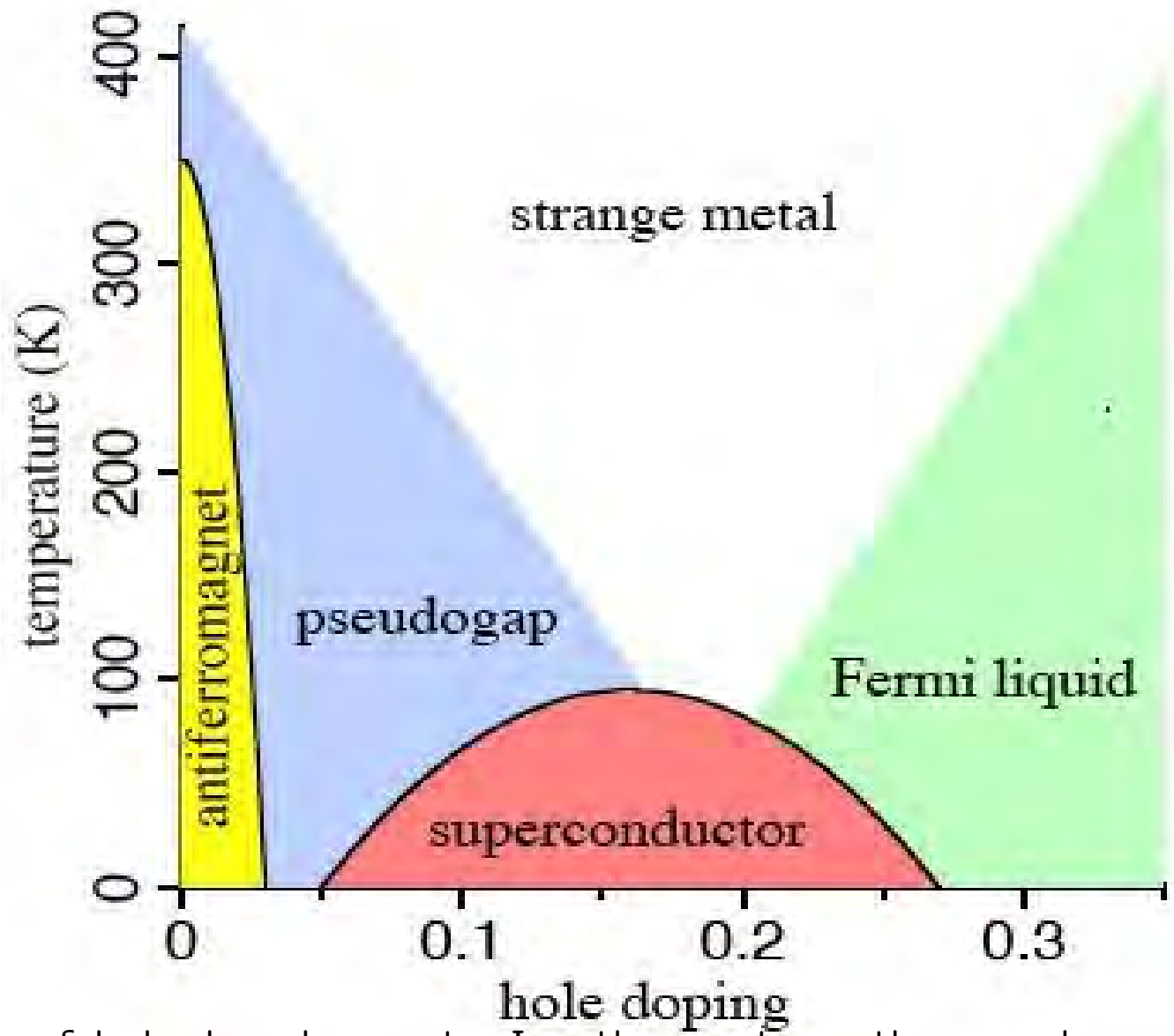

Phase diagram of hole-doped cuprates.In other systems the pseudogap region is much smaller, the superconducting region can shrink to almost nothing etc.

Linear Resistivity

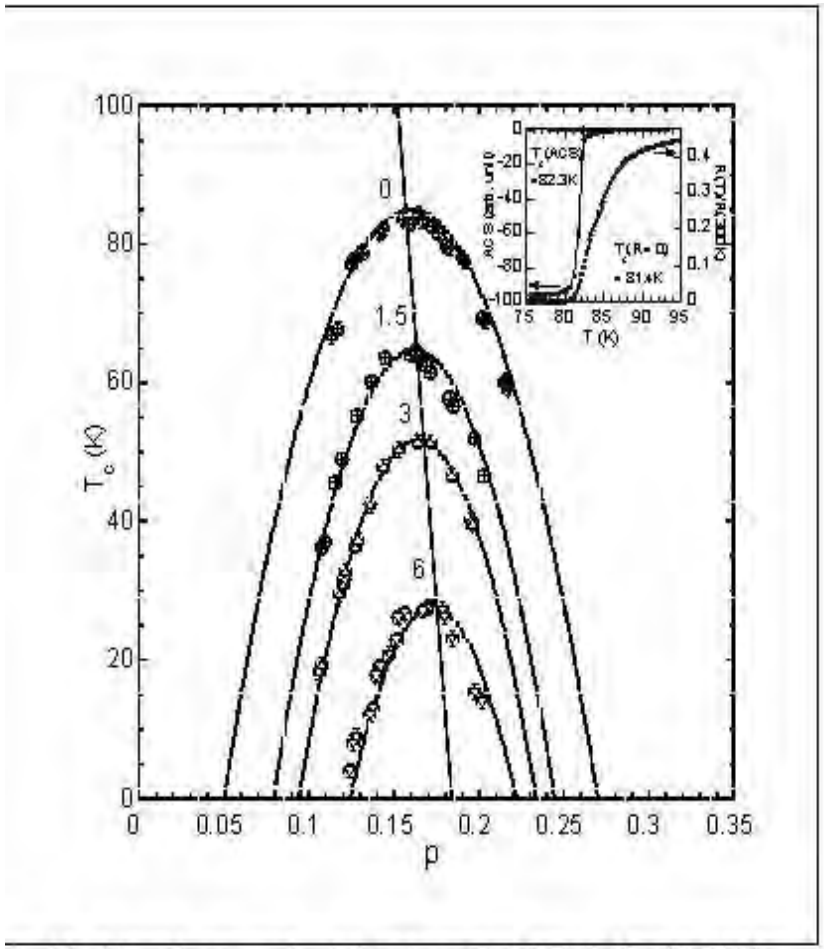

S. H. Naqib et. al., Physica C 387, 365 (2003)

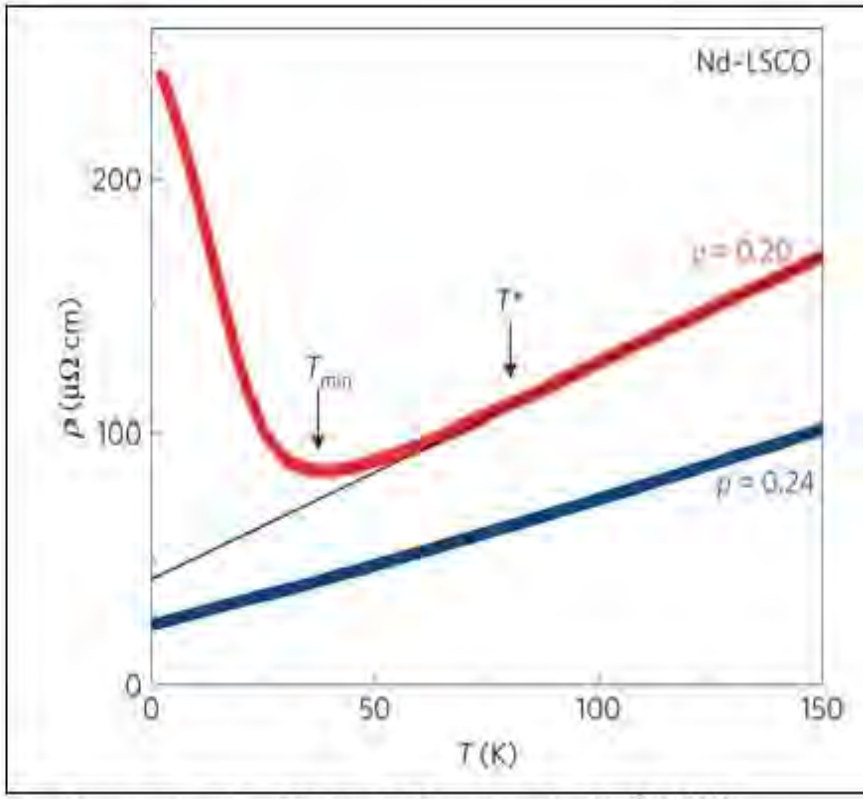

R. Daou et. al., Nature Physics 5, 31 (2009)
& R. A. Cooper, et. al., Science 323, 603(2009)
Nicolas Doiron-Leyraud, et. al., arXiv:0905.0964

- Suppress superconducting dome with *Zn* substitution or large magnetic field
- Linear temperature dependence of resistivity around the critical point

Linear Heat Capacity

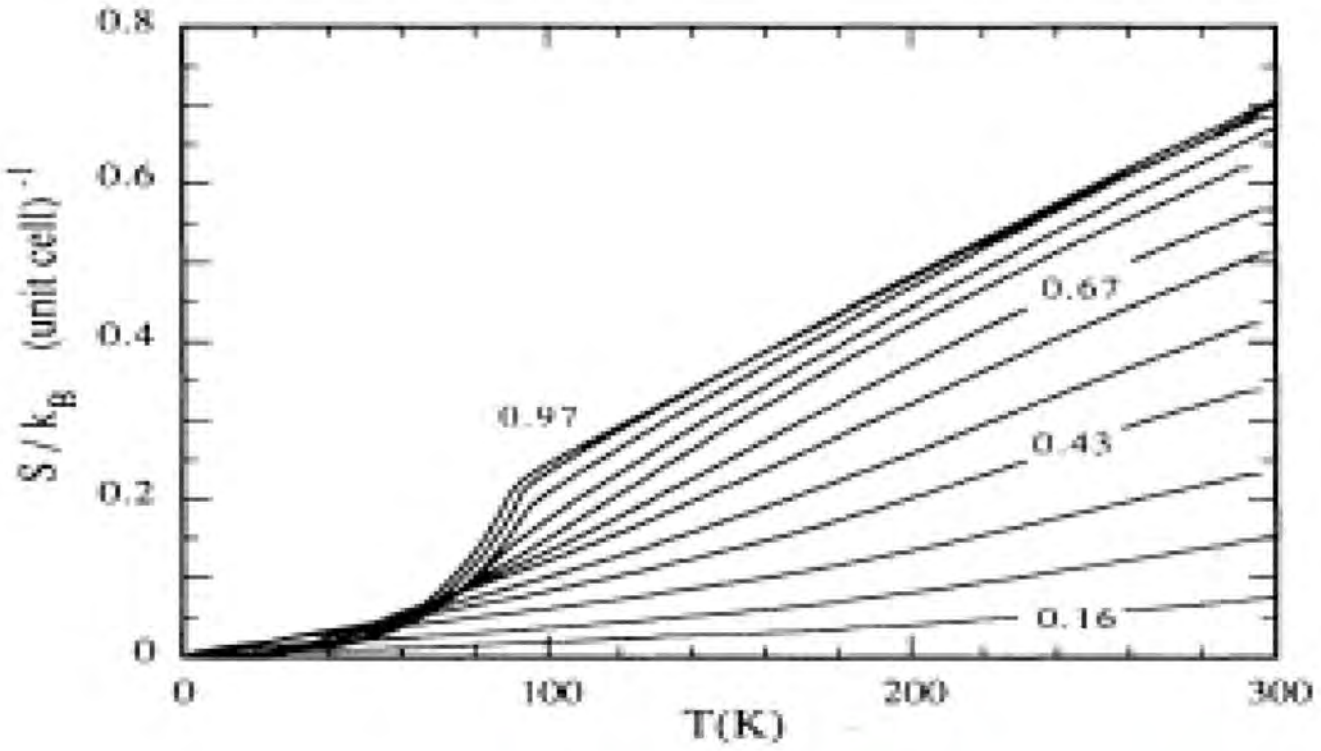

[Loram et. al. PRL 71, 11, 1993]

AC conductivity

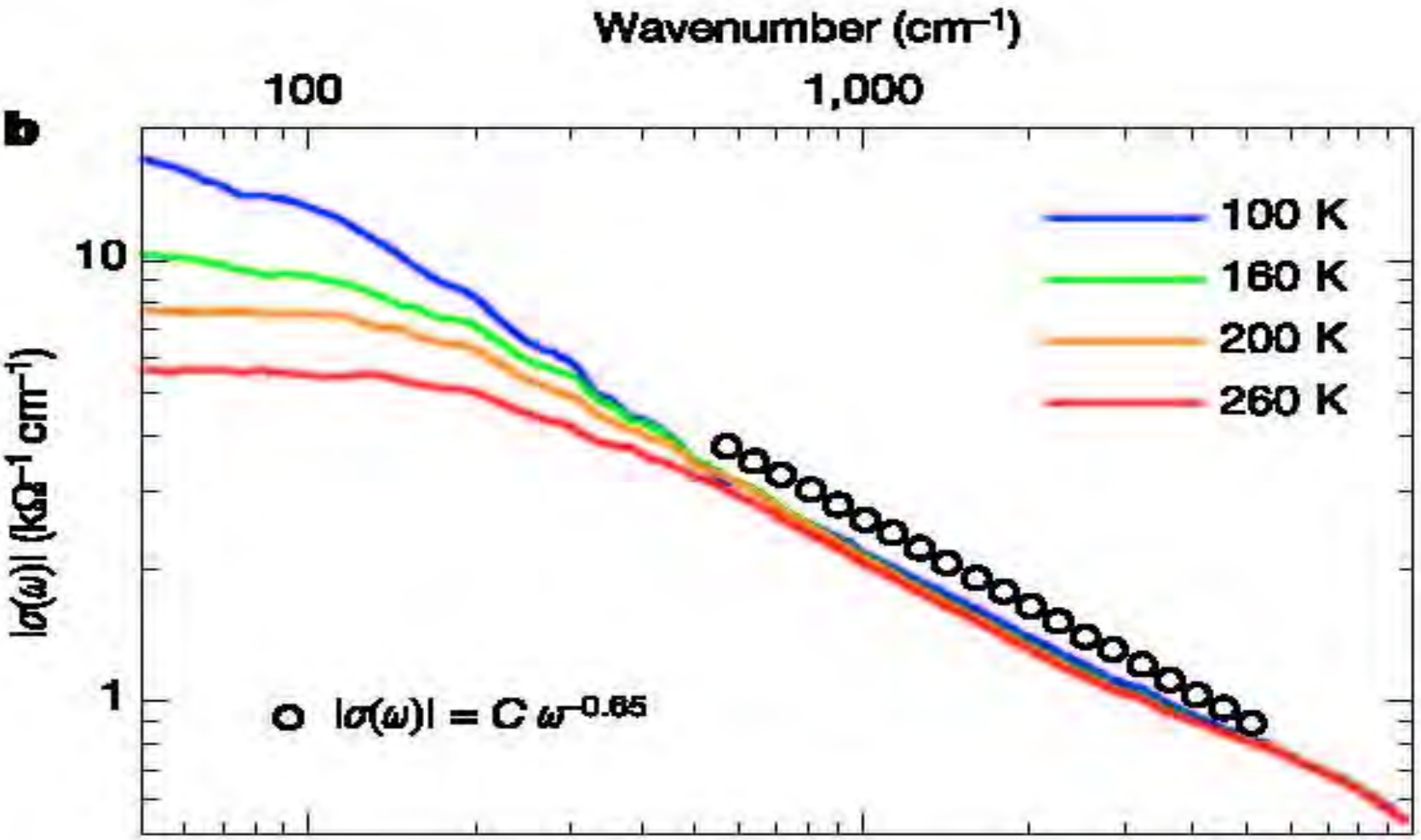

van der Marel+Molegraaf+Zaanen+Nussinov+Carbone+Damascelli+Eisaki+Greven+Kes+Li, Nature 425 (2003) 271

Conductivity

- It is main characteristic transport coefficient in a finite density system.

$$J^i(\omega,\vec{k}) = \sigma^{ij}(\omega,\vec{k})\ E_j(\omega,\vec{k})$$

- Can be calculated from a Kubo formula

$$\sigma^{ij}(\omega,\vec{k}) = \frac{G_R^{ij}(\omega,\vec{k})}{i\omega} \quad , \quad G_R^{ij} \equiv \langle J^i\ J^j \rangle$$

- Various limits are of experimental importance

$$\vec{k} \to 0 \quad \to \quad \sigma^{ij}(\omega,T) \quad \to \quad \text{AC conductivity}$$

$$\omega \to 0 \quad \text{and} \quad \vec{k} \to 0 \quad \to \quad \sigma^{ij}(T) \quad \to \quad \text{DC conductivity}$$

- The limits $\omega \to 0$ and $\vec{k} \to 0$ do not commute.

Romatchke+Son (2009)

- We can use the drag calculation to calculate the DC conductivity for massive carriers

$$\rho = \frac{T_f}{Jt}\ g_{xx}^E(r_h)\ e^{k\phi(r_h)}$$

RETURN

AC Conductivity: derivation

To compute the frequency depended current correlator we perturb we start with a general diagonal metric ansatz

$$ds^2 = -D(r)dt^2 + B(r)dr^2 + C(r)(dx_i dx^i) \quad , \quad A'_t = q\frac{\sqrt{D(r)B(r)}}{Z(\phi)C(r)^{\frac{p-1}{2}}}$$

In the backreacted case we must turn on perturbations

$$A_i = a_i(r)e^{i(\omega t)} \quad , \quad g_{ti}(r,t) = z_i(r)e^{i\omega t}$$

From the r, x_i Einstein equation we obtain

$$z'_i - \frac{C'}{C}z_i = -ZA'_t\ a_i$$

while from the gauge field equations

$$\partial_r\left(ZC^{\frac{p-3}{2}}\sqrt{\frac{D}{B}}a'_i\right) + ZC^{\frac{p-3}{2}}\sqrt{\frac{B}{D}}\omega^2\ a_i = \frac{q}{C}\left(z'_i - \frac{C'}{C}z_i\right)$$

Substituting we obtain

$$\partial_r\left(ZC^{\frac{p-3}{2}}\sqrt{\frac{D}{B}}a'_i\right) + ZC^{\frac{p-3}{2}}\left(\sqrt{\frac{B}{D}}\omega^2 - \frac{q^2\sqrt{DB}}{ZC^{p-1}}\right)a_i = 0$$

We can map to a Schrödinger problem

$$\frac{dz}{dr} = \sqrt{\frac{B}{D}} \quad , \quad a_i = \frac{\Psi}{\sqrt{\bar{Z}}} \quad , \quad \bar{Z} = ZC^{\frac{p-3}{3}}$$

$$-\frac{d^2\Psi}{dz^2}+V_{eff}\Psi=\omega^2\Psi \quad , \quad V_{eff}=\frac{q^2 D}{ZC^{p-1}}+\frac{1}{4}\left(\frac{\partial_z \bar{Z}}{\bar{Z}}\right)^2+\frac{1}{2}\partial_z\frac{\partial_z\bar{Z}}{\bar{Z}}$$

Near an AdS boundary the potential asymptotes to

$$V_{eff}\simeq\frac{(p-1)(p-3)}{4z^2}+\frac{q^2}{Z_b}\left(\frac{z}{\ell}\right)^{2(p-2)}+\cdots$$

When $p=3$ the leading behavior is given by

$$V_{\perp,p=3}=-\frac{k}{2}\Delta(2\Delta-1)\ r^{2\Delta-2}+\cdots$$

The frequency dependent conductivity is given by

$$\sigma(\omega)=\frac{1-\mathcal{R}}{1+\mathcal{R}}-\frac{i}{2\omega}\frac{\dot{Z}}{Z}\Big|_{\text{boundary}}$$

Roberts+Horowitz (2009), Goldstein+Kachru+Prakash+Trivedi (2009)

At extremality, near the singularity at $r=r_0$, $D=c_D(r-r_0)^2$, $B=c_B/(r-r_0)^2$ and

$$V\simeq\frac{\nu^2-\frac{1}{4}}{z^2}+\cdots \quad , \quad \nu^2-\frac{1}{4}=\frac{q^2c_B}{Z_0C_0^{p-1}}$$

Calculation of the reflection coefficient then gives

$$\sigma\sim\omega^{2\nu-1}$$

Goldstein+Kachru+Prakash+Trivedi (2009)

Brief summary of results

- We will describe the IR asymptotics of strongly coupled systems at finite density driven by a leading relevant operator.

- To do this we will have to parametrize the gravitational EHT and it will depend on two real constants (γ, δ).

- For zero charge density we will scan the IR landscape and characterize theories by the nature of their spectra and their low temperature thermodynamics. Both 1st order and continuous transitions exist.

- At finite charge density we will find all near-extremal solutions and calculate the low-temperature conductivity, in order to characterize the dynamics. We will also analyze two families of exact solutions.

- We will find that some regions in the (γ, δ) plane will be excluded as unphysical.

- In another large region the has continuous spectra, we will find the most general quantum critical behavior, generalizing AdS_2 and Lifshitz backgrounds.

- For all (γ, δ) except when $\gamma = \delta$ the entropy vanishes at extremality.

- There is a codimension-one space, where the IR resistivity is linear in the temperature

- When the scalar operator is not the dilaton, then in 2+1 dimensions, the IR resistivity has the same scaling as the entropy (and heat capacity).

- We will find the first holographic examples of Mott insulators at finite density.

- Generically the charge-induced entropy dominates the one without charge carriers.

The charged spectra, at zero density and conductivity

• We can also analyze the spectrum of current fluctuations that now depends on γ.

♠ $\frac{\gamma}{\delta} > \frac{3}{2}$ or $\frac{\gamma}{\delta} < -\frac{1}{2}$: When the UV dimension of the scalar $\Delta < 1$ then the potential diverges both in the UV and the IR and the spectrum is discrete and gapped. This resembles to an insulator. Otherwise it is a conductor.

♠ $-\frac{1}{2} < \frac{\gamma}{\delta} < \frac{3}{2}$. The spectral problem is unacceptable and therefore the spin-1 spectrum unreliable.

• The AC Conductivity at zero charge density:

When $|\delta| < 1$ the effective potential is

$$V_{eff} \simeq \frac{c}{z^2} \quad , \quad c = \frac{(\gamma\delta + 1 - \delta^2)\gamma\delta}{(1-\delta^2)^2} \quad , \quad \sigma \sim \omega^n \quad , \quad n = \sqrt{4c+1} - 1$$

- It becomes $n=-\frac{2}{3}$ iff

$$\gamma=\frac{\delta^2-1}{3\delta} \quad \text{or} \quad \gamma=\frac{2(\delta^2-1)}{3\delta}$$

- The DC conductivity can calculated (using Karch-O'Bannon) to be

$$\sigma=e^{-k\phi_0}(\kappa T)^{\frac{2k\delta+2}{\delta^2-1}}\sqrt{\langle J^t\rangle^2+e^{2(\gamma+k)\phi_0}(\kappa T)^{\frac{4[1+(\gamma+k)\delta]}{1-\delta^2}}}\,,$$

$$\rho_{\text{light}}\sim T^{\frac{2\gamma\delta}{\delta^2-1}} \quad , \quad \rho_{\text{drag}}\sim\frac{T^{\frac{2k\delta+2}{1-\delta^2}}}{\langle J^t\rangle}$$

- In the first case we can attain linear resistivity when

$$\gamma=\gamma_{\text{linear}}\equiv\frac{\delta^2-1}{2\delta}\,.$$

The extremal AC conductivity

$$p = 3 \quad \sigma \sim \omega^n\,, \qquad n = \left| \frac{(\delta-\gamma)(3\gamma+5\delta)-12}{(\delta-\gamma)(\gamma+3\delta)-4} \right| - 1\,.$$

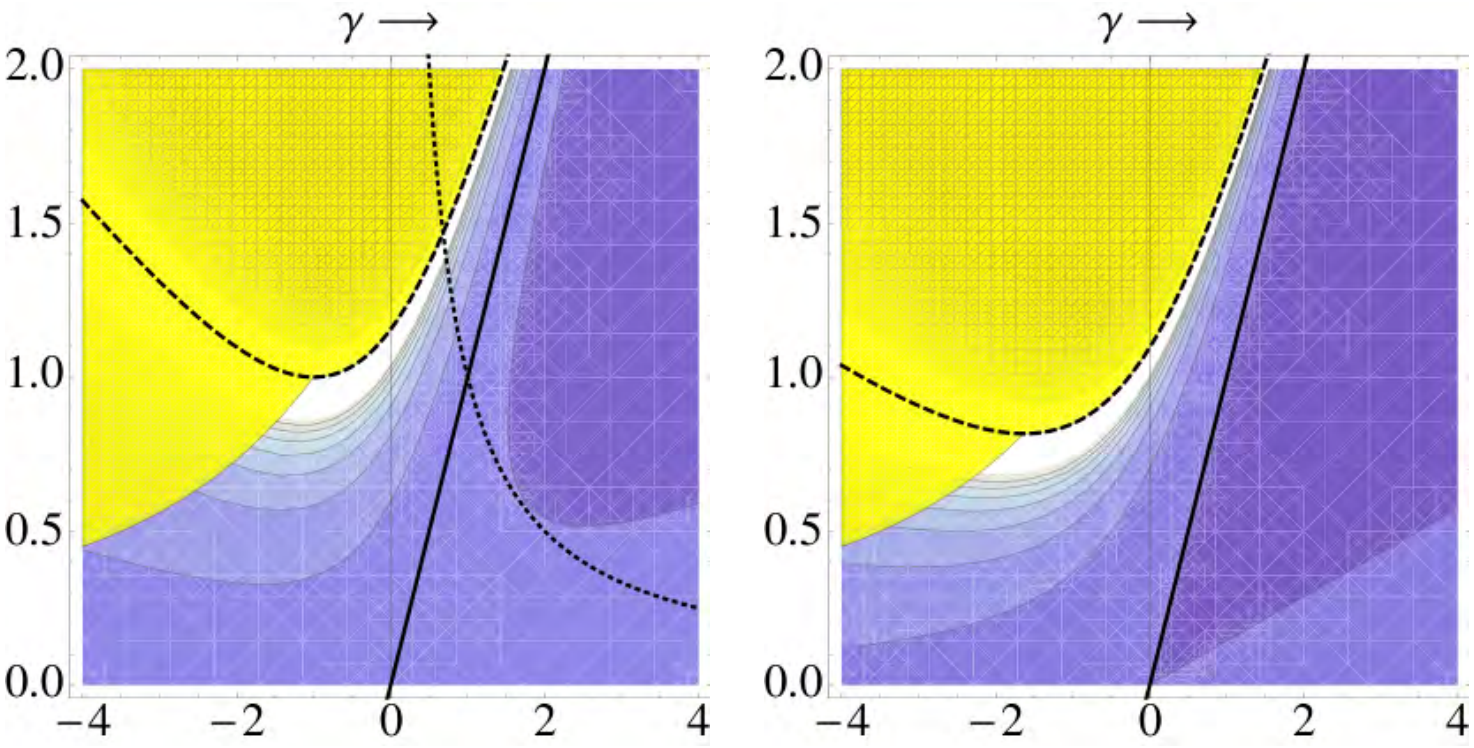

Contour plot of the scaling exponent n in the (γ, δ) upper half plane for $p = 3$ (left figure $0 \le \delta \le \sqrt{\frac{5}{3}}$) and $p = 4$ (right figure, $0 \le \delta \le \sqrt{\frac{4}{3}}$). Left figure: Contours correspond to $n = 1.52, \ldots, 8.36$, starting with $n = 1.52$ in the upper right corner and increasing in steps of 0.76. The black solid line $\gamma = \delta$ is $n = 2$, and brighter colors correspond to larger n. Right figure: Contours correspond to $n = 2.2, \ldots, 12.1$, starting with $n = 2.2$ in the lower right corner and increasing in steps of 1.1. The black solid line $\gamma = \delta$ is again at

$n = 2$. In the yellow regions the computation of n cannot be trusted, since an explicit AdS completion of the space-time is needed to render the thermodynamics well-defined. The scaling exponent diverges to $+\infty$ along the dashed black line in both cases.

The near-extremal DC conductivity

- For massive charge carriers

$$\rho \sim T^m\,, \qquad \frac{4k(\delta-\gamma)+2(\delta-\gamma)^2}{4(1-\delta(\delta-\gamma))+(\delta-\gamma)^2}$$

- The exponent becomes unity for two values of γ

$$\gamma_\pm = 3\delta + 2k \pm 2\sqrt{1+(\delta+k)^2}\,.$$

- For a non-dilatonic scalar, $k=0$ and the temperature dependence of the entropy and the resistivity are the same. Therefore, the entropy also scales linearly with T.
- For the Lifshitz solutions, we must take $\delta=0$ and $\gamma=-\sqrt{\frac{4}{(z-1)}}$. In this case we obtain that

$$m_p = \frac{2+k\sqrt{4(z-1)}}{z}\,,$$

- When $k=0$ this is in agreement with Hartnoll+Polchinski+Silverstein+Tong

Drag calculation of DC conductivity

.

Gubser (2005), Karch+O'Bannon (2007)

$$S_{NG} = T_f \int d^2\xi \sqrt{\hat{g}} + \int d\tau A_\mu \dot{x}^\mu \,, \qquad \hat{g}_{\alpha\beta} = g_{\mu\nu}\partial_\alpha x^\mu \partial_\beta x^\nu \,,$$

In a direction with translation invariance we have the following world-sheet Poincaré conserved currents

$$\pi^\alpha_\mu = \bar{\pi}^\alpha_\mu + A_\mu \eta^{\alpha\tau} = T_f \sqrt{\hat{g}} \hat{g}^{\beta\alpha} g_{\nu\mu} \partial_\beta x^\nu + A_\mu \eta^{\alpha\tau} \,,$$

The bulk and boundary equations are

$$\partial_\alpha \bar{\pi}^\alpha_\mu = 0 \quad , \quad T_f \sqrt{\hat{g}} \hat{g}^{\sigma\beta} g_{\mu\nu} \partial_\beta x^\nu + q F_{\mu\nu} \dot{x}^\nu = 0 \,.$$

We now consider a space-time metric in a generic coordinate system and a bulk gauge field

$$ds^2 = -g_{tt}(r) dt^2 + g_{rr}(r) dr^2 + g_{xx}(r) dx^i dx^i \quad , \quad A_{x^1} = -Et + h(r) \quad , \quad A_t(r)$$

We choose a static gauge with $\sigma = r$ and $\tau = t$ and make the ansatz

$$x^1 = X = vt + \xi(r) \,,$$

which is motivated by the expectation that the motion of the string will make it have a profile that is dragging on one side as it lowers inside the bulk space.
The boundary equation for $\mu = t$ and $\mu = x$ are equivalent and become

$$T_f \frac{\hat{g}_{\sigma\tau}}{\sqrt{-\hat{g}}} g_{tt} + Ev = 0 \quad \to \quad \bar{\pi}_x = E \,.$$

Solving we obtain

$$\xi' = \sqrt{\frac{g_{rr}}{g_{tt}g_{xx}}}\frac{\sqrt{g_{tt}-g_{xx}v^2}}{\sqrt{T_f^2 g_{tt}g_{xx}-\bar{\pi}_x^2}}\bar{\pi}_x\,.$$

To ensure we have a real solution, there must be a turning point at $r = r_s$

$$v^2 = \frac{g_{tt}(r_s)}{g_{xx}(r_s)}\,, \qquad \bar{\pi}_x = -T_f\sqrt{g_{tt}(r_s)g_{xx}(r_s)}$$

Finally as v is constant we obtain

$$T_f\sqrt{g_{tt}(r_s)g_{xx}(r_s)} = -E \quad , \quad \frac{dp}{dt} = -\bar{\pi}_x + qE\,,$$

and the steady state solution is $\bar{\pi}_x = E$. For small velocities we obtain

$$\bar{\pi}_x \simeq -T_f g_{xx}(r_h)\; v + \mathcal{O}(v^2) \quad , \quad J^x = J^t\; v \simeq \frac{J^t\bar{\pi}_x}{T_f g_{xx}(r_h)} \simeq \frac{J^t}{T_f g_{xx}(r_h)}E\,,$$

and we obtain the DC conductivity and related resistivity as

$$\sigma \simeq \frac{J^t}{T_f g_{xx}(r_h)}\,, \qquad \rho \simeq \frac{T_f g_{xx}(r_h)}{J^t} = \frac{T_f g_{xx}^E(r_h)e^{k\phi(r_h)}}{J^t}\,.$$

In the case that $k = 0$

$$\frac{\rho(T)}{S(T)^{\frac{2}{p-1}}} = \text{constant}\,.$$

Vacuum solutions in the Einstein-Dilaton theory

$$V(\lambda) \sim V_0 \lambda^{2Q} \quad , \quad \lambda \equiv e^{\phi} \to \infty$$

- The solutions can be parameterized in terms of a fake superpotential

$$V = \frac{64}{27} W^2 - \frac{4}{3} \lambda^2 \, W'^2 \quad , \quad W \geq \frac{3}{8} \sqrt{3V}$$

The crucial parameter resides in the solution to the diff. equation above. There are three types of solutions for $W(\lambda)$:

Gursoy+E.K.+Mazzanti+Nitti

1. Generic Solutions (bad IR singularity)

$$W(\lambda) \sim \lambda^{\frac{4}{3}} \quad , \quad \lambda \to \infty$$

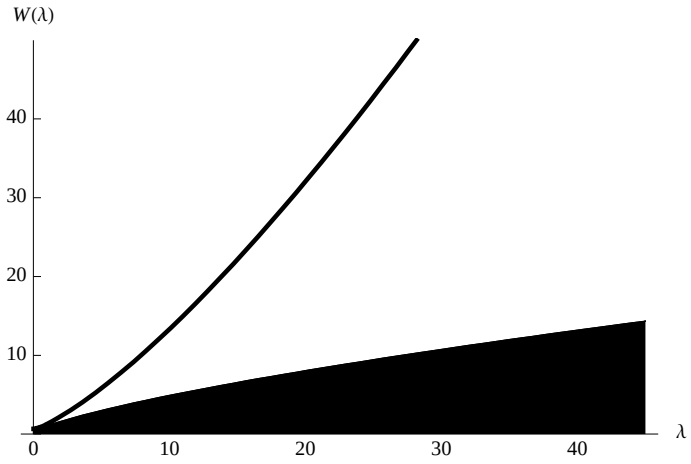

2. Bouncing Solutions (bad IR singularity)

$$W(\lambda) \sim \lambda^{-\frac{4}{3}} \quad , \quad \lambda \to \infty$$

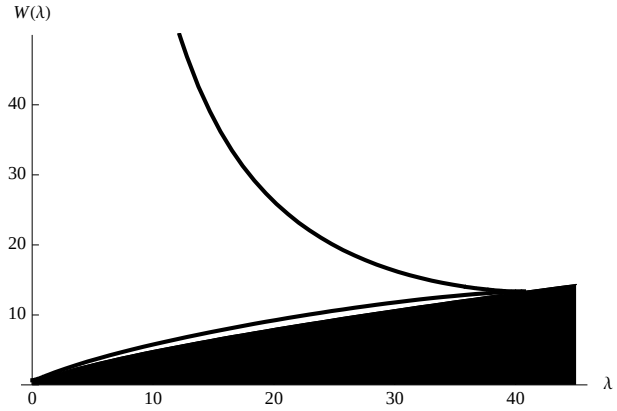

3. The "special" solution.

$$W(\lambda) \sim W_\infty \lambda^Q \quad , \quad \lambda \to \infty \quad , \quad W_\infty = \sqrt{\frac{27V_0}{4(16-9Q^2)}}$$

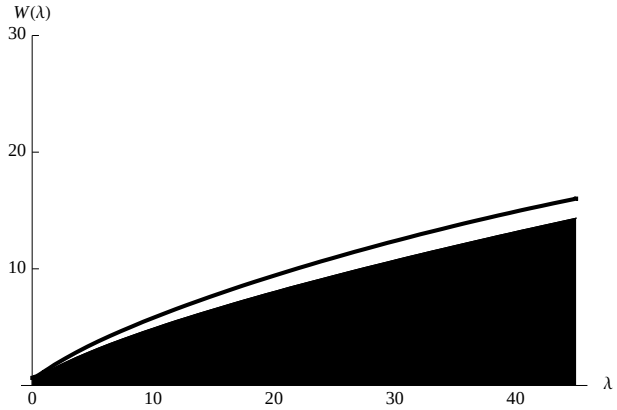

Good+repulsive IR singularity if $Q < \frac{4\sqrt{2}}{3}$

• For $Q > \frac{4}{3}$ all solutions are of the bouncing type (therefore bad).

• There is another special asymptotics in the potential namely $Q = \frac{2}{3}$. Below $Q = \frac{2}{3}$ the spectrum changes to continuous without mass gap.

In that region a finer parametrization of asymptotics is necessary

$$V(\lambda) \sim V_0 \ \lambda^{\frac{4}{3}} \ (\log \lambda)^P$$

• For $P > 0$ there is a mass gap, discrete spectrum and confinement of charges. There is also a first order deconfining phase transition at finite temperature.

• For $P < 0$, the spectrum is continuous, without mas gap, and there is a transition at T=0 (as in N=4 sYM).

• At $P = 0$ we have the linear dilaton vacuum. The theory has a mass gap but continuous spectrum. The order of the deconfining transition depends on the subleading terms of the potential and can be of any order larger than two.

Gurdogan+Gursoy+E.K.

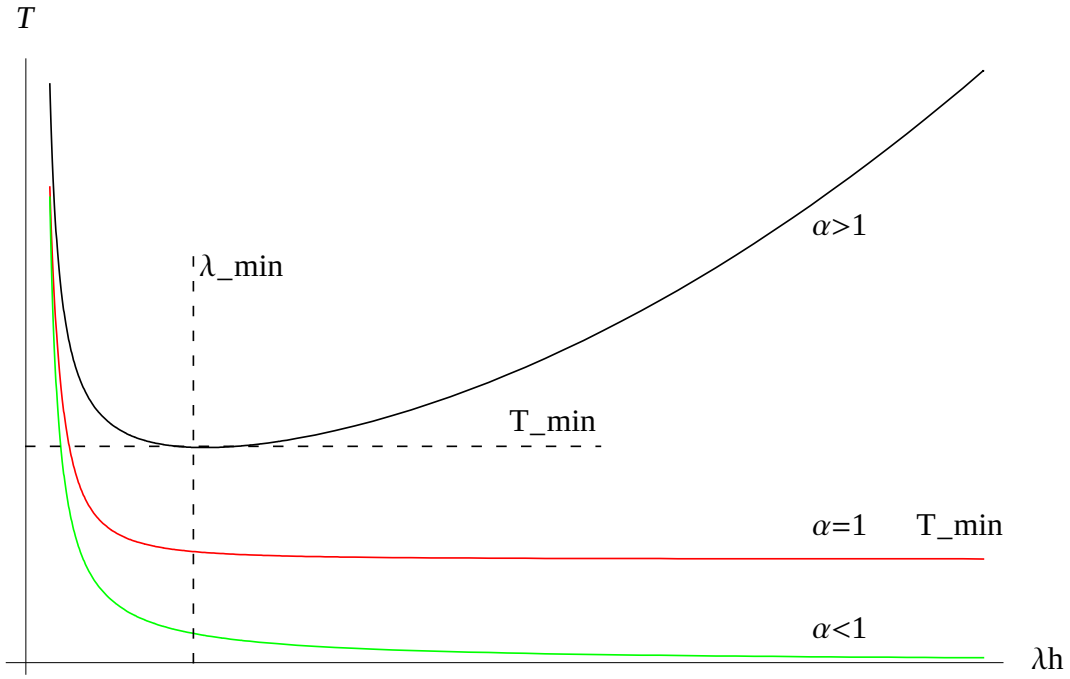
T
λ_min
α>1
T_min
α=1
T_min
α<1
λh

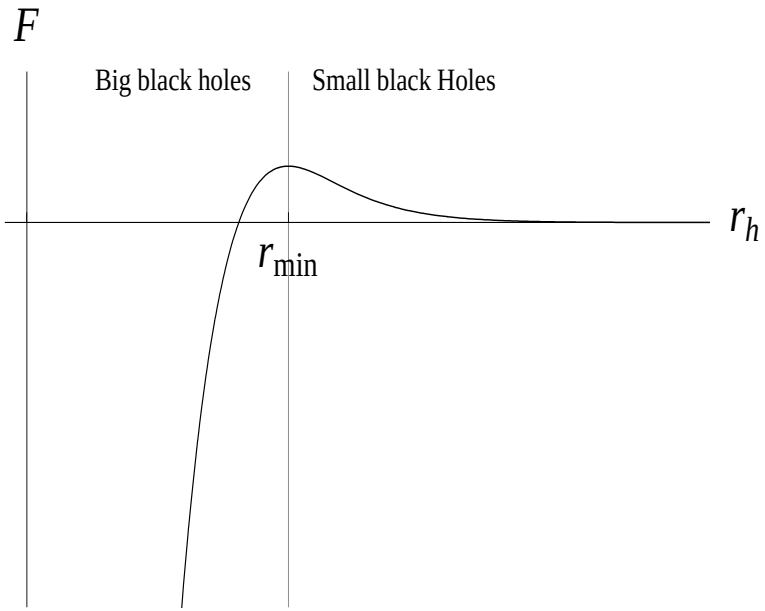
F
Big black holes
Small black Holes
r_h
r_{min}

Classification of zero temperature solutions

For any positive+monotonic potential $V(\lambda)$, $\lambda \equiv e^{\phi}$ with the asymptotics :

$$V(\lambda) = V_0 + V_1\lambda + V_2\lambda^2 + \ldots \quad V_0 > 0, \qquad \lambda \to 0$$

$$V(\lambda) = V_\infty \lambda^{2Q} (\log \lambda)^P, \quad V_\infty > 0, \qquad \lambda \to \infty$$

the zero-temperature superpotential equation has three types of solutions, that we name the *Generic*, the *Special*, and the *Bouncing* types:

• A continuous one-parameter family that has a fixed power-law expansion near $\lambda = 0$, and reaches the asymptotic large-λ region where it grows as

$$W \simeq C_b\ \lambda^{4/3} \qquad \lambda \to \infty \quad , \quad C_b > 0$$

These solutions lead to backgrounds with "bad" (i.e. non-screened) singularities at finite r_0,

$$b(r) \sim (r_0 - r)^{1/3}, \qquad \lambda(r) \sim (r_0 - r)^{-1/2}$$

We call this solution *generic*.

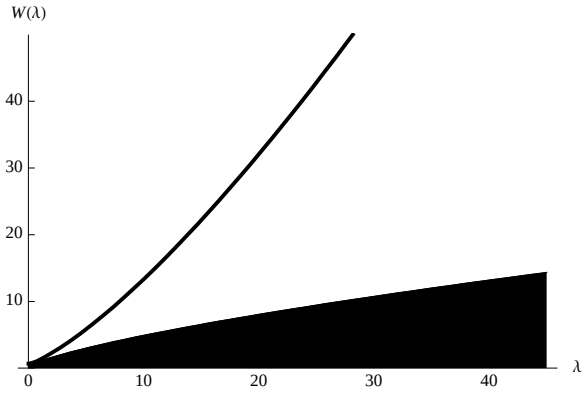

• A unique solution, which also reaches the large-λ region, but slower:

$$W(\lambda) \sim W_\infty \lambda^Q (\log \lambda)^{P/2}, \qquad W_\infty = \sqrt{\frac{27 V_\infty}{4(16 - 9Q^2)}}$$

This leads to a repulsive singularity, provided $Q < 2\sqrt{2}/3$ [**?**]. We call this the *special* solution.

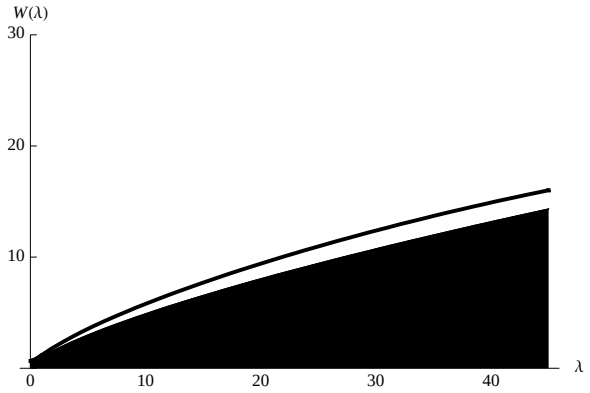

• A second continuous one-parameter family where $W(\lambda)$ does not reach the asymptotic region. These solutions have two branches that both reach $\lambda = 0$ (one in the UV, the other in the IR) and merge at a point λ_* where $W(\lambda_*) = \sqrt{27V(\lambda_*)/64}$. The IR branch is again a "bad" singularity at a finite value r_0, where $W \sim \lambda^{-4/3}$, and

$$b(r) \sim (r_0 - r)^{1/3}, \qquad \lambda(r) \sim (r_0 - r)^{1/2}.$$

We call this solution *bouncing*.

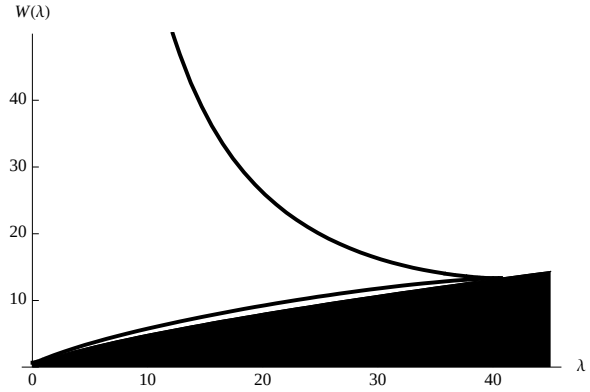

The special solution marks the boundary between the generic solutions, that reach the asymptotic large-λ region as $\lambda^{4/3}$ and the bouncing ones, that don't reach it.

If $Q > 4/3$, only bouncing solutions exist.

In all types of solutions the UV corresponds to the region $\lambda \to 0$ on the W_+ branch. There the behavior of W_+ is universal: a power series in λ with *fixed* coefficients, plus a subleading non-analytic piece which depends on an arbitrary integration constant C_w:

$$W = \sum_{i=1}^{\infty} W_i \lambda^i + C_w \lambda^{16/9} e^{-\frac{16W_0}{9W_1}\frac{1}{\lambda}} [1 + O(\lambda)]$$

All the power series coefficients W_i are completely determined by the coefficients in the small λ expansion of $V(\lambda)$, the first few being:

$$W_0 = \frac{\sqrt{27V_0}}{8}, \quad W_1 = \frac{V_1}{16}\sqrt{\frac{27}{V0}}, \quad W_2 = \frac{\sqrt{27}(64V_0V_2 - 7V1^2)}{1024V_0^{3/2}}$$

RETURN

The $\gamma\delta = 1$ solutions

$$ds^2 = -\frac{V(r)dt^2}{\left[1-\left(\frac{r_-}{r}\right)^{3-\delta^2}\right]^{\frac{4(1-\delta^2)}{(3-\delta^2)(1+\delta^2)}}} + e^{\delta\phi}\frac{dr^2}{V(r)} + r^2\left[1-\left(\frac{r_-}{r}\right)^{3-\delta^2}\right]^{\frac{2(\delta^2-1)^2}{(3-\delta^2)(1+\delta^2)}}\left(dx^2+dy^2\right),$$

$$V(r) = \left(\frac{r}{\ell}\right)^2 - 2\frac{m\ell^{-\delta^2}}{r^{1-\delta^2}} + \frac{(1+\delta^2)q^2\ell^{2-2\delta^2}}{4\delta^2(3-\delta^2)^2 r^{4-2\delta^2}} \quad , \quad (r_\pm)^{3-\delta^2} = \ell^{2-\delta^2}\left[m \pm \sqrt{m^2 - \frac{(1+\delta^2)q^2}{4\delta^2(3-\delta^2)^2}}\right]$$

$$e^{\phi} = \left(\frac{r}{\ell}\right)^{2\delta}\left[1-\left(\frac{r_-}{r}\right)^{3-\delta^2}\right]^{\frac{4\delta(\delta^2-1)}{(3-\delta^2)(1+\delta^2)}} \quad , \quad \mathcal{A} = \left(\Phi - \frac{q\ell^{2-\delta^2}}{(3-\delta^2)r^{3-\delta^2}}\right)dt \quad , \quad \Phi = \frac{q\ell^{2-\delta^2}}{(3-\delta^2)r_+^{3-\delta^2}}$$

where the parameters m and q are integration constants linked to the gravitational mass and the electric charge. There is an overall scale ℓ

$$\ell^2 = \frac{\delta^2-3}{\Lambda}.$$

RETURN

The $\gamma = \delta$ solutions

$$ds^2 = -V(r)dt^2 + e^{\delta\phi}\frac{dr^2}{V(r)} + r^2\Big(dx^2 + dy^2\Big)$$

$$V(r) = \left(\frac{r}{\ell}\right)^2 - 2m\ell^{-\delta^2}r^{\delta^2-1} + \frac{q^2}{4(1+\delta^2)r^2}$$

$$e^{\phi} = \left(\frac{r}{\ell}\right)^{2\delta} \quad , \quad \mathcal{A} = \left(\Phi - \frac{\ell^{\delta^2}q}{(1+\delta^2)r^{1+\delta^2}}\right)dt \quad , \quad \Phi = \frac{q\ell^{\delta^2}}{(1+\delta^2)r_+^{1+\delta^2}}$$

- There is a "BPS condition" for the existence of a horizon

$$m \geq \frac{2q^{\frac{3-\delta^2}{2}}}{1+\delta^2}$$

- U(r) has two roots $0 < r^- < r^+$. The two coincide at the extremality limit, $(1+\delta^2)m = 2q^{\frac{3-\delta^2}{2}}$.

- There are two distinct regimes:

$$0 \leq \delta^2 \leq 1 \qquad\qquad 1 \leq \delta^2 \leq 3$$

- $0 \leq \delta^2 \leq 1$

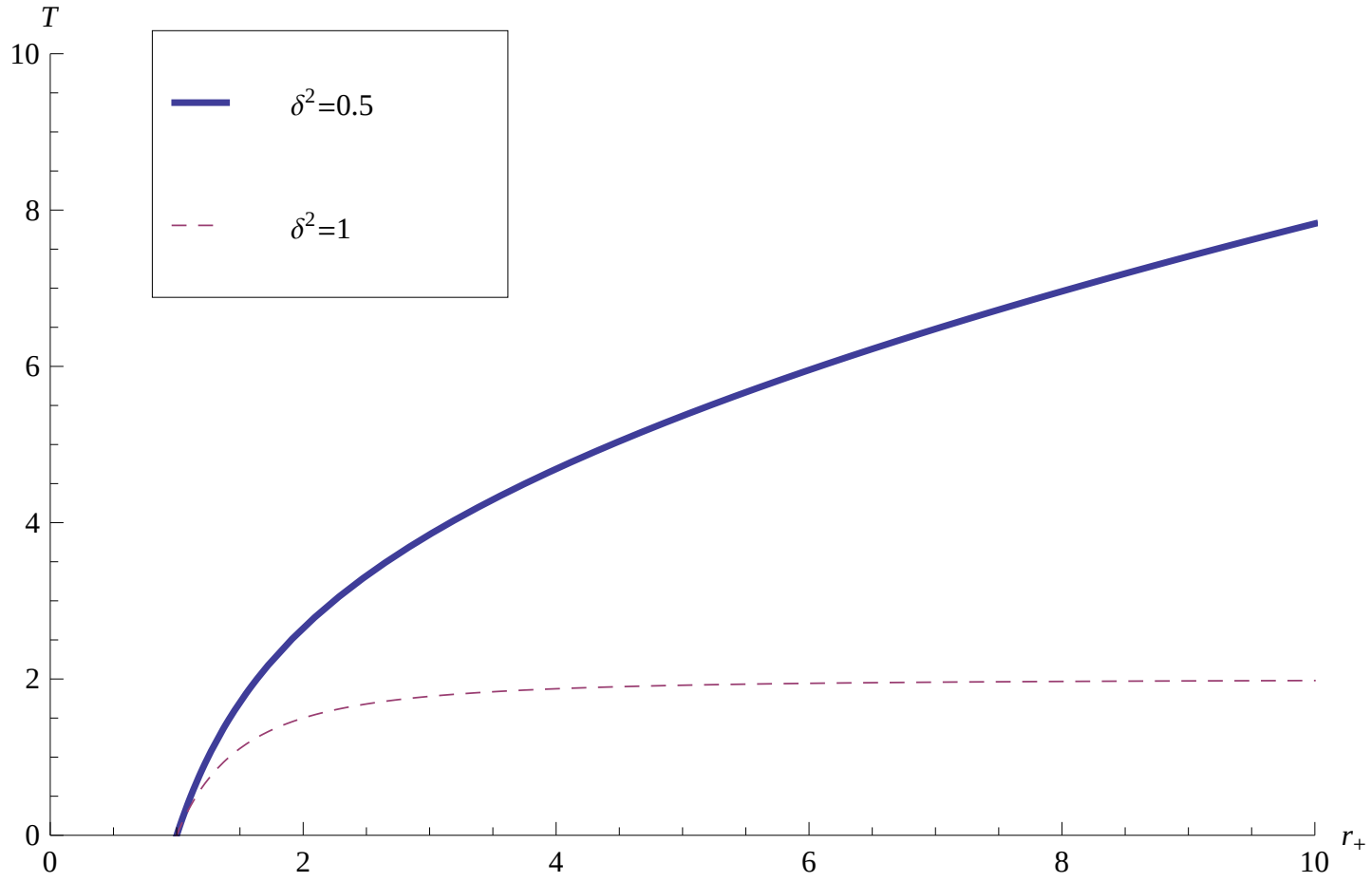

- Temperature as a function of horizon position

- $0 \leq \delta^2 \leq 1$

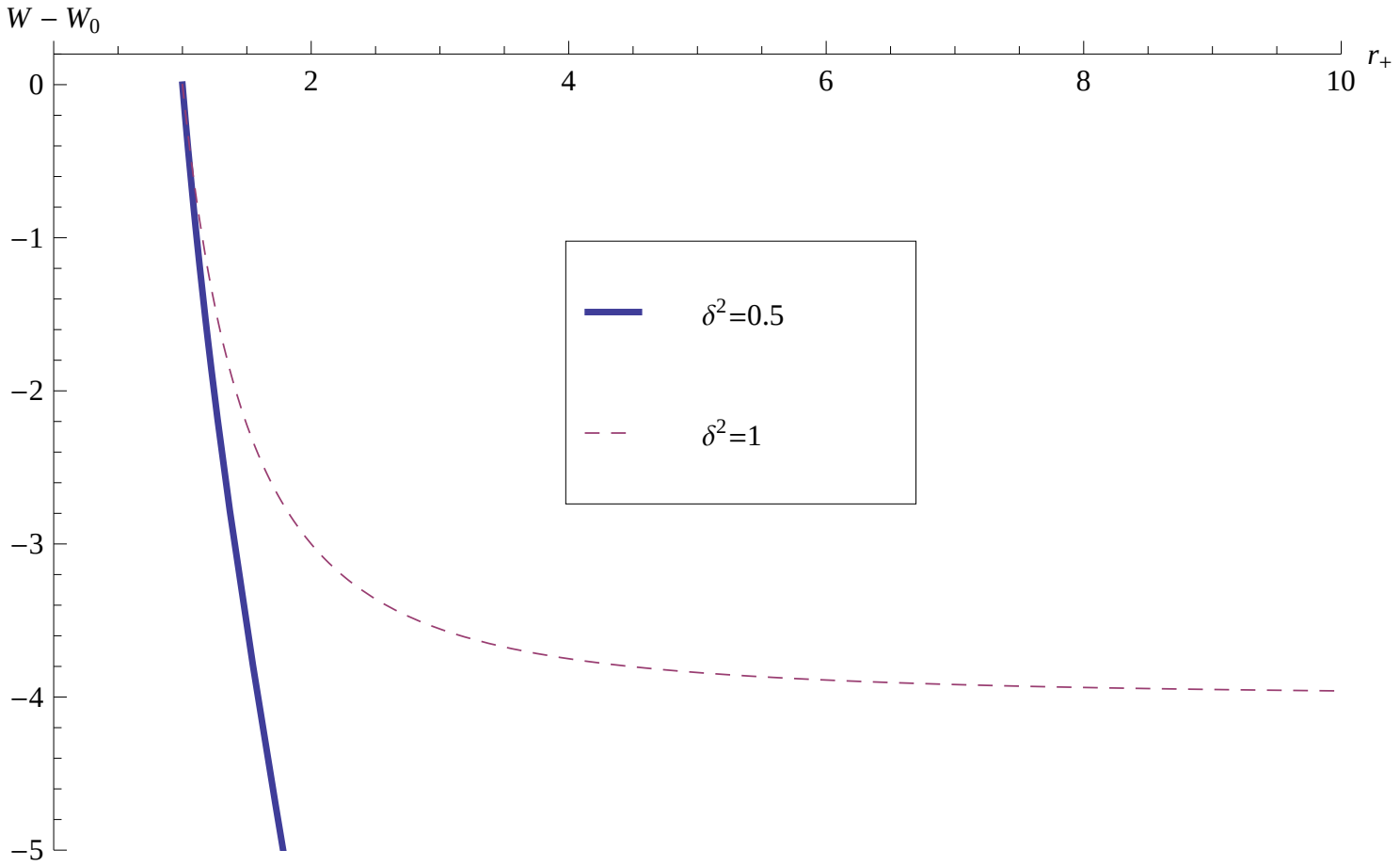

- Difference of free energies vs horizon position

- The BH always dominates

- $1 \leq \delta^2 \leq 3$

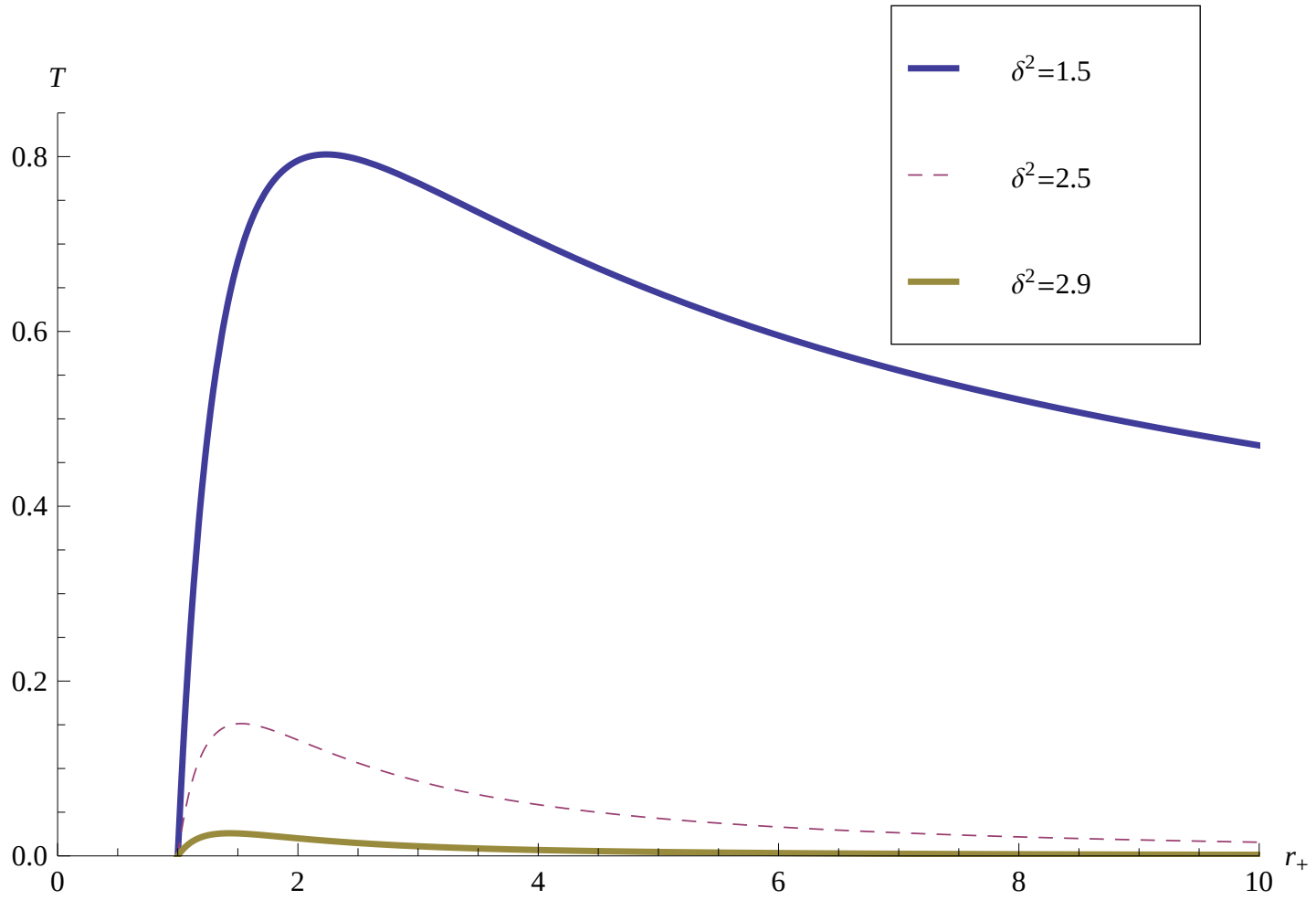

- Temperature vs horizon position

- $1 \leq \delta^2 \leq 3$

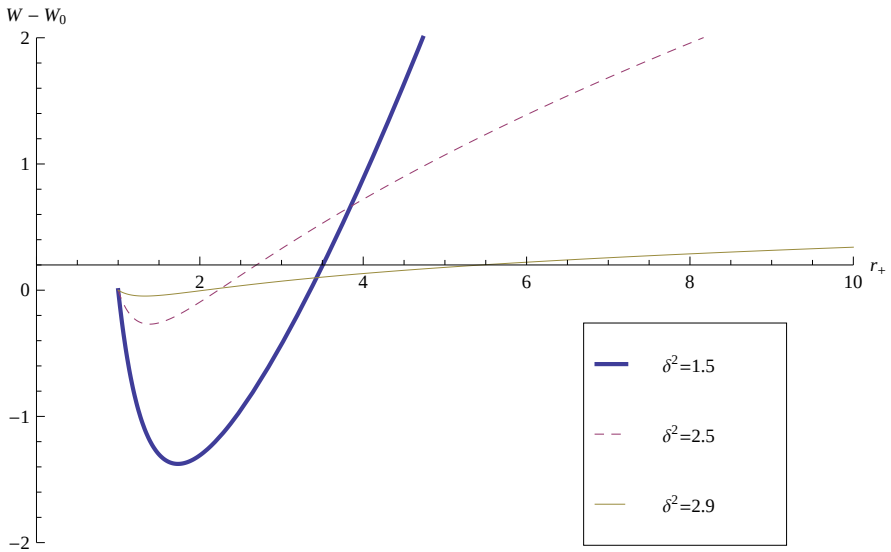

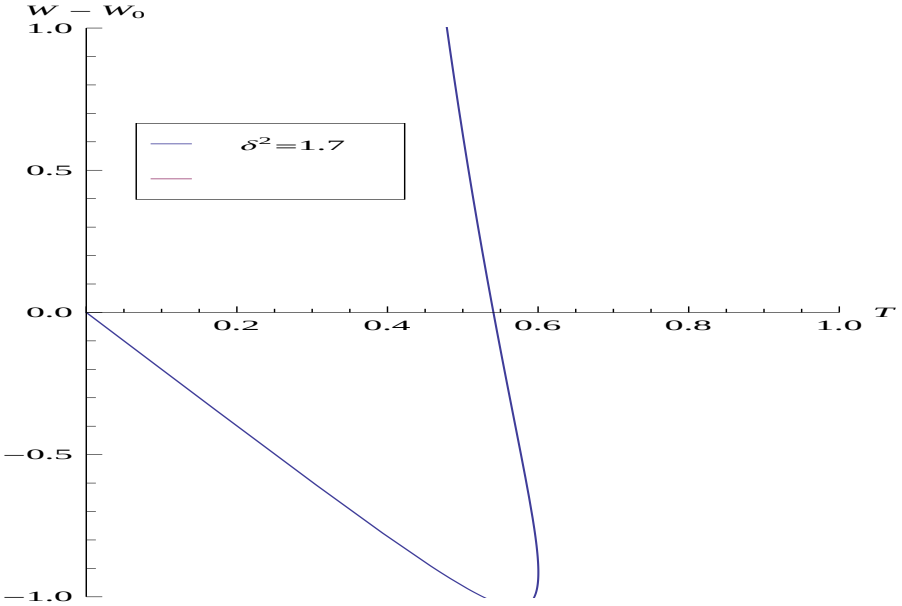

- Difference of free energies as a function of horizon position and temperature.

- The BH dominates at low temperatures up to the phase transition

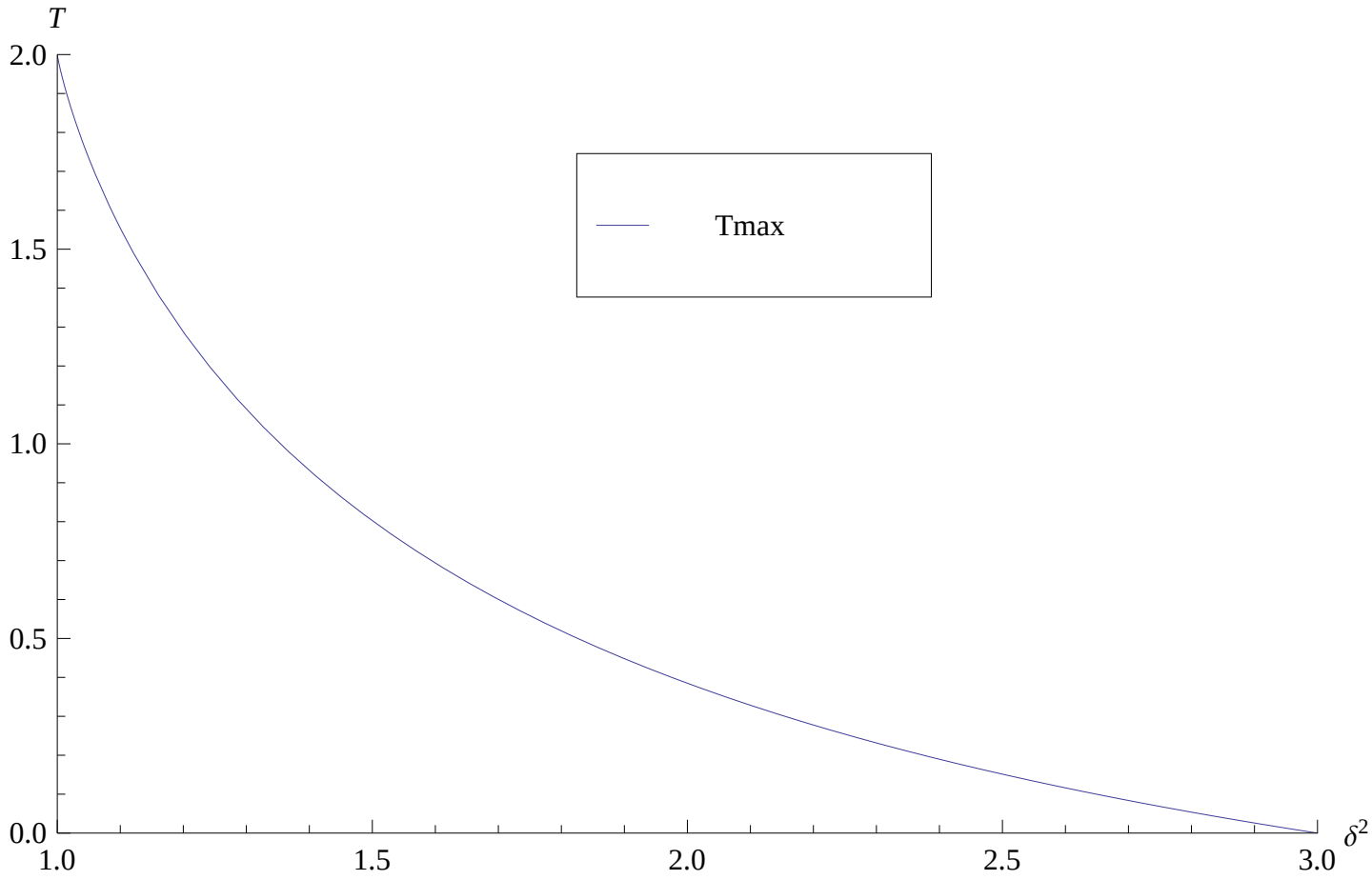

- The maximum temperature as a function of δ^2.

Conductivity of the $\gamma\delta = 1$ solutions

In the first two regimes $0 \leq \delta^2 \leq 1 + \frac{2}{\sqrt{3}}$ the AC conductivity is

$$\sigma(\omega) \simeq \omega^n\,, \qquad n = \frac{(3-\delta^2)(5\delta^2+1)}{|3\delta^4 - 6\delta^2 - 1|} - 1\,.$$

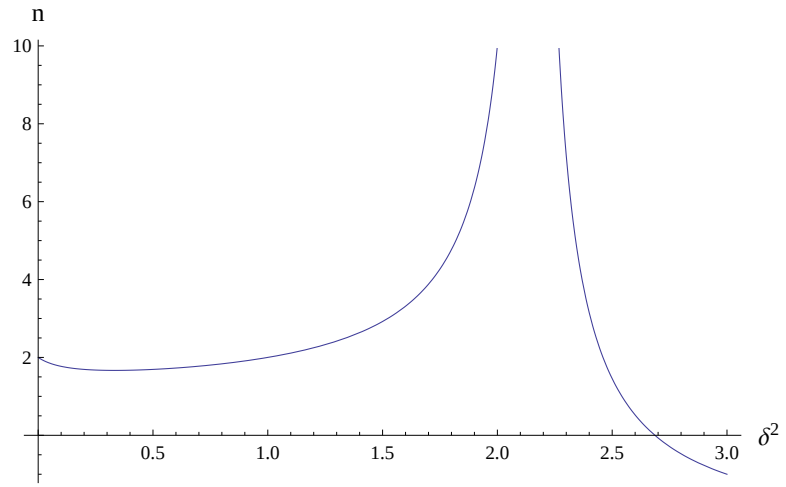

- The exponent is always larger than 5/3 in the region, $0 \leq \delta^2 < 1 + \frac{2}{\sqrt{3}}$ and diverges at $\delta^2 = 1 + \frac{2}{\sqrt{3}}$.

- The system behaves as a conductor.

- The system is again conducting for $\frac{1}{4}(5+\sqrt{33}) < \delta^2 < 3$.

The DC resistivity is plotted below.

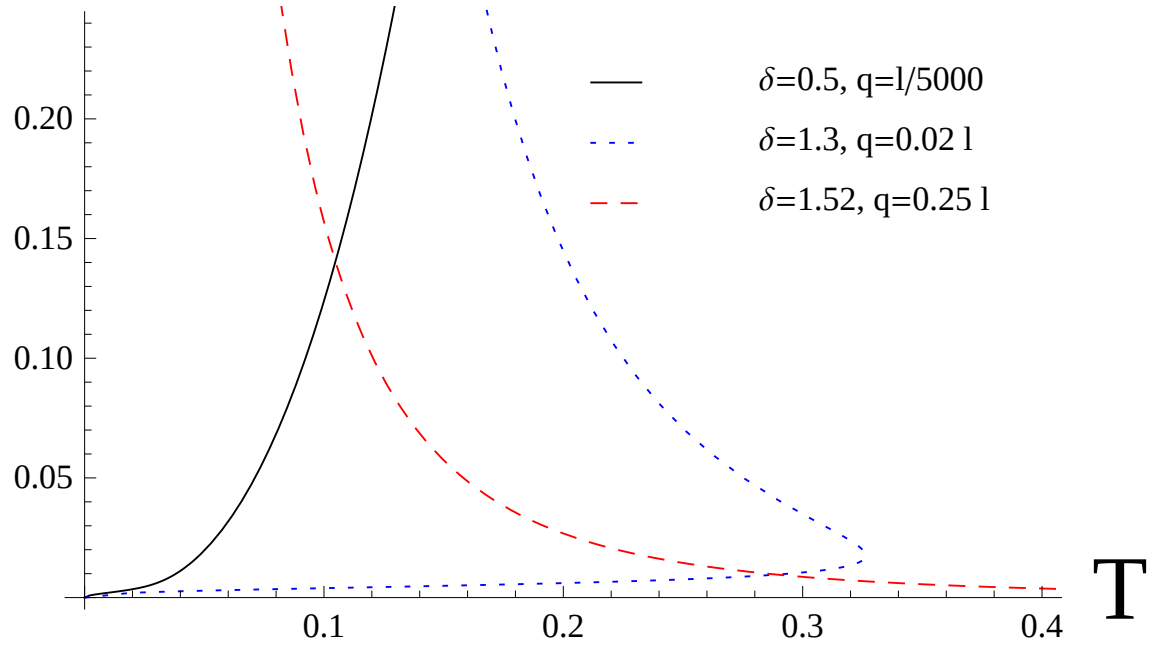

The leading behavior at low temperature is

$$\rho_{\text{leading}} \sim \frac{T_f}{J^t}\left(\frac{q}{\ell}\right)^{\frac{2\delta(\delta(3-\delta^2)+(1+\delta^2)k)}{1+6\delta^2-3\delta^4}} (\ell T)^{\frac{2(\delta^2-1)(\delta^2-1+2k\delta)}{1+6\delta^2-3\delta^4}}$$

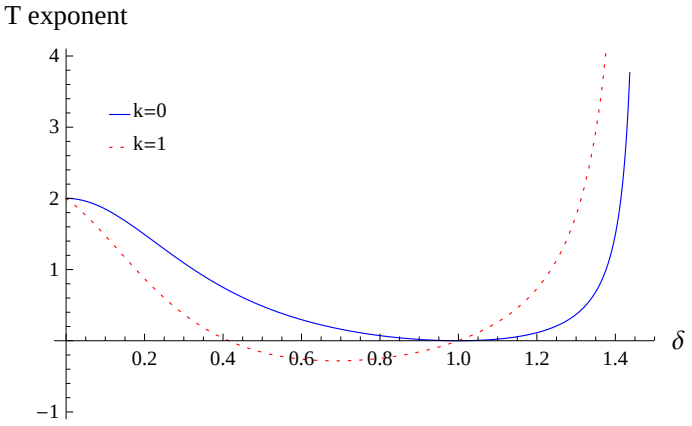

- It is one at $\delta^2 = 1 + \frac{2}{\sqrt{5}}$.

QC systems with Schröndiger symmetry

• The solutions found, can be put in a different coordinate system that realizes $z = 2$ Schröndiger symmetry.

Son, Balasubramanian+McGreevy

• Consider the simplest example: AdS-Schwarzschild Black hole in light-cone coordinates boosted by an arbitrary boost.

$$ds^2 = \frac{\ell^2}{r^2}\left[\frac{(1-f(r))}{4b^2}(dx^+)^2 - (1+f(r))dx^+dx^- + (1-f(r))b^2(dx^-)^2 + dx^2 + dy^2 + \frac{dr^2}{f(r)}\right]$$

• This realizes $z = 2$ non-relativistic Schrödinger symmetry in 2 spatial dimensions.

Golberger (08), Barbon+Fuertes(08), Maldacena+Martelli+Tachikawa (08)

• One can compute the conductivities using the Karch-O'Bannon formalism applied in this context

Kim+Yamada (10)

The conductivity in the absence of magnetic field (but with light-cone electric field) reads

$$\rho = \frac{\rho_0}{\sqrt{\frac{J^2}{t^2 A(t)} + \frac{t^3}{\sqrt{A(t)}}}}\,,\ A(t) = t^2 + \sqrt{1+t^4} \quad , \quad t = \frac{\pi \ell T b}{\sqrt{2b\tilde{E}_b}}\,,\ J^2 = \frac{64\sqrt{2}\langle J^+\rangle^2}{(\tilde{\mathcal{N}} b\cos^3\theta)^2(2b\tilde{E}_b)^3}.$$

When the "drag" term dominates

$$\rho \sim t\sqrt{t^2+\sqrt{1+t^4}}$$

showing a transition from linear to quadratic behavior.

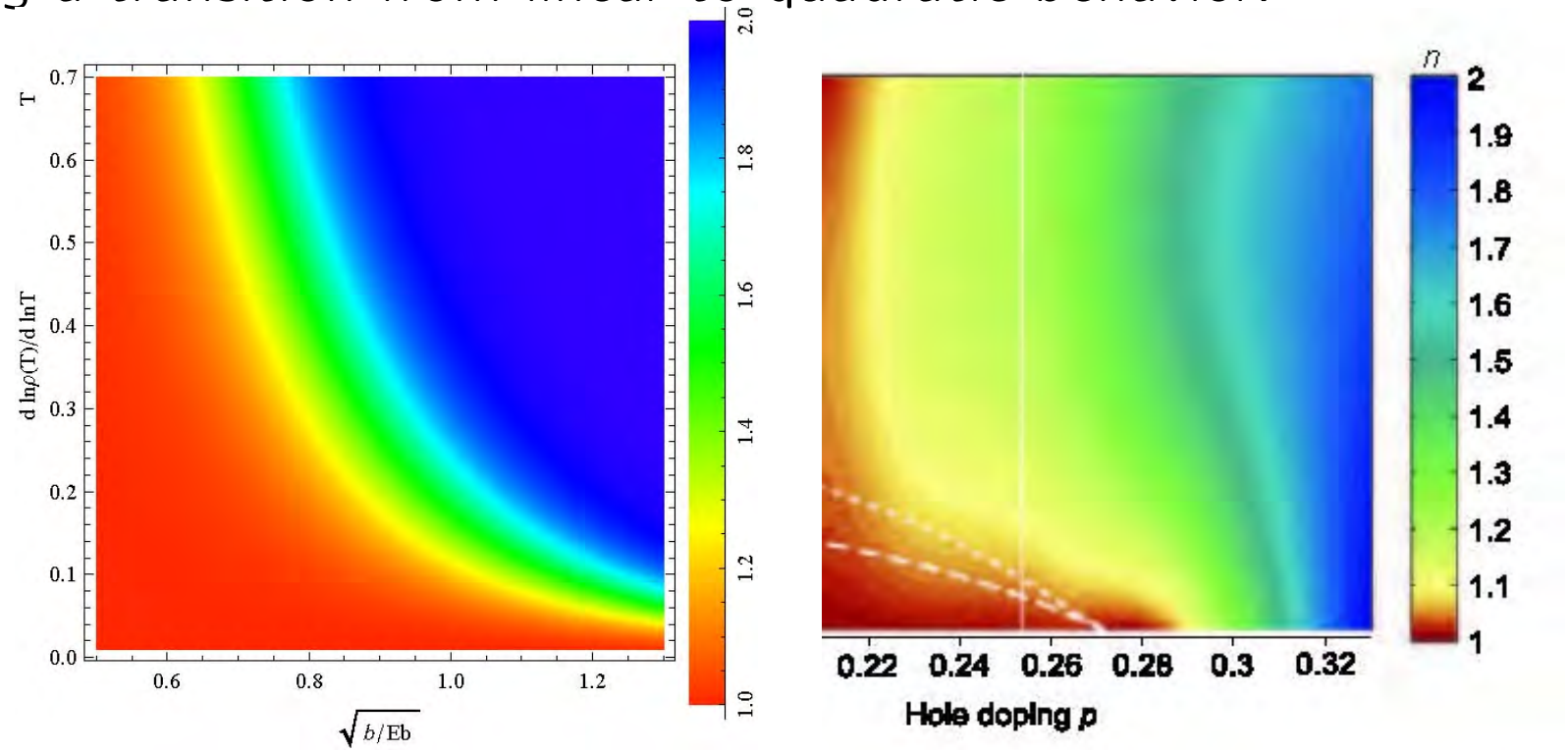

$La_{2-x}Sr_xCuO_4$ in R. A. Cooper et al., Science **323**, 603 (2009).

• This transition can be achieved by decreasing the light-cone electric field, E_b. It interpolates between AdS and z=2 Lifshitz scaling.

.

- By parametrizing $\rho = a_1 T + a_2 T^2$ we obtain $\alpha_1 \sim \sqrt{E_b}$ and $\rho_2 = constant$.

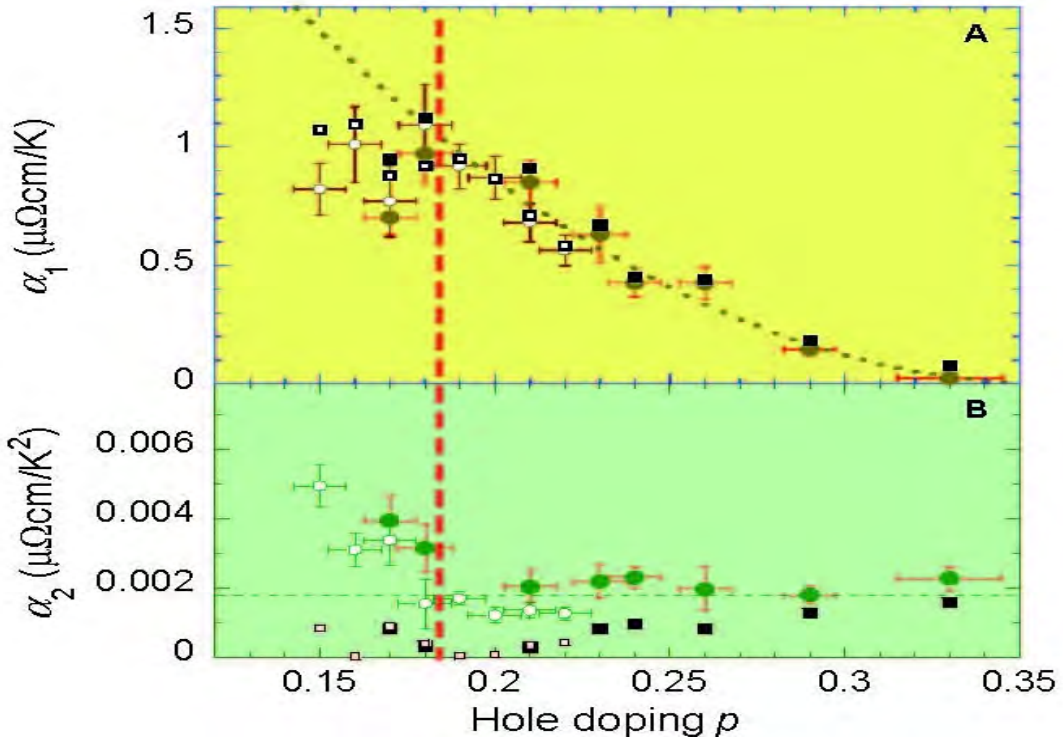

$La_{2-x}Sr_xCuO_4$ in R. A. Cooper et al., Science **323**, *603 (2009).*

Resistivity at non-zero magnetic field

At finite magnetic field

$$\sigma^{yy} = \sigma_0 \frac{\sqrt{\mathcal{F}_+(t) J^2 + t^4 \sqrt{\mathcal{F}_+(t)\mathcal{F}_-(t)}}}{\mathcal{F}_-(t)} \quad , \quad \sigma^{yz} = \bar{\sigma}_0 \frac{\mathcal{B}}{\mathcal{F}_-(t)}$$

$$\mathcal{F}_\pm = \sqrt{\left(\mathcal{B}^2 + t^4\right)^2 + t^4} \mp \mathcal{B}^2 + t^4 \quad , \quad \mathcal{B} = \frac{\tilde{B}_b}{2b\tilde{E}_b}$$

- The scaling variable $\mathcal{B} = \frac{\tilde{B}_b}{2b\tilde{E}_b}$ seems to be in agreement with experimental data

$Tl_2Ba_2CuO_{6+\delta}$ in A. W. Tyler et al., Phys. Rev. B **57**, *R278 (1998).*

- The inverse Hall angle is defined as the ratio between Ohmic conductivity and Hall conductivity as

$$\cot \Theta_H = \frac{\sigma^{yy}}{\sigma^{yz}}$$

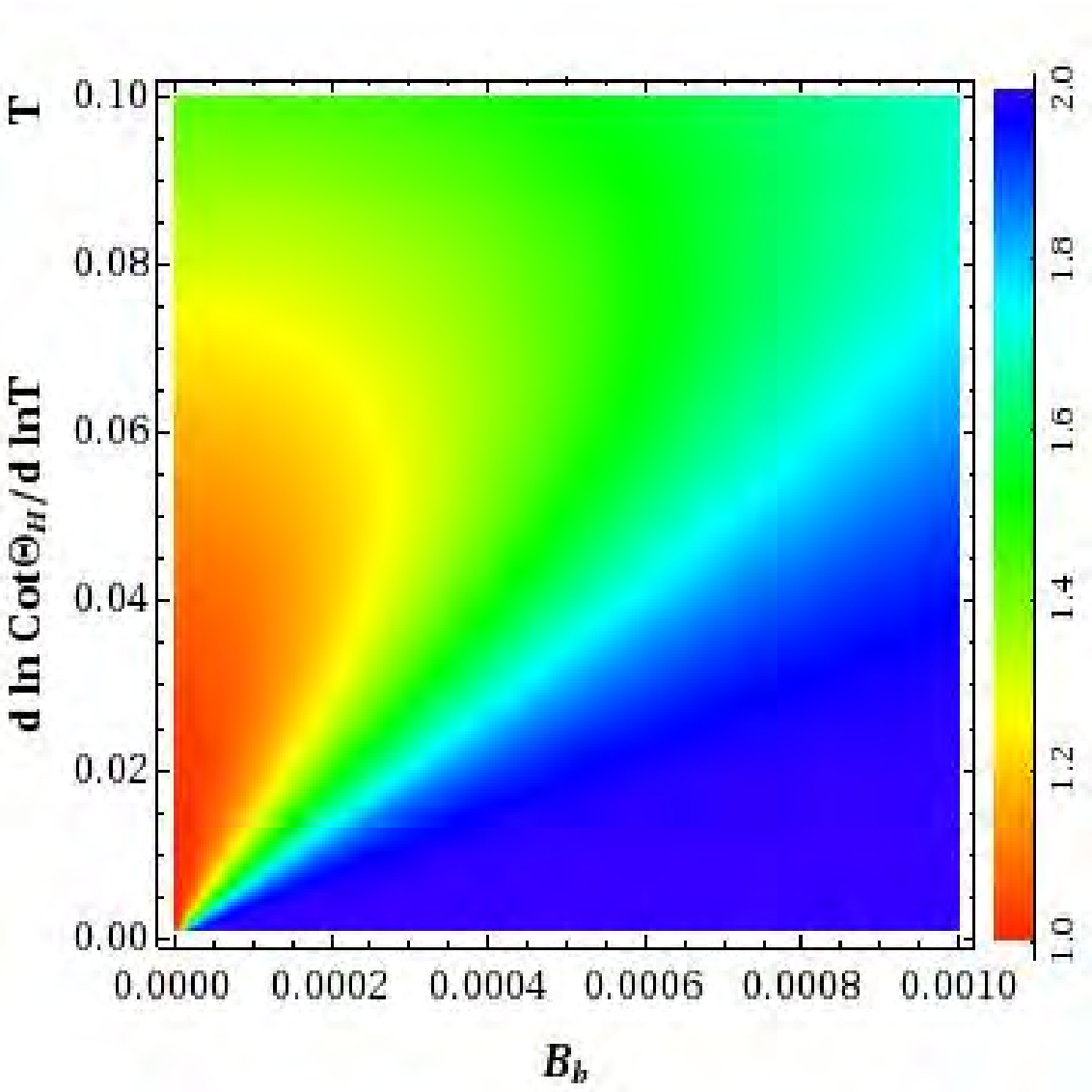
T
0.10
0.08
0.06
0.04
0.02
0.00
d ln CotΘ_H/d lnT
0.0000
0.0002
0.0004
0.0006
0.0008
0.0010
B_b
2.0
1.8
1.6
1.4
1.2
1.0

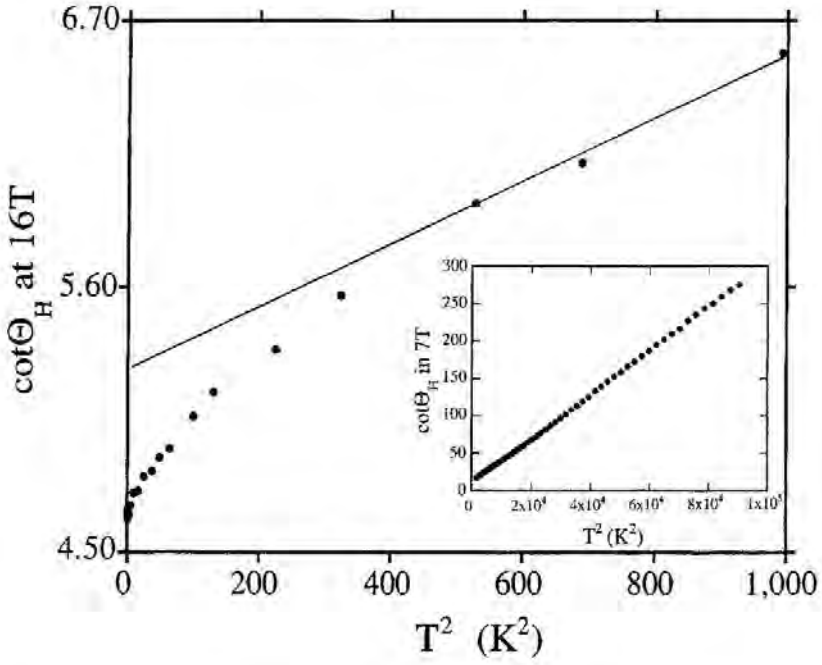

FIG. 8. The cotangent of the Hall angle plotted against T^2 below 30 K. The low-temperature data deviate significantly from the $A+BT^2$ dependence seen at high temperatures (inset), whose extrapolation is shown by the solid line.

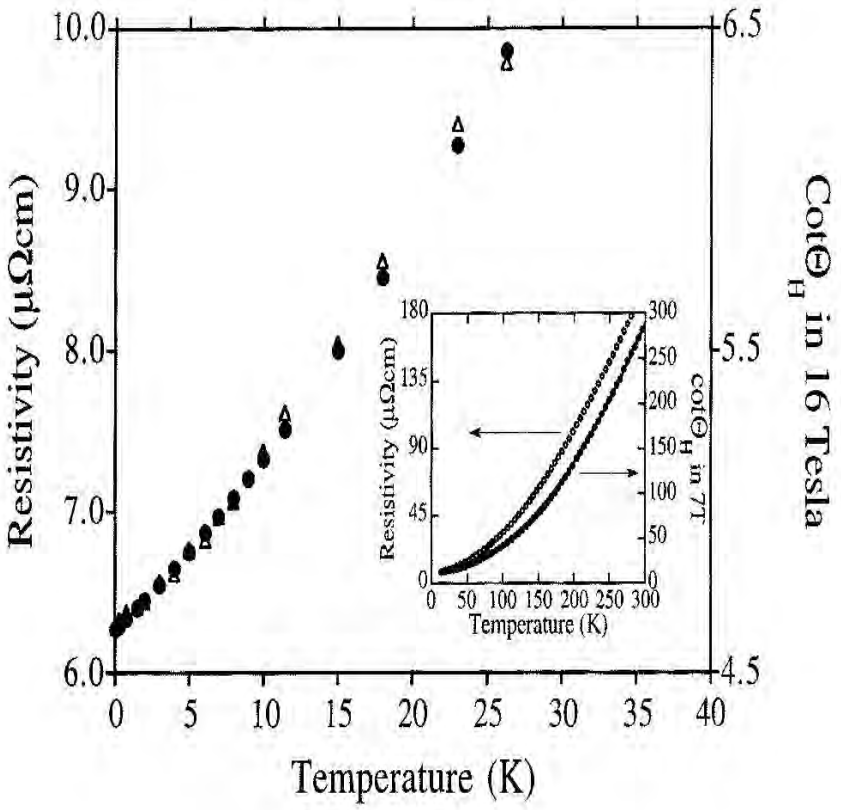

The resistivity and $cot\Theta_H$ are correlated at low temperatures in $Tl_2Ba_2CuO_{6+\delta}$

Mackenzie et al. Phys. Rev. B **53**, *5848 (1996).*

The Hall Conductivity $R_H = \left.\frac{\rho_{yz}}{B}\right|_{B=0}$ is constant in the two different regimes (linear and quadratic)

$$R_H \simeq \frac{\bar{\sigma}_0}{\sigma_0^2 J^2} \sim E_b$$

and decreases with doping.

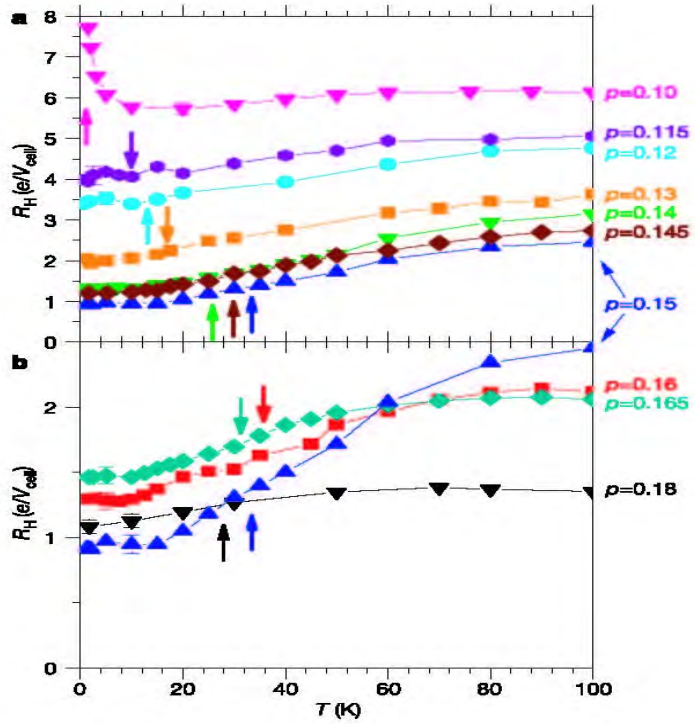

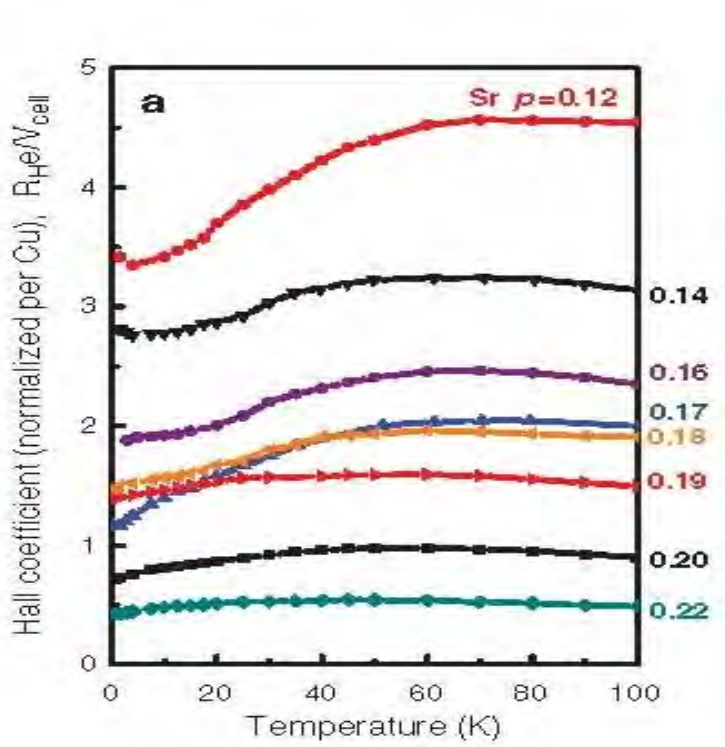

$Bi_2Sr_{2-x}La_xCuO_{6+\delta}$ from F. F. Balakirev et al., NATURE 424 (2003) 912; Phys. Rev. Lett. **102**, *017004 (2009).*

- The magnetoresistance

$$\frac{\Delta\rho}{\rho} = \frac{\rho_{yy}(B) - \rho_{yy}(0)}{\rho_{yy}(0)}$$

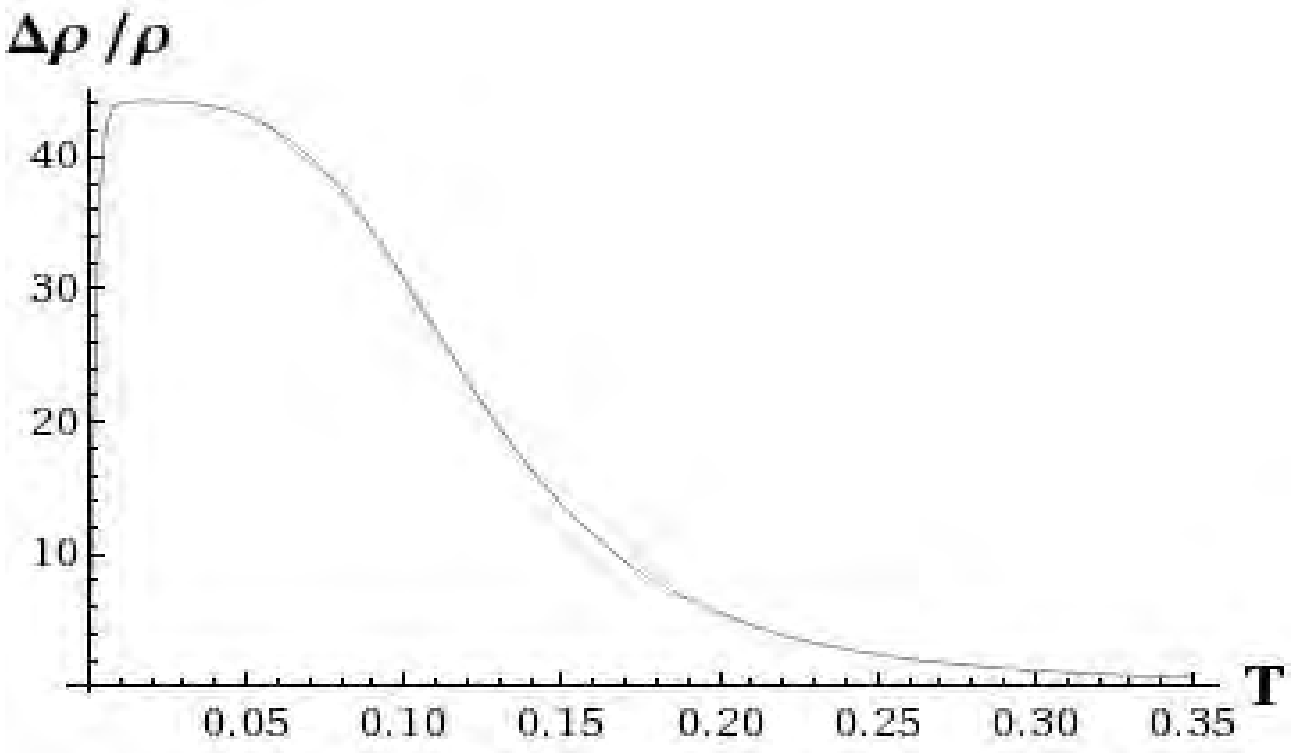

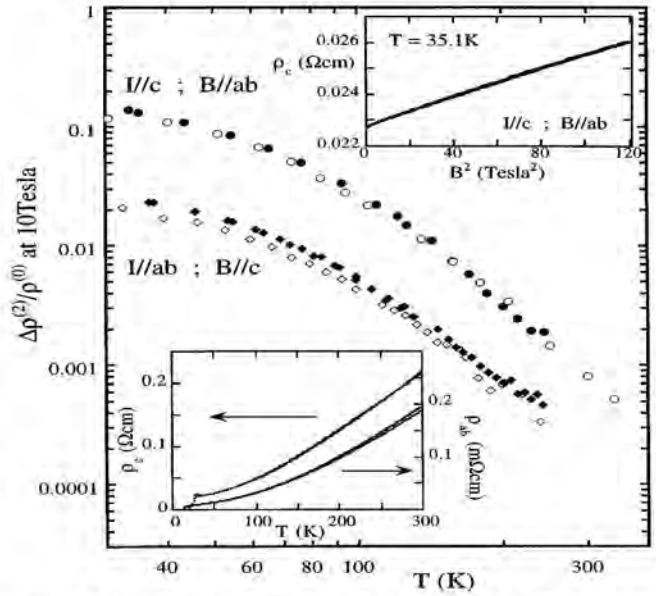

FIG. 1. T dependences of the B^2 terms $\Delta\rho^{(2)}/\rho^{(0)}$ at 10 T for c-axis MR (circles) and a-b plane MR (diamonds) in overdoped $Tl_2Ba_2CuO_6$. Data for two crystals are shown in each case. Bottom inset: Zero-field $\rho_c(T)$ and $\rho_{ab}(T)$ for the crystals shown in the main figure. Top inset: MR field sweep at 35.1 K for $\mathbf{I} \parallel c$, $\mathbf{B} \parallel ab$.

N. E. Hussey et al., Phys. Rev. Lett, **76**, *122 (1996).*

- We find that the modified Köhler rule

$$\tilde{K} = (\cot\Theta_H)^2 \frac{\Delta\rho}{\rho} \simeq \text{temperature} \quad \text{independent}$$

is valid in regions (linear+quadratic), as demanded by data,

J. M. Harris et al., Phys. Rev. Lett, **75**, *1391 (1995).*

- We also find that the Köhler rule

$$K = \rho^2 \frac{\Delta\rho}{\rho} \simeq \text{temperature} \quad \text{independent}$$

is approximately valid in the same regions.

This is not supported by the data at high temperatures but is valid at low temperatures.

The β functions

The second order equations for the system of two scalars plus metric can be written as first order equations for the β-functions

Gursoy+Kiritsis+Nitti

$$\frac{d\lambda}{dA} = \beta(\lambda, T) \quad , \quad \frac{dT}{dA} = \gamma(\lambda, T)$$

The equations of motion boil down to two partial non-linear differential equations for β, γ.

Such equations have also branches as for DBI and non-linear scalar actions the relation of $e^{-A}A'$ with the potentials is a polynomial equation of degree higher than two.

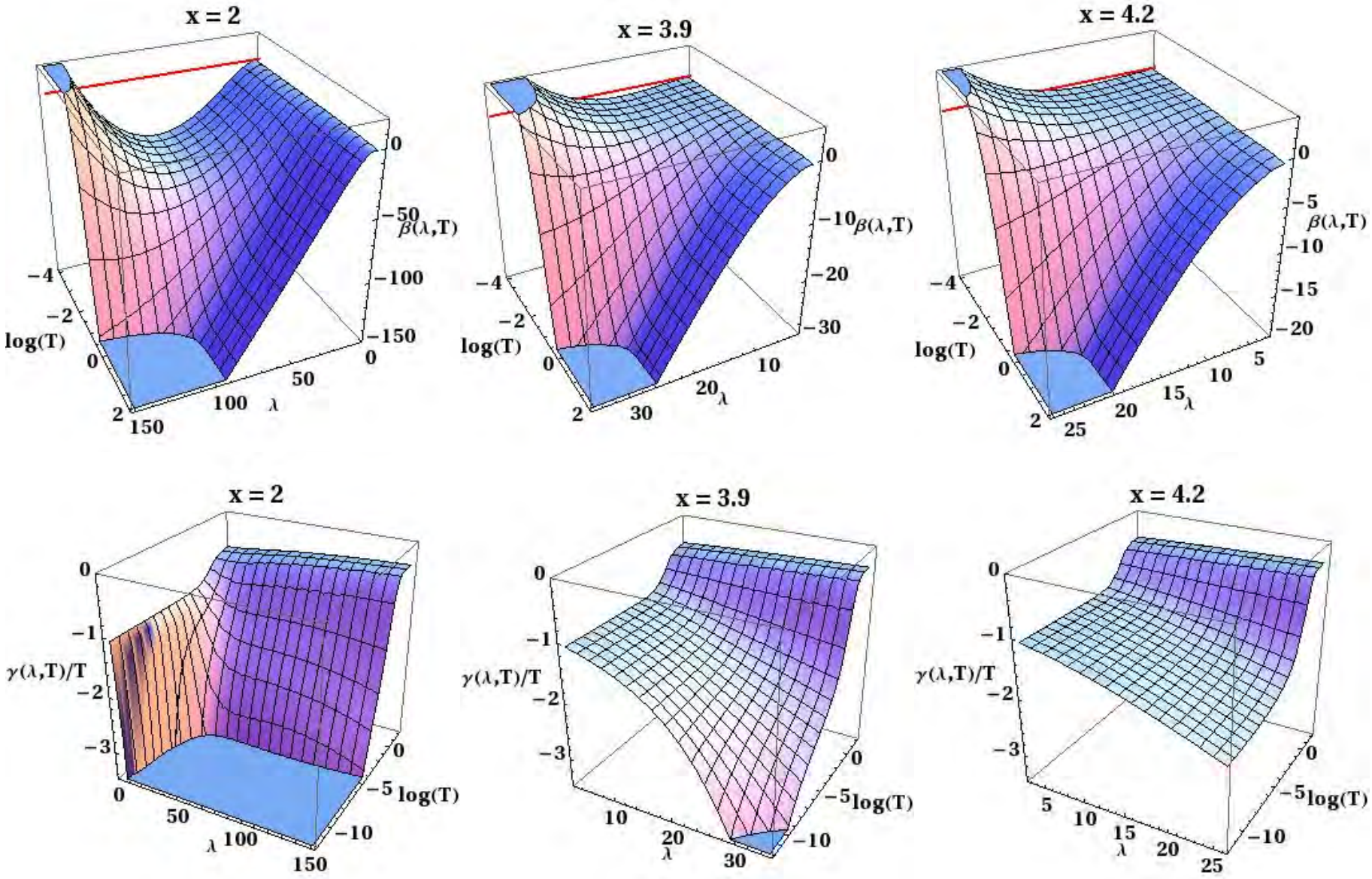

The red lines are added on the top row at $\beta = 0$ in order to show the location of the fixed point.

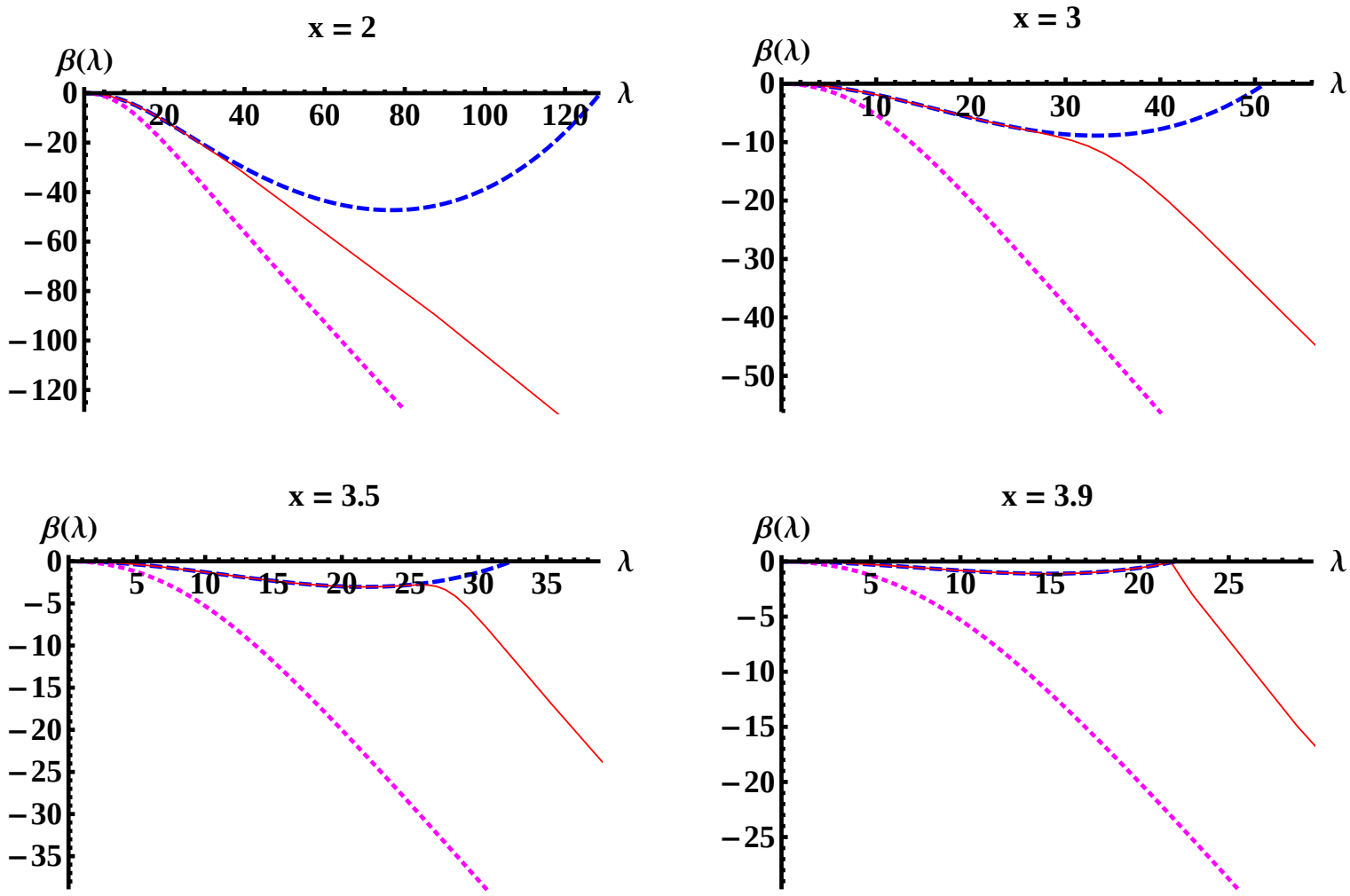

The β-functions for vanishing quark mass for various values of x. The red solid, blue dashed, and magenta dotted curves are the β-functions corresponding to the full numerical solution $(d\lambda/dA)$ along the RG flow, the potential $V_{\text{eff}} = V_g - xV_{f0}$, and the potential V_g, respectively.

The free energy

The free energy difference between the ChS and ChSB $m_q = 0$ solutions

Chiral symmetry breaking solution favored whenever it exists ($x < x_c$)

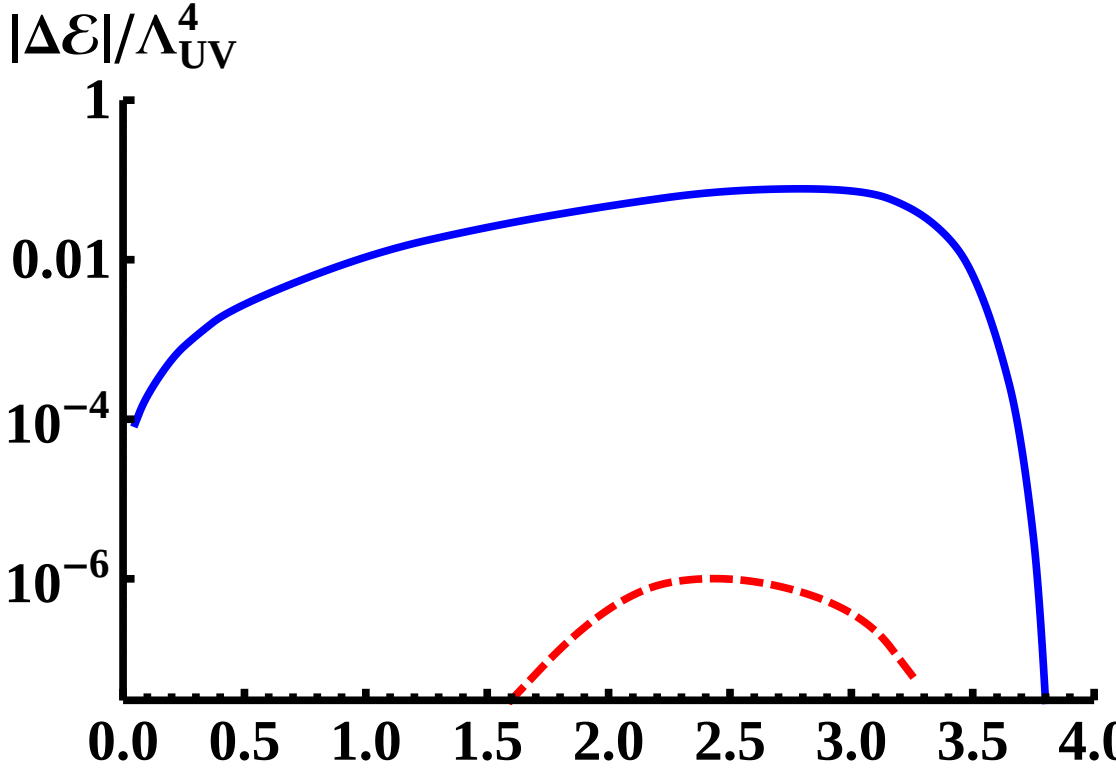

- The Efimov minima have free energies ΔE_n with

$$\Delta E_0 > \Delta E_1 > \Delta E_2 > \cdots$$

BKT scaling, II

We can derive

$$\Delta_{\rm IR}(4-\Delta_{\rm IR}) = -m^2_{\rm IR}\ell^2_{\rm IR} = G(\lambda_*, x) \ ,$$

where

$$G(\lambda, x) \equiv \frac{24a(\lambda)}{h(\lambda)(V_g(\lambda) - xV_{f0}(\lambda))} \ .$$

and by matching behaviors

$$\sigma \sim \frac{1}{r^3_{\rm UV}} \exp\left(-\frac{2K}{\sqrt{\lambda_* - \lambda_c}}\right) \sim \frac{1}{r^3_{\rm UV}} \exp\left(-\frac{2\hat{K}}{\sqrt{x_c - x}}\right) \ .$$

x_c and λ_c are defined by $G(\lambda_*(x_c), x_c) = 4$ and $G(\lambda_c, x) = 4$, respectively, so that $\lambda_* = \lambda_c$ at $x = x_c$. we obtain

$$K = \frac{\pi}{\sqrt{\frac{\partial}{\partial\lambda}G(\lambda_c, x)}} \ ; \qquad \hat{K} = \frac{\pi}{\sqrt{-\frac{d}{dx}G(\lambda_*(x), x)\Big|_{x=x_c}}} \ .$$

.

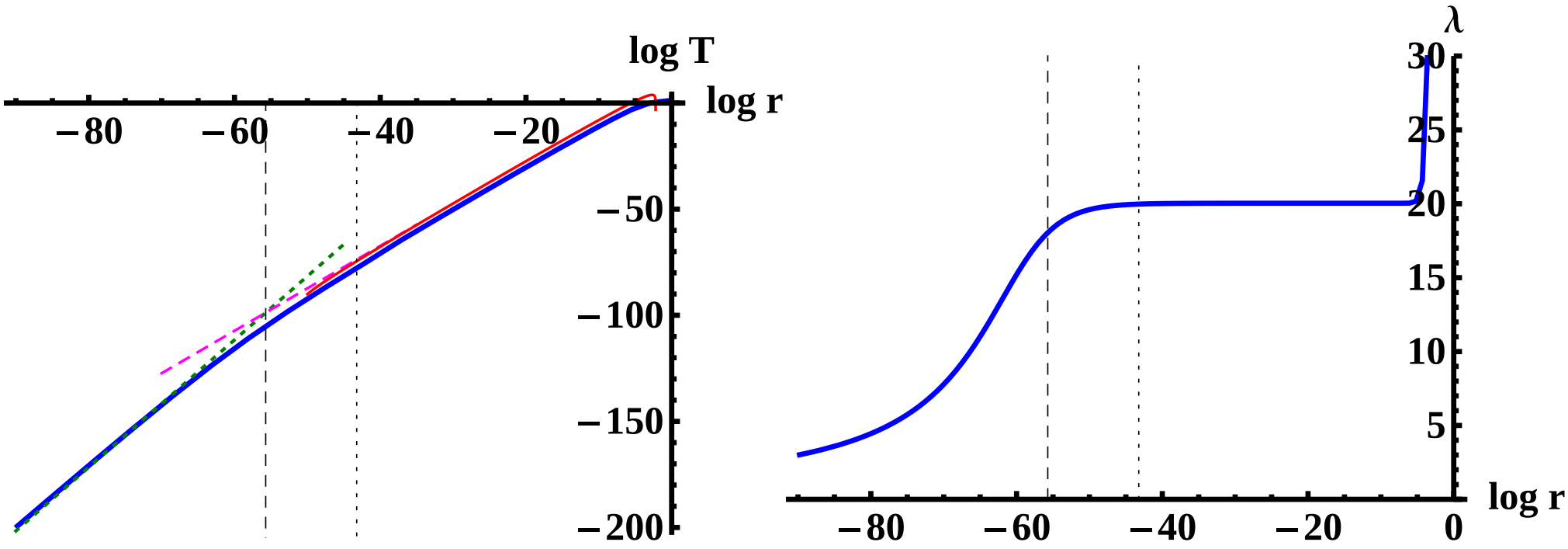

The tachyon $\log T$ (left) and the coupling λ (right) as functions of $\log r$ for an extreme walking background with $x = 3.992$. The thin lines on the left hand plot are the approximations used to derive the BKT scaling.

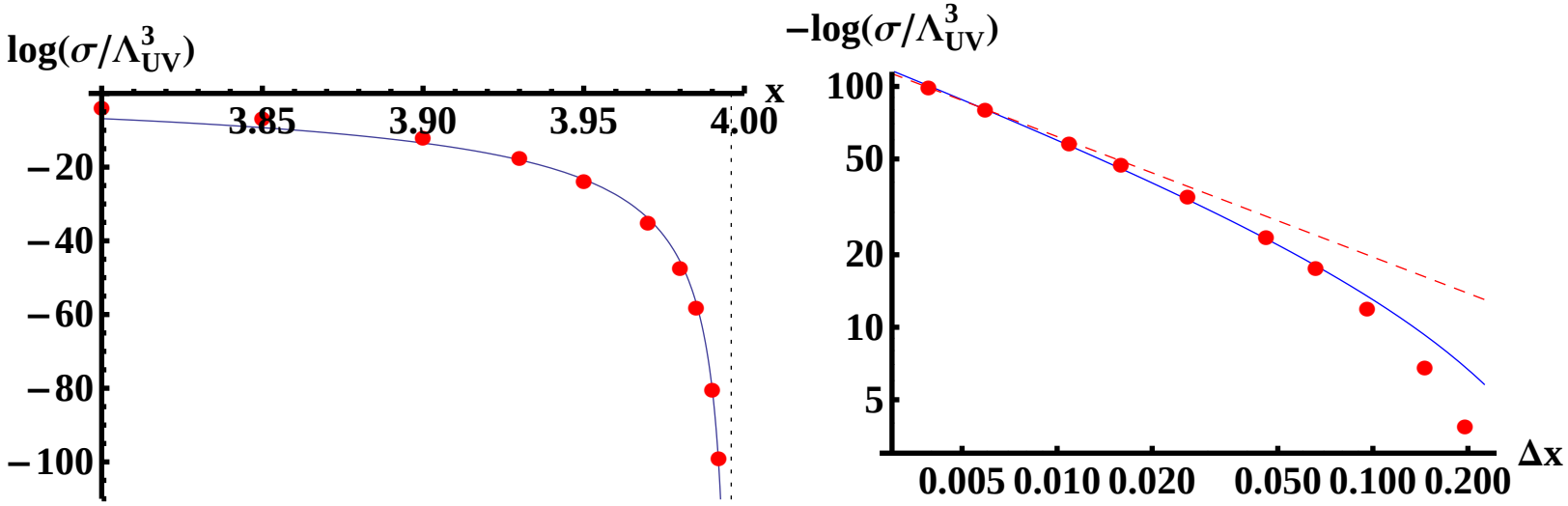

Left: $\log(\sigma/\Lambda^3)$ as a function of x (dots), compared to a BKT scaling fit (solid line). The vertical dotted line lies at $x = x_c$. Right: the same curve on log-log scale, using $\Delta x = x_c - x$.

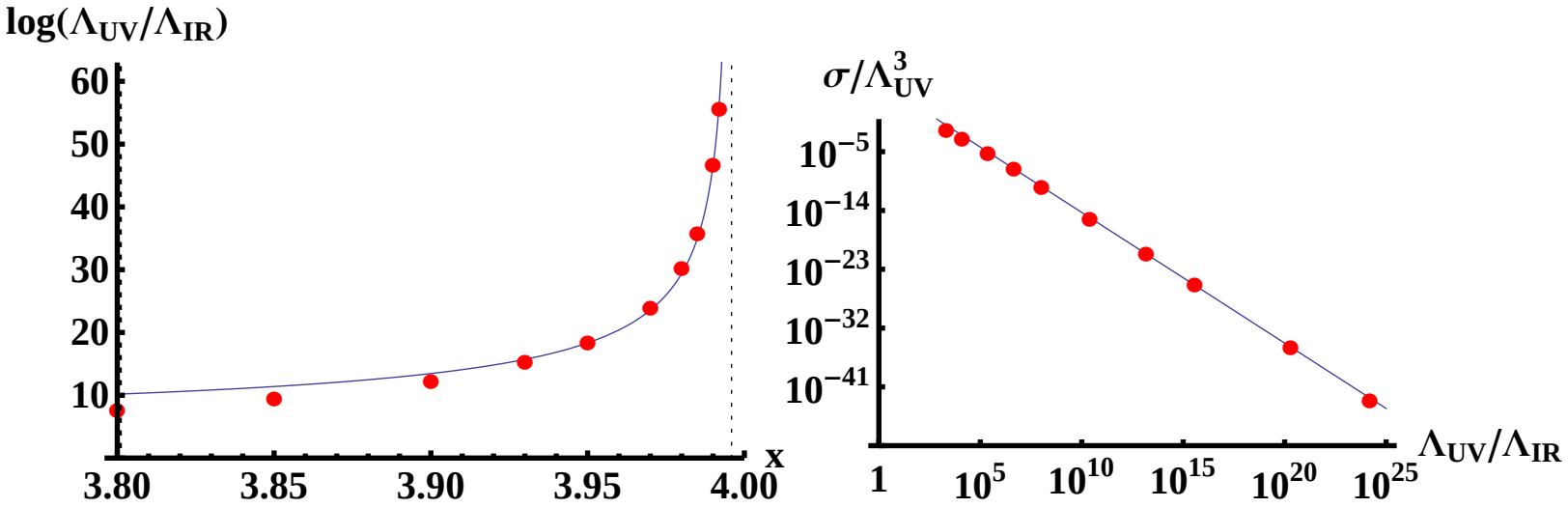

Left: $\log(\Lambda_{UV}/\Lambda_{IR})$ as a function of x (dots), compared to a BKT scaling fit (solid line). Right: σ/Λ^3 plotted against $\Lambda_{UV}/\Lambda_{IR}$ on log-log scale.

Effective potential and phase transitions

Iqbal+Liu+Mezei+Si, Jensen, Faulkner+Horowitz+Roberts

- In the scaling region we obtain

$$V_{eff}(\alpha) = -C\alpha^{\frac{d}{\Delta_-}} - (2d-1)\left(\frac{4\pi T}{d}\right)^d - \frac{(2d-1)\Delta_-(d-2\Delta_-)}{4d}\left(\frac{4\pi T}{d}\right)^{d-2\Delta_-}\alpha^2 + \ldots$$

- In the presence of a double-trace deformation on the field theory side

$$\delta\mathcal{L} \sim g\ \mathcal{O}^2$$

the effective potential at zero temperature becomes

$$V_{eff}(\alpha)\Big|_{T=0} \simeq g\alpha^2 - C\alpha^{\frac{d}{\Delta_-}}$$

- a stable symmetry-breaking vacuum exists with vev

$$\alpha \simeq \left(\frac{2g\Delta_-}{dC}\right)^{\frac{\Delta_-}{d-2\Delta_-}}$$

- Adding temperature in the presence of the double-trace deformation we obtain the effective potential

$$V_{eff}(\alpha) \simeq -C\alpha^{\frac{d}{\Delta_-}} - ET^d + g_{eff}\alpha^2 + \ldots$$

where g_{eff} is the temperature-shifted effective double-trace coupling

$$g_{eff} = g + GT^{d-2\Delta_-}$$

• The normal vacuum becomes unstable when $g_{eff} < 0$. The critical temperature T_c that separates the stable from the unstable regime is obtained :

$$g_{eff} = 0 \quad \Leftrightarrow \quad T_c \simeq \left(-\frac{g}{G}\right)^{\frac{1}{d-2\Delta_-}}$$

• At finite density:

$$g_c(\rho) = \frac{2d-1}{d}\rho^2 C_1 A_1^{\frac{d-2}{\Delta_-}}(\rho)\left(C_2 A_1^2(\rho) + \frac{d-2}{\Delta_-}A_2(\rho)\right)$$

• $A_{1,2}, C_{1,2}$ can be determined analytically

E.K.+Niarchos

• In the vicinity of the quantum critical point we observe the following scaling of the vev

$$\langle \mathcal{O} \rangle \sim (g_c - g)^{\frac{\Delta_-}{d-2\Delta_-}}$$

RETURN

Horizon values of τ, λ

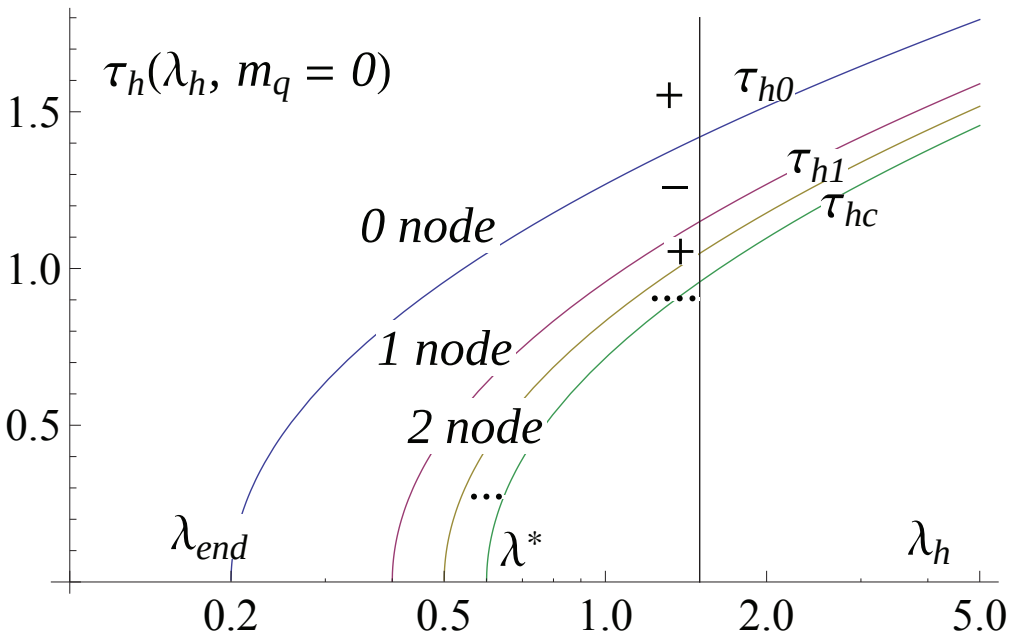

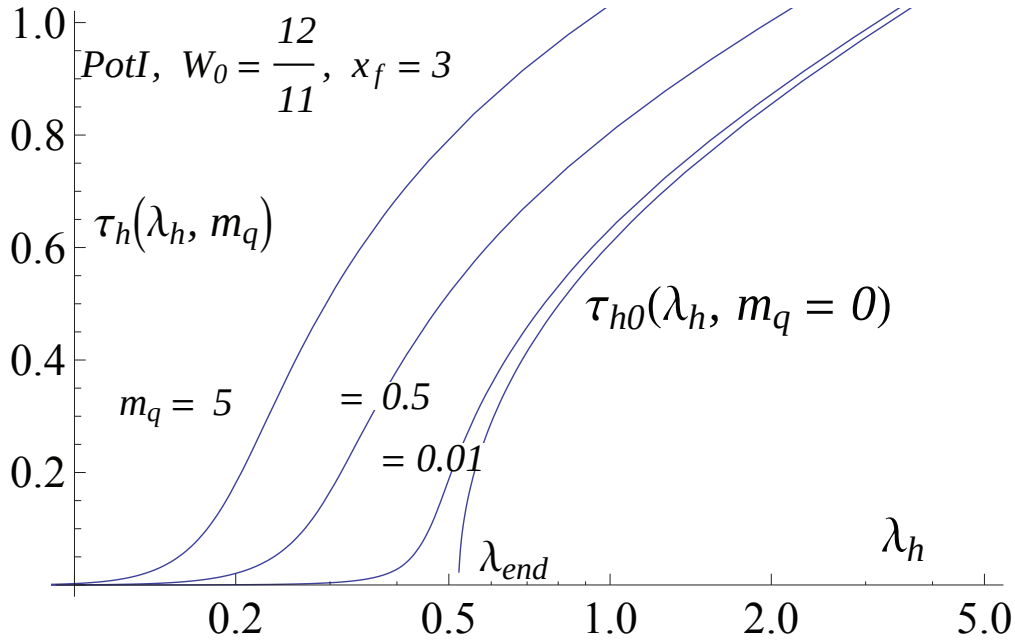

Detailed plan of the presentation

- Title page 0 minutes
- Bibliography 1 minutes
- The plan 2 minutes
- Introduction 4 minutes
- Effective Holographic Theories 7 minutes
- Einstein-scalar-U(1) theory 10 minutes
- Finite density scaling 12 minutes
- Scaling IR asymptotics 13 minutes
- The hidden scale invariance 16 minutes
- Scaling and hyperscaling at finite density 21 minutes
- (Lifshitz) Scaling of the broken-symmetry phase. 23 minutes
- Constant Scalar 25 minutes
- Running Scalar 27 minutes
- Extremal Geometries 28 minutes

- The holographic effective potential. 38 minutes
- The effective action 40 minutes
- EHT with two scalar fields 41 minutes
- A startup example: V-QCD 43 minutes
- Condensate dimension at the IR fixed point 44 minutes
- The symmetry-breaking regime 45 minutes
- BKT scaling 47 minutes
- Finite temperature 54 minutes
- The phase diagram for potential II_2. 56 minutes
- Outlook 57 minutes

- Naked singularities 60 minutes
- Solutions at Zero Charge Density 66 minutes
- Charged near extremal solutions 70 minutes
- Mott-like spectra 71 minutes
- Exact Charged solutions 72 minutes
- Solutions with $\gamma\delta = 1$ 75 minutes
- A typical Phase diagram 77 minutes
- Linear Resistivity 78 minutes
- Linear Heat Capacity 79 minutes
- AC conductivity 80 minutes
- Conductivity 81 minutes
- AC Conductivity: Derivation 85 minutes
- Brief Summary of Results 87 minutes
- The charged spectra, at zero density and conductivity 89 minutes
- The extremal AC conductivity 92 minutes

- The near-extremal DC conductivity 94 minutes
- Drag calculation of DC conductivity 98 minutes
- Vacuum solutions in the Einstein-Dilaton theory 102 minutes
- Classification of zero temperature solutions 106 minutes
- The $\gamma\delta = 1$ solutions 110 minutes
- Charged solutions $\gamma = \delta$ 117 minutes
- Conductivity of the $\gamma\delta = 1$ solutions 124 minutes
- QC systems with Schröndiger symmetry 129 minutes
- Resistivity at non-zero magnetic field 136 minutes
- The β functions 138 minutes
- The free energy 140 minutes
- BKT scaling, II 142 minutes
- Effective Potential and phase transitions 144 minutes
- Horizon values of λ, τ 146 minutes